Aalto-yliopisto
Insinööritieteiden
korkeakoulu

Tim-Oliver Latta

Identification and impact assessment of parameters on open stoping in the Kylylahti mine

Master's thesis submitted in partial fulfilment of the requirements for the degree of Master of Science in Technology

Espoo:	10.09.2020
Supervisor:	Prof. Mikael Rinne
Advisor:	M.Sc. Markus Malmberg

Aalto University
School of Engineering

Aalto University, P.O. BOX 11000, 00076 AALTO
www.aalto.fi

Abstract of master's thesis

Author Tim-Oliver Latta

Title of thesis Identification and impact assessment of parameters on open stoping in the Kylylahti mine

Master programme European Mining, Minerals and Environmental Programme (EMMEP) **Code** ENG211

Thesis supervisor Prof. Mikael Rinne

Thesis advisor(s) M.Sc. Markus Malmberg

Date 10.09.2020 **Number of pages** 95+21 **Language** English

Abstract

The stoping performance has a paramount effect on the economic viability of underground mining operations. Increasing volumes of overbreak diminish the ore quality and impose additional hauling expenditures. In contrast, any form of valuable material left inside the stope reduces the operational profit immediately. Knowing the parameters which affect stoping positively or negatively is of great interest to any mine planning engineer, as it allows more predictive and accurate production numbers.

This study is devoted to identifying important parameters to affect longhole open stoping in the Kylylahti mine. The introduction to stope planning is done by means of a comprehensive literature review on different dilution quantification and stope design methods. A further theoretical part of this study describes well-researched factors that are considered to have a solitary impact on generated stope overbreak and ore loss. Besides the importance of geological information on rock mass and formations, the accuracy of proper stope design as well as drilling and blasting pattern govern the success in stope efficiency.

The examination of the stope data revealed several parameters that steer the stope efficiency. Few parameters such as stope dimensioning tend to affect longitudinal and transverse stoping likewise. Main focus here is put on the correlation of varying stope sizes and associated overbreak. The inclination of stope walls is also found to affect both stoping methods accordingly. Visual and numerical observations showed strong sensitivity of stoping towards structural formations such as foliation in the Gap zone or in the lower Wombat orebody. The mining sequence is a parameter that mainly governs the distribution of ore overbreak and ore loss in longitudinal stopes. Dependencies on the stope locations with associated overbreak correspond to transverse stopes only. A compelling new insight is demonstrated that states the correlation of ore overbreak in primary stopes and the ore loss in secondary stopes. Conclusively, different methods are documented that provoke or prevent excessive overbreak and ore loss. The study concludes with suggestions on how to improve stoping based on the results of the stoping parameter identification.

Keywords Longhole Open Stoping, Blasthole Open Stoping, Longitudinal Stoping, Transverse Stoping, Dilution Control, Overbreak, Ore loss, Stoping Parameters, Underground Mining, Stope Design, Stope Geometry, Cavity Monitoring System, CMS

Acknowledgements

First and foremost, I would like to thank my thesis supervisor professor Mikael Rinne for providing me with this opportunity and the helpful feedback during my thesis and studies. At this point, I also would like to express my gratitude towards Boliden's technology department and especially Daniel Sandström for making the thesis possible in the first place.

This thesis could not have been done without the support from Boliden Kylylahti Oy. Thus, I would like to express my gratitude particularly towards Jaakko Kilponen, Antti Pihko and Kirsi Eronen who have made my stay on-site and in the office more than comfortable.

Next, I would like to say thank you to Juha-Matti Kekki who not only helped me through the difficulties in understanding Kylylahti's geology but also, for making my entire stay in the Kylylahti house more enjoyable and teaching me the Finnish culture.

I would like to take the opportunity to thank my family and my friends for the enduring support throughout my EMC years and during my thesis. A special thanks must be expressed to Christian for all the feedback on the thesis and my brother Niclas who kept me motivated and focused during my studies.

Finally, I would like to thank Markus Malmberg. If it were not for you, I would have never been able to learn so many different things about the operation, about stoping and how to look at and beyond underground mining operations. Thank you for your patience with me, our almost daily talks in the office and for showing me around outside of Polvijärvi.

Espoo, 10.09.2020

T.Latta

Tim-Oliver Latta

Table of Content

Abstract
Acknowledgements
Table of Content i
Symbols iv
Abbreviations v
List of Figures vii
List of Tables xi
1 Introduction 1
1.1 Aim and objectives 1
1.2 Research questions 1
2 Dilution 3
2.1 Terminology 3
2.2 Quantification of dilution 5
2.3 Equivalent linear overbreak/sloughing 6
2.4 Dilution density 8
3 Empirical stope design 10
3.1 Rock mass classification 10
3.2 Stability graph method 11
3.3 ELOS design method 12
4 Factors causing unplanned dilution 14
4.1 Geological factors 14
4.2 Drilling and blasting factors 14
4.3 Stope design 16
4.3.1 Stope height and length 16
4.3.2 Stope inclination 17
4.3.3 Hydraulic radius 18
4.3.4 Stress state 18
4.3.5 Mining sequence and stope type 20
4.3.6 Undercutting 21
4.3.7 Others 22
5 The Kylylahti mine 23
5.1 Regional setting 24
5.2 Local setting 24
5.3 Mineralisation 26
5.4 Geotechnical properties of rock mass 29
5.5 Mining method 30
5.5.1 Longitudinal stoping 31

5.5.2 Transverse stoping 32
6 Database information 36
6.1 General data overview 37
6.2 Stope geometry 38
6.2.1 Longitudinal stopes 38
6.2.2 Transverse stopes 41
6.3 Macro application 44
7 Results and key parameters of longitudinal stoping 47
7.1 Ore loss and overbreak results 47
7.2 Mining sequence and mining direction 49
7.2.1 Mining sequence 49
7.2.2 Mining direction 50
7.3 Stope design 52
7.3.1 Longitudinal stope dimensioning 52
7.3.2 Hanging wall inclination 53
7.3.3 Geometric complexity 54
7.4 Geological formations 56
7.4.1 Presence of structures 56
7.4.2 Black schist zone 59
8 Results and key parameters of transverse stoping 61
8.1 Ore loss and overbreak results 61
8.2 Mining sequence and stope types 63
8.3 Stope design 65
8.3.1 Transverse stope dimensioning 65
8.3.2 Effects of dip inclination 67
8.4 Stope sub-type and environment 68
8.5 Post-mining conditions of primary stopes 72
9 Best and bad practices for overbreak reduction 75
9.1 Best practices 75
9.2 Bad practices 76
9.3 Suggestions on precautions and improvements 76
10 Discussion 78
10.1 Benefits and drawbacks of macro application 78
10.2 Critical assessment of key parameter results 79
10.3 Lack of interdependent influences 81
10.4 The multi-causation of stoping parameters 82
10.5 Missing and omitted parameters 86

11 Conclusion 87
12 Recommendations 89
Bibliography 91
Appendix 1 96
Appendix 2 100
Appendix 3 103
Appendix 4 106
Appendix 5 111
Appendix 6 112
Appendix 7 115

Symbols

r		Correlation Factor/Coefficient
r_x		Radius
π		Pi
σ_1	[MPa]	Major Principal Stress
σ_2	[MPa]	Intermediate Stress
σ_3	[MPa]	Minor Stress

Abbreviations

A	Stress Factor
ANFO	Ammonium Nitrate and Fuel Oil
Au	Gold
AutoCAD	Computer-Aided Design Software
B	Joint Orientation Factor
C	Gravity Factor
cm	Centimetres
CMS	Cavity Monitoring System
Co	Cobalt
CRF	Cemented Rock Fill
Cu	Copper
DD	Dilution Density
DISS	Sulphide Disseminations
e.g.	Exempli Gratia (For Example)
ELOS	Equivalent Linear Lost Ore
ELOS	Equivalent Linear Overbreak/Sloughing
et al.	Et Alia (And Others)
FW	Footwall
Ga	Giga-Annum
HR	Hydraulic Radius
HW	Hanging Wall
i.e.	Isto Es (That is)
J_a	Joint Alteration Number
J_n	Joint Set Number
J_r	Joint Roughness Number
J_w	Joint Water Reduction Factor
K	Stress Ratio
LBS	Longitudinal Bench Stoping
LHD	Load Haul Dump Loader
LOM	Life of Mine
m	Metres
m^2	Square Meters
m^3	Cubic Metres
MPa	Megapascal
MS	Massive Sulphide Lenses
N	Stability Number
N’	Modified Stability Number
Ni	Nickel
NKSB	North Karelia Schist Belt
NNE	North-North-East
Q	Rock Tunneling Quality Index
RMR	Rock Mass Rating
RQD	Rock Quality Designation
S	Shape Factor
SMS	Semi-Massive Sulphide Lenses
SRF	Stress Reduction Factor
SSW	South-South-West

TBS	Transverse Bench Stoping
UCS	Uniaxial Compressive Strength
Zn	Zinc

List of Figures

Figure 2.1: Planned and unplanned dilution in a stope cross-section (after Mitri et al. (2010), modified by Latta) 4

Figure 2.2: Classification of dilution (after Villaescusa (1998), modified by Latta) 5

Figure 2.3: Application of ELOS method (after Clark (1998), from Hughes (2011), modified by Latta) 7

Figure 2.4: Application of ELLO method (after Clark (1998), modified by Latta) 7

Figure 2.5: Half-prolate ellipsoid used for dilution density approach (after Henning & Mitri (2007), modified by Latta) 8

Figure 3.1: Modified stability graph (after Potvin (1988), from Capes (2009)) 12

Figure 3.2: Dilution graph method (after Clark (1998)) 13

Figure 4.1: Factors to influence blasting (after Wang (2004), modified by Latta) 15

Figure 4.2: Anticipated dilution density (DD) for varying strike length and mining depths (after Henning (2007)) 16

Figure 4.3: Dilution density prediction with varying stope height and strike length (after Henning & Mitri (2007)) 17

Figure 4.4: Anticipated dilution density regarding stope height and aspect ratio (after Henning & Mitri (2007)) 17

Figure 4.5: Hanging wall angle sensitivity on overbreak (after Henning & Mitri (2007)) . 18

Figure 4.6: ELOS versus HR for different stress conditions K=1.5, K=2, K=2.5 (after Clark (1998,) from Wang (2004)) 19

Figure 4.7: Relaxation depth versus HR with different stress ratio K (after Wang (2004)) 20

Figure 4.8: Impact of major principal stress orientation on overbreak (after Henning & Mitri (2007)) 20

Figure 4.9: Overbreak associated with different stope types (after Henning & Mitri (2007)) 21

Figure 4.10: Illustrative scheme of undercutting effect on hanging wall stability (after Wang (2004), modified by Latta) 22

Figure 5.1: Location of Kylylahti mine, processing plant and corresponding smelter (after DFAT (2020), modified by Latta) 23

Figure 5.2: Kylylahti complex in cross-section view with local geological rock mass (after Kontinen (2005)) 25

Figure 5.3: Semi-massive massive ore domains of the Kylylahti deposit (looking east) per orebody allocation 27

Figure 5.4: DISS mineralisation (left) and in contrast to the SMS-MS domains (brown) on the right 27

Figure 5.5: Single sulphide grain from Kylylahti consisting of multiple different minerals (after Kekki (2020b)) 29

Figure 5.6: Schematic illustration of the longitudinal mining sequence (looking west) (after Malmberg & Svensson (2019), modified by Latta) 32

Figure 5.7: Transverse stoping sequence as per level (after Malmberg & Svensson (2019), modified by Latta) 33

Figure 5.8: Typical 1-3-5 pattern in transverse open stoping (after Ghasemi (2012)) 34

Figure 5.9: Mining sequence in upper Wombat orebody in Kylylahti 35

Figure 6.1: Stope database compilation (after Henning (2007), modified by Latta) 36

Figure 6.2: Longitudinal stope distribution across the Kylylahti orebodies 37

Figure 6.3: Transverse stope distribution across the Kylylahti orebodies 38

Figure 6.4: Width frequency of longitudinal stopes 39

Figure 6.5: Length frequency of longitudinal stopes 39

Figure 6.6: Height frequency of longitudinal stopes 40

Figure 6.7: Hanging and footwall dip in longitudinal stopes 41

Figure 6.8: Width frequency of transverse stopes 41

Figure 6.9: Length frequency of transverse stopes 42

Figure 6.10: Height frequency of transverse stopes 43

Figure 6.11: Hanging and footwall dip in transverse stopes 43

Figure 6.12: Scheme of a longitudinal stope with corresponding boxes in plan-view 45

Figure 6.13: QR-Code for illustration of macro input data 46

Figure 7.1: Ore loss and overbreak in longitudinal stope sidewalls 47

Figure 7.2: Ore loss in end walls over LOM in Wallaby 49

Figure 7.3: Avg. ore loss in the end walls of longitudinal stopes in Wombat 51

Figure 7.4: Avg. ore overbreak in the end walls of longitudinal stopes in Wombat 51

Figure 7.5: Scatter plot of stope length versus waste overbreak for Wallaby longitudinal stopes, r = 0.41 52

Figure 7.6: Scatter plot of waste overbreak versus hydraulic radius for longitudinal stopes in Wombat, r = 0.15 53

Figure 7.7: Hanging wall analysis of total overbreak in longitudinal stopes 54

Figure 7.8: Total overbreak after newly introduced geometric complexity in Wallaby longitudinal stopes 55

Figure 7.9: Waste overbreak after geometric complexity for longitudinal stopes in Wombat 56

Figure 7.10: Waste overbreak per level in longitudinal stopes for the Wombat orebody ... 57

Figure 7.11: Black schist foliation next to the Gap and on top of the Wombat ore lens encapsulating stope 380jpL2 57

Figure 7.12: Waste overbreak of longitudinal stopes in the lower levels after drift location in Wombat 58

Figure 7.13: Visual layering of black schist overbreak in production levels 240 and 270 looking west 59

Figure 7.14: Cross-section illustration of the planned stope 270L2 (green) and its CMS scan (red) indicating uniform layer overbreak from black schist in the footwall (east) 60

Figure 8.1: Ore loss and overbreak in transverse stope sidewalls 62

Figure 8.2: Schematic overview of stope type classification after vertical extraction 64

Figure 8.3: Transverse stope types versus total overbreak 65

Figure 8.4: Secondary stope strike length versus total overbreak results in the sidewalls, r = 0.6 66

Figure 8.5: Hydraulic radius of secondary stopes versus total overbreak results in the sidewalls, r = 0.6 67

Figure 8.6: Dip angles of hanging/footwall in secondary stopes versus overbreak/ore loss, r_{HW} = -0.64 and r_{FW} = -0.76 68

Figure 8.7: Sequential stope splitting shown for stope 560ppL14/1,2 and 3 69

Figure 8.8: Transverse sidewalls overbreak per sub-type after orebody location 71

Figure 8.9: Post-mining issue in form of excessive primary stope ore overbreak 72

Figure 8.10: Ore overbreak and ore loss causation in transverse stopes 73

Figure 8.11: Schematic illustration of ore overbreak and ore loss correlation 74

Figure 10.1: Total overbreak in primary stopes against production levels in Wombat 82

Figure 10.2: Comparison of drift design and mining direction in level 560 and 620 shows drastic strike shift in Wombat 85

Figure 10.3: Overbreak in transverse stopes located in the levels 500 – 620 86

List of Tables

Table 3.1: ELOS classification (after Clark (1988)) 13

Table 5.1: Overview of ore type classification in Kylylahti (after Malmberg & Svenson (2019), modified by Latta) 28

Table 5.2: General overview of rock mass properties in Kylylahti (after SRK Consulting (2007), modified by Latta) 30

Table 5.3: Production numbers of the Kylylahti operation from 2019 (after Malmberg & Svenson (2019)) 31

Table 6.1: Summary of stope geometry properties 44

Table 7.1: Statistical summary of longitudinal stopes in Wallaby 48

Table 7.2: Statistical summary of longitudinal stopes in Wombat 48

Table 7.3: Geometric complexity classification 55

Table 8.1: Statistical summary of primary transverse stopes 62

Table 8.2: Statistical summary of secondary transverse stopes 63

Table 8.3: Transverse sub-types with different side and end wall environments 70

Table 8.4: Combined stope sub-type results 71

Table 10.1: Benefits and drawbacks of the macro utilisation when establishing the ELOS and ELLO database 79

Table 10.2: Frequency of transverse stope sub-types 81

Table 10.3: Total overbreak in transverse stopes per ore type (see chapter 5.3) summarized per production levels 84

1 Introduction

In a world which becomes more competitive, the mining sector must keep track of the market development to sustain its profitability and achieve sufficient supply. The concepts that help achieve these goals vary greatly. They range from the implementation of newly developed automation projects to process optimisation whilst embracing digitalisation. Some mining operations do not allow for these improvements to be implemented due to their restrictive production rates or their short mine life. The affected mining operations must look after different approaches to increase value.

In underground mining, especially in longhole open stope mining, the production performance is monitored and assessed by checking hauled tonnages from the LHD scale and comparing them against planned tonnages. However, the single comparison of tonnages does not indicate the real conditions of the stopes being mined out. Dilution is a common issue causing mining operations to suffer elevated operational expenditures. The stope assessment must be extended towards the comparison of the actual stope conditions and the planned design by using the Cavity Monitoring System (CMS). Extensive research was conducted over the past decades to allow more predictability in stope stability and stope performance. This study attempts to analyse the stoping data of the Kylylahti mine and determine the most crucial parameter regarding its stope performance. The superordinate goal of the parameter identification aims to facilitate more accurate stope and production planning. This will eventually help to achieve minimized costs in loading and hauling and maximized revenue due to decreased overbreak and ore loss, respectively.

1.1 Aim and objectives

As the ore production is expected to be completed in Autumn 2020, the Kylylahti operation provides a vast dataset of more than 150 stopes to study. Due to different mining methods, the data presents great insights in how different mining methods have affected the production in general.

The first research objective principally focuses on the identification of influencing stoping parameters. The determination of these factors is done by means of overbreak and ore loss analyses. The second objective attempts to reveal best and bad practices on stope efficiency. Best practices are defined as methods or factors that prevent or reduce overbreak and ore loss occurrence. Bad practices are considered as conditions or methods that promote excessive dilution and ore loss. The ultimate goal is to find factors and methods that help to understand stoping better and improve the stope performance.

1.2 Research questions

The research questions are established to guide through the study and help to achieve the main objectives. The first set of research questions attempts to help with the determination of influencing stoping factors. Since the data mainly comprises stope planning parameters, the research questions are formulated as the following:

1. How is stope planning done in Kylylahti?
2. Is there a principal difference in longitudinal and transverse stoping performance?
3. How does the mining sequence influence stoping?
4. Does stope dimension variation affect overbreak likelihood?
5. To what extent does the geology affect stoping?

The determination of best practices follows the answering of the first research objective. The study attempts to reveal if distinct factors can help to prevent overbreak and ore loss. Emphasis is additionally laid on methods, that have to be avoided or reconsidered as they provoke excessive dilution. There are no explicit research questions necessary regarding the second objective because the examination of bad and best practices is highly dependent on the successful identification of stoping parameters.

2 Dilution

As the world economy becomes increasingly competitive, so does the mining sector. One of the major goals of every mining corporation is to increase its profitability. Some mining operations, such as the Kylylahti mine, are not eligible to be upgraded with newest technology due to their limited overall production. They need to seek different approaches in their performance surge. Since Kylylahti is mined in a combination of longitudinal and transverse longhole open stoping, stopes are typically assessed on their accuracy and deviation from original plans. Dilution is known as the major driver for increasing operational costs and decreasing profitability (Henning & Mitri, 2007). The main emphasis in high grade areas is put on the ore recovery (Malmberg, 2020a).

The term dilution is introduced in this chapter which is considered one of the most critical stope assessment parameters. Starting with the terminology of planned and unplanned dilution, the explanation of different interpretations for dilution quantification is explained next. The chapter concludes with the presentation of important factors that potentially promote or inhibit dilution.

2.1 Terminology

Dilution is a well-known, yet underestimated parameter when analysing the stope performances (Henning & Mitri, 2007). It is commonly assessed in combination with ore recovery. In best practice, the operation would return a maximization in ore recovery in contrast to the minimization of dilution. Yet, Clark (1998) points out the contradicting interrelation between dilution and ore recovery. The planning department needs to accept a certain degree of dilution to attain a desired ore recovery (Clark, 1998).

Wright (1983) defines dilution as any material considered non-ore which is intruding the mining operation. The repercussions are additional operational expenditures due to increase tonnages to haul and transport but also a cutback on the total ore grade being extracted.

Dilution can be further subdivided into planned and unplanned dilution. Another expression for these terms is internal and external dilution, respectively (Villaescusa, 1998). Figure 2.1 illustrates a scheme that visualises how dilution definitions are used in practice. Scoble and Moss (1994) suggest a definition of planned and unplanned dilution as follows:

- *Planned dilution* is referred to as any non-ore material i.e. waste rock and also ore below the applied cut-off grade that is situated within the stope delineation and mined out with the ore.

- *Unplanned dilution* considers any non-ore material (below cut-off grade) which is derived from rock or backfill outside the stope boundaries.

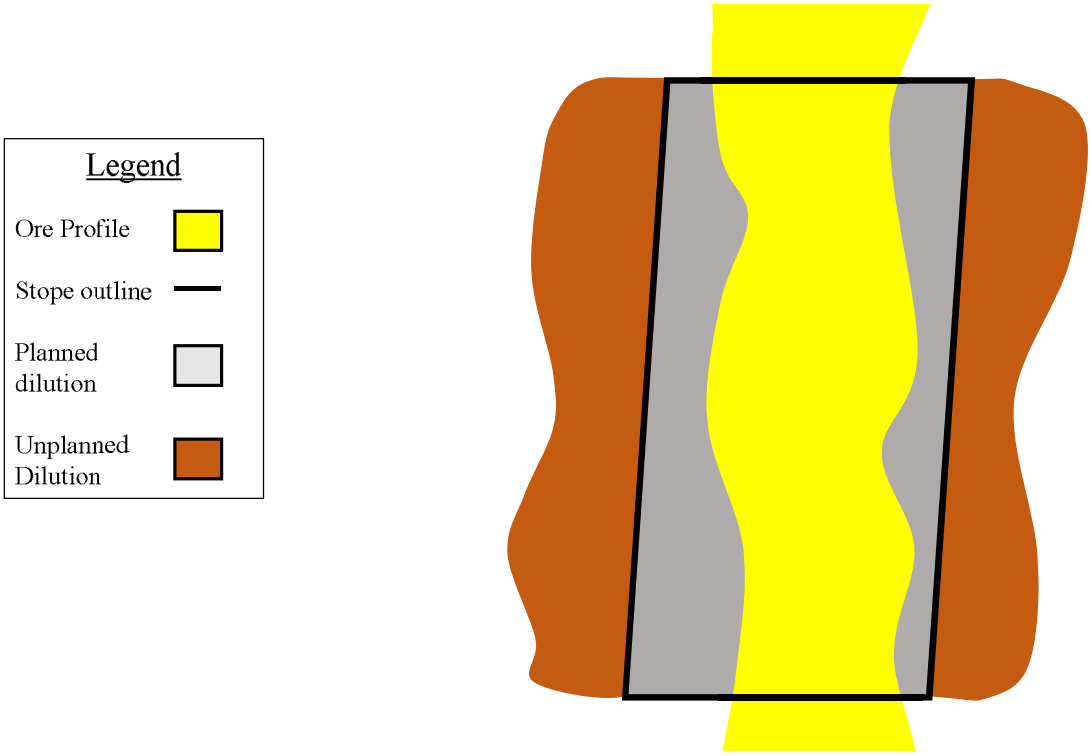

Figure 2.1: Planned and unplanned dilution in a stope cross-section (after Mitri et al. (2010), modified by Latta)

Reasons for planned dilution are mostly related to mining method restrictions. A more complex and irregular orebody dictates over the level of accuracy and appropriateness of used equipment (Trevor, 1991). Elbrond (1994) found that drilling and blasting equipment promote planned dilution because of their relative inflexibility to follow contacts between ore and non-ore material (below cut-off grade).

Unplanned dilution is related to non-ore material breaking into the stope and is triggered by unstable stope walls. Sloughage of backfill material of adjacent stopes, waste intrusion from hanging and footwall as well as blast-induced overbreak are major causes for unplanned dilution. (Scoble & Moss, 1994)

According to Villaescusa (1998), dilution does not refer to overbreak of non-ore material only. The Figure 2.2 shows a scheme that explains potential causes of dilution and ore loss as well as their interrelationship. The bottom row plots potential causes for unplanned, planned and geological dilution. The top row refers to common expressions for unplanned and planned dilution. External dilution is a term frequently used in mining for unplanned dilution with internal dilution describing planned and even geological dilution.

It must be noted that the distinction between planned and geological dilution lays within its origin. Planned dilution is mostly driven by mining methods and can be relatively easily calculated. The geological impact on planned dilution happens due to insufficient exploration that requires ore models to be designed differently. Due to those possible ore model alterations, dilution in form of new low-grade or below cut-off material can intersect preliminary ore blocks.

Any form of economically valuable ore material (above cut-off grade) that has not been mined and mucked out is referred to as ore loss. Ore loss is typically pronounced by improper rock fragmentation due to insufficient or inaccurate drilling and blasting. Unplanned pillar instalments used for increasing stope wall stability and incomplete mucking on ground floor are additional causes. (Villaescusa, 1998)

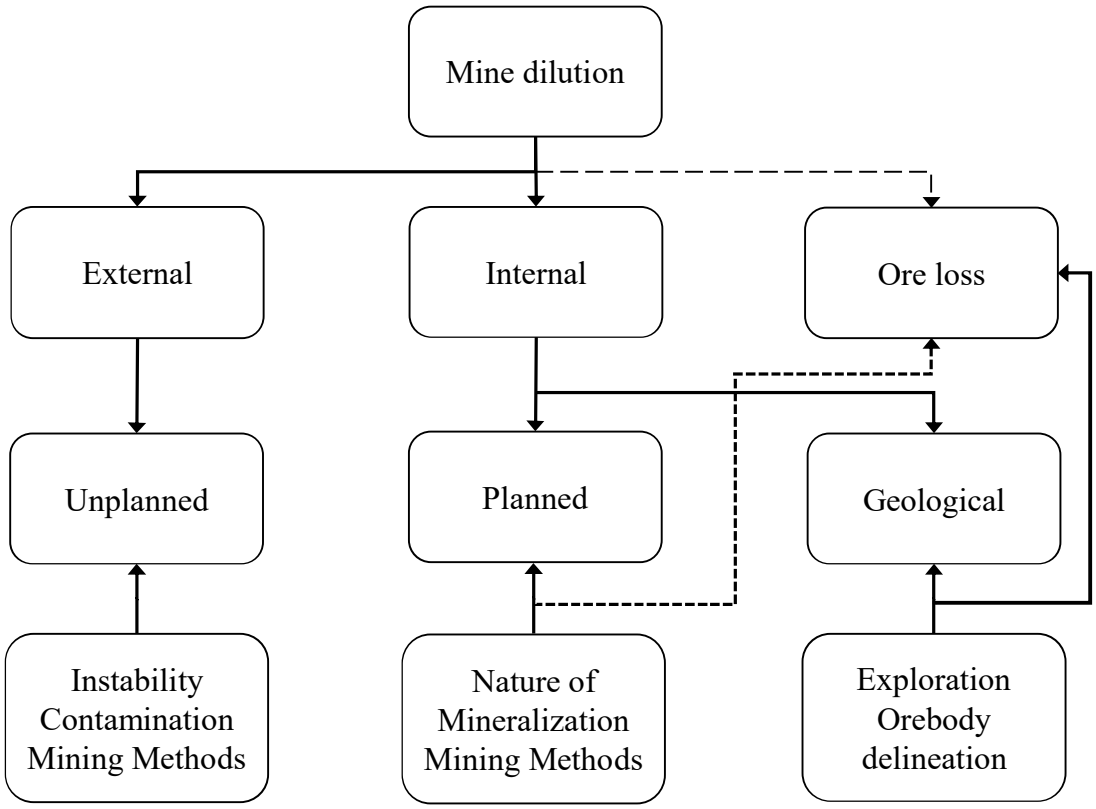

Figure 2.2: Classification of dilution (after Villaescusa (1998), modified by Latta)

The main focus of this thesis lays on unplanned dilution and ore losses. In the further part of this study, it is decided that dilution refers to unplanned dilution to ease an understanding of the context. Ore losses shall be mentioned separately. The term overbreak is used as alternative for unplanned dilution (Henning & Mitri, 2007).

2.2 Quantification of dilution

Mining companies principally decide individually how they express dilution. The methods to calculate dilution vary greatly as observed by Pakalnis (1986) who found ten different approaches to do so whilst studying 22 different mine sites in Canada. Scoble and Moss (1994) identified the two following equations to be the most abundant calculation used to determine dilution:

$$Dilution = \frac{Tonnes\ of\ waste\ mined}{Tonnes\ of\ ore\ mined} \quad (1)$$

$$Dilution = \frac{Tonnes\ of\ waste\ mined}{Tonnes\ of\ ore\ mined + tonnes\ of\ waste\ mined} \quad (2)$$

Pakalnis et al. (1995) proposed Equation (1) to be used as the standard procedure to allow for dilution quantification as it is more receptive to stope wall sloughage. On the other hand, Henning and Mitri (2008) reveal the susceptibility of Equation (1) compared to Equation (2) while using a 2:1 sloughage-to-ore ratio test. According to Equation (1), the dilution totals 200 % as opposed to only 66 % if Equation (2) is applied. It must be mentioned that dilution will be expressed as percentages only.

Another drawback of the equations is their susceptibility and inappropriateness towards stope comparison with varying mining widths (Henning & Mitri, 2008). As an example, a stope has steeply dipping sidewalls, is 1.5 metres wide and suffers 0.3 metres overbreak from the stope walls. The unplanned dilution returns eventually a dilution factor of 40 %. Assuming the overbreak remains equal and the stope width is twice as wide, the dilution factor changes automatically by half and would be 20 %.

2.3 Equivalent linear overbreak/sloughing

The dilution comparison of longitudinal stopes is rather complicated due to the strong dependency on the individual stope width (Henning & Mitri, 2008). Dunne and Pakalnis (1996) suggested the equivalent linear overbreak or sloughing (ELOS) method. It allows for greater accuracy when comparing unplanned dilution in longitudinal stopes. Overbreak is typically irregularly sized rock mass which caves into the stope whereas sloughing is rather a thin layer of material sliding down into the open space. Both are understood to affect stope performance similarly which is why in this study, no distinction is made. Both are perceived as unplanned material caving into the stoping area.

The equivalent linear overbreak or sloughing (ELOS) expresses dilution in terms of a volumetric measure (Clark, 1998). The calculation requires the information of planned stope design and the actual stope scan obtained from the Cavity Monitoring System (CMS). The CMS uses laser technique temporarily installed in the open void to obtain post-blasting conditions. That enables the creation of a three-dimensional mesh of data points into an AutoCAD software e.g. Surpac (Clark, 1998). Dunne and Pakalnis (1996) proposed the dilution to be calculated in form of unplanned material which had come off the stope walls as volume per square metre of wall. The mathematical notation is formulated as follows:

$$ELOS\ [m] = \frac{Volume\ of\ measured\ overbreak\ from\ stope\ surface\ [m^3]}{Area\ of\ stope\ surface\ [m^2]} \qquad (3)$$

The results express the actual overbreak along the respective stope surface. They do not express an estimate of equivalent layer thickness with approximate volume using a 2D section. The ore loss calculations can be similarly computed. The term for this method is called equivalent linear lost ore (ELLO) and focuses on underbreak instead of overbreak (Clark, 1998). Figure 2.3 and Figure 2.4 portray the idea and the conversion of irregular overbreak and ore loss into equivalent layers.

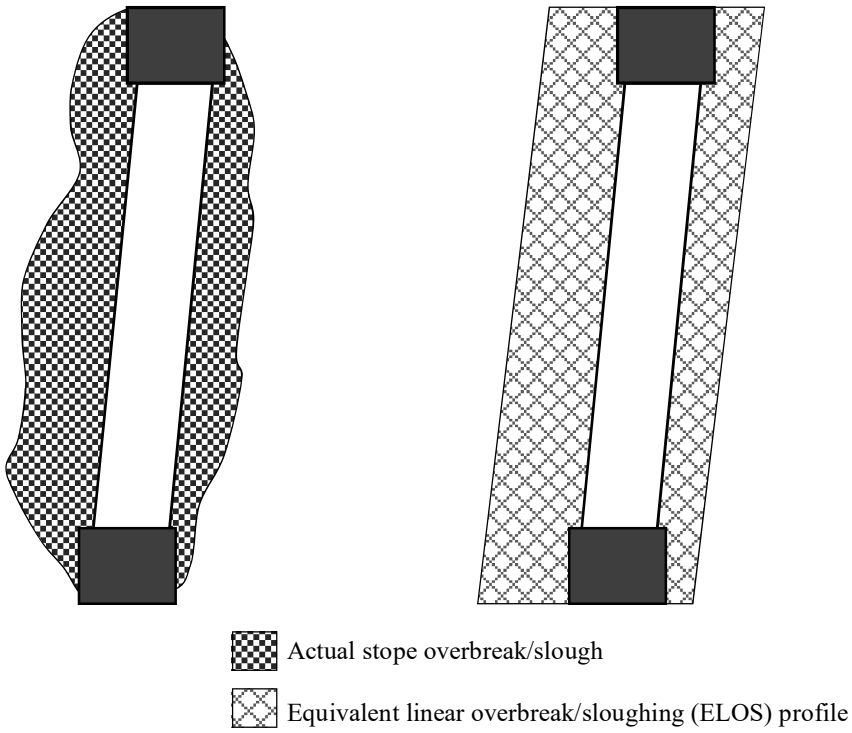

Figure 2.3: Application of ELOS method (after Clark (1998), from Hughes (2011), modified by Latta)

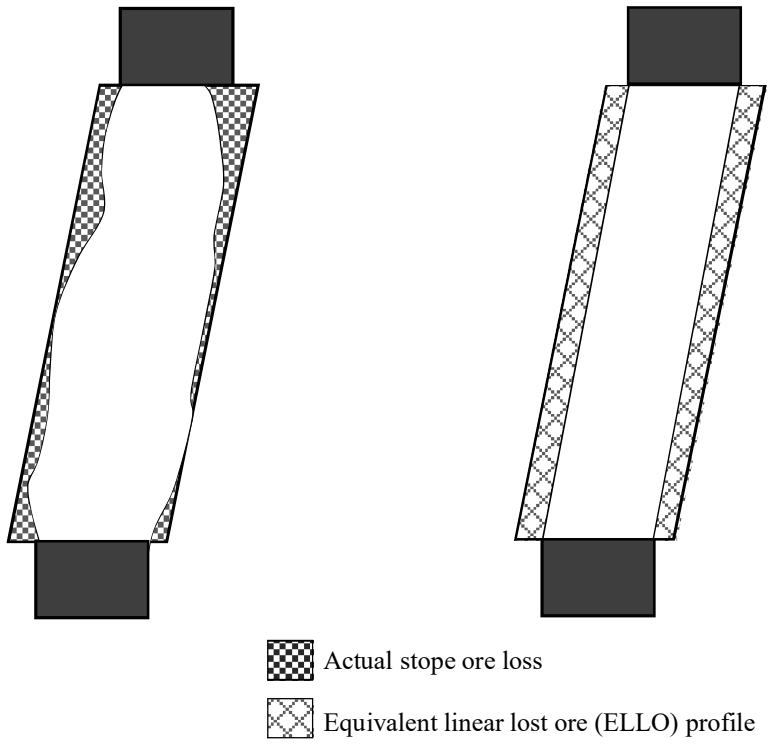

Figure 2.4: Application of ELLO method (after Clark (1998), modified by Latta)

2.4 Dilution density

The equivalent linear overbreak/sloughing (ELOS) method is an improvement to conventional dilution interpretation in a way that allows mines to compare different mining methods (Clark, 1998). Henning and Mitri (2007) stress the simplification of assuming overbreak to occur equally distributed along the stope wall. They conceive overbreak to be more accurately expressed as a half-prolate ellipsoid whose overbreak volume can be formulated as follows:

$$Volume\ of\ half-prolate\ ellipsoid\ [m^3] = (\frac{2\pi}{3}) * r_1 * r_2 * r_3 \quad (4)$$

where: r1, r2 and r3 refer to the perpendicular, vertical, and horizontal radius distance from the centre of the stope wall contact. The mid-span and mid-height of the particular stope wall is conceived as the centre of the ellipsoid.

An illustration attempt is made in the Figure 2.5. The application of overbreak volume represented by a half-prolate ellipsoid allows a more precise overbreak prediction over the entire stope wall. Its natural shape does not cover the stope wall edges and produces the largest quantity of overbreak in the mid-span of the stope wall.

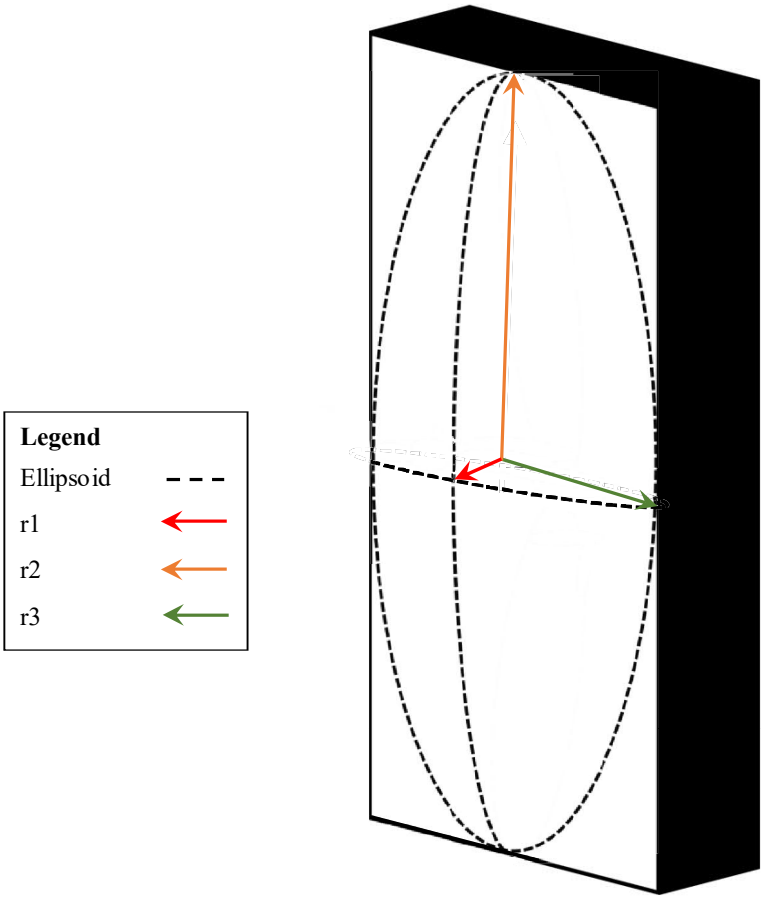

Figure 2.5: Half-prolate ellipsoid used for dilution density approach (after Henning & Mitri (2007), modified by Latta)

The half-prolate ellipsoid approach is a convenient tool when using numerical modelling. The assessment of real case studies applied dilution density differently as shown in Equation (5) and (6) (Henning, 2007).

$$Dilution\ density\ [m] = \frac{Half\ prolate\ ellipsoid\ volume\ [m^3]}{Area\ of\ exposed\ surface\ [m^2]} \quad (5)$$

$$Dilution\ density_{CMS}\ [m] = \frac{Volume\ of\ overbreak\ measured\ from\ CMS\ [m^3]}{Area\ of\ exposed\ stope\ wall\ [m^2]} \quad (6)$$

3 Empirical stope design

The individual stope performance in terms of ore recovery, overbreak and ore loss, is predominately driven by the stope design. Several studies have been conducted over the past decades to obtain better understandings on rock mass characteristics. Empirical methods have been found appropriate when evaluating rock mass properties and their impact on open excavation or stope stability. Any stope instability incurs additional operational costs and deteriorates working environments with regard to safety. This chapter introduces briefly to the most common empirical methods of rock mass classification and stope design. Apart from the original and modified stability graph number, the ELOS stability method is discussed.

3.1 Rock mass classification

When planning stopes, the more information on the rock mass is available, the more accurate the planning procedure is likely to become (Villaescusa, 1998). The rock mass classification is widely used to allow the characterization of rock mass including their quality, strength, and structural composition. Three common methods which help to assess rock mass properly are as follows:

- Rock Quality Designation (RQD)

The rock quality designation (RQD) analyses diamond drill core samples to evaluate rock quality (Deere, et al., 1967). In practice, the samples are analysed according to their present conditions. Flawless, unbroken pieces of sizes greater than 10 centimetres are examined against the total length of the individual drill core log. The length of each piece is then summed up and divided by the total dimension of the log. Equation (7) shows the mathematical expression (Deere & Deere, 1988). The drawback of the RQD is considered to be the estimation of a single criteria only. Other methods such as the Q-classification and the rock mass rating (RMR) consider multiple factors at once (Suorineni, 1998).

$$RQD\ [\%] = \frac{\sum Core\ pieces > 10\ cm\ [cm]}{Total\ length\ of\ drill\ core\ log\ [cm]} * 100 \qquad (7)$$

- Rock Mass Rating (RMR)

The ultimate goal besides the determination of rock mass is to provide with suggestions on adequate support (Bieniawski, 1976). Recommendations are made on the excavation dimensions and the support installation. If required, the results propose the potential rock support implementation of either rock bolting, wire mesh, shotcrete application or steel sets (Bieniawski, 1989). The parameters are as the following (Bieniawski, 1989):

1) Strength of intact rock material
2) Rock quality designation (RQD)
3) Spacing of discontinuities
4) Condition of discontinuities
5) Groundwater conditions
6) Orientation of discontinuities

- Rock Tunnelling Quality Index (Q)

The rock tunnelling quality index, also known as Q-classification, has been developed by Barton et al. (1974). Similar to the RMR, the Q-classification is a multi-parameter method. It aims principally for suggestions on additionally implemented rock support. In the following, the mathematical expression of the Q-index is shown in Equation (8).

$$Rock\ tunnelling\ quality\ index\ = \frac{RQD}{J_n} * \frac{J_r}{J_a} * \frac{J_w}{SRF} \quad (8)$$

where RQD = Rock quality designation
J_n = Joint set number
J_r = Joint roughness number
J_a = Joint alteration number
J_w = Joint water reduction factor
SRF = Stress reduction factor

3.2 Stability graph method

Underground mining is known to profit from the adoption of rock mass classification techniques (Hoek, 2007). Mining methods such as open stoping heavily rely on accurate interpretation on how the rock mass is likely to perform when excavated (Capes, 2009). The most popular method is the stability graph method (Mathews et al., 1981) and its modification after Potvin (1988). The ELOS stability method is an alternative provided by Clark (1998).

Two main parameters which are utilised for the stability methods are the stability number (N) or and the hydraulic radius (HR). The modified stability number N' is used in the updated version after Potvin (1988). With help of the stability method, stope geometry and rock mass properties are both incorporated. Increasing the predictability of the stope stability is the ultimate goal. The stability method incorporates besides the Q-Index factors such as stresses, the joint orientation and gravity (Brady & Brown, 2005). Equation (9) summarizes how to calculate the modified stability number N'. Appendix 1 comprises further visual explanation of the stress factor A, the joint orientation factor B and the gravity factor C.

$$Stability\ number\ N' = Q' * A * B * C \quad (9)$$

Another equation that Mathews et al. (1981) incorporate into the stability method is referred to as hydraulic radius (HR) or shape factor (S) (Brady & Brown, 2005). The HR is formulated as the quotient of the open stope surface area and the respective perimeter as shown in Equation (10). The idea behind the integration of the HR is to account for the geometry of the respective stope dimensions (Capes, 2009).

$$Hydraulic\ radius\ [m]\ = \frac{Area\ of\ open\ stope\ surface\ [m^2]}{Perimeter\ of\ respective\ surface\ [m]} \quad (10)$$

The stope stability can be assessed and predicted by plotting the two numerical values in the modified stability graph chart (Figure 3.1). The chart distinguishes between three different zones. These regions are defined as stable, transition and caving zone. Further efforts were

made (Nickson, 1992) to include support requirements into the graph. The original version from Matthews et al. (1981) is attached in Appendix 1.

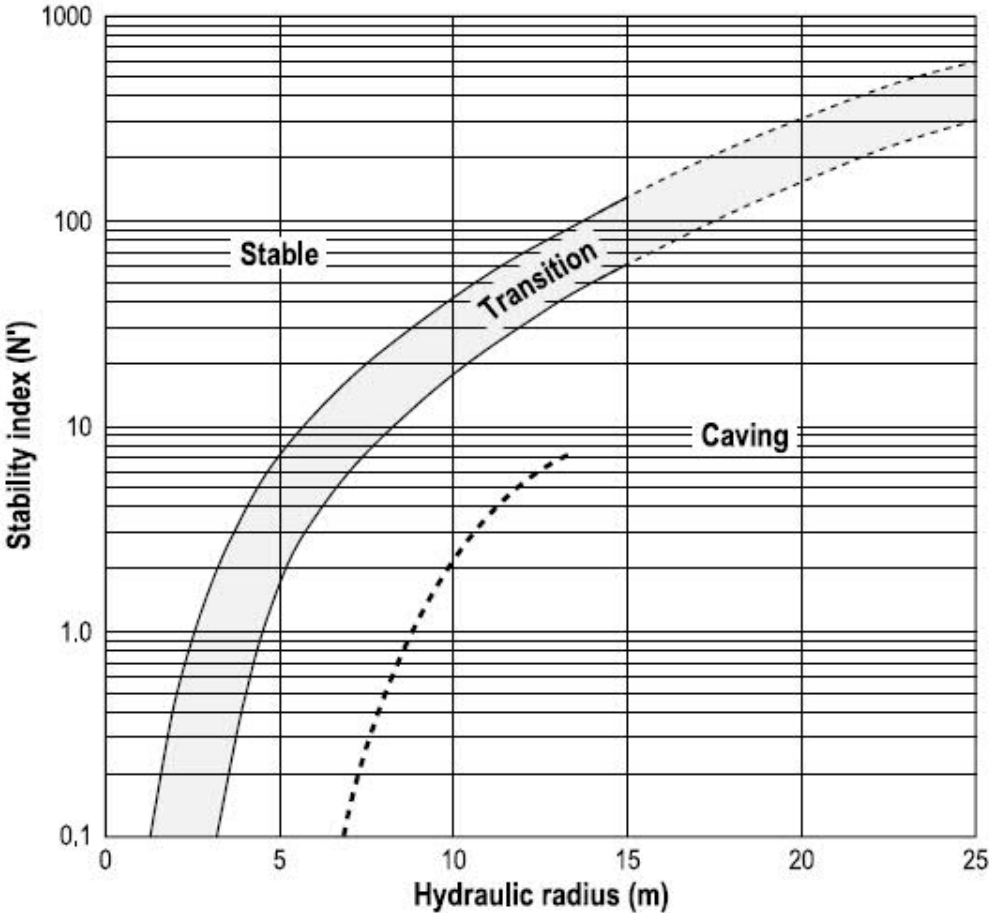

Figure 3.1: Modified stability graph (after Potvin (1988), from Capes (2009))

3.3 ELOS design method

A different approach to stope design is presented in form of the dilution graph method developed by Clark (1998). The technique attempts to derivate stope stability from occurring dilution in form of overbreak or slough. The main difference is the switch in input values which are in this method ELOS results (Figure 3.2). Clark (1998) concluded from the results the distinction into categories as shown in Table 3.1. Two additional plots are enclosed in Appendix 1 to illustrate how the stopes in Kylylahti performed based on the introduced ELOS design method.

Table 3.1: ELOS classification (after Clark (1998))

ELOS classification			
Category	**Classification**	**ELOS**	**Description**
I	Blast damage only	< 0.5 m	○ Minimal overbreak only with no support needed
II	Minor sloughing	0.5 m - 1.0 m	○ Stope support should be considered ○ Slight wall instability due to further blasting-induced vibrations
III	Moderate sloughing	1.0 m - 2.0 m	○ Stope support highly recommended ○ Significant overbreak associated with wall instability
IV	Severe sloughing	> 2.0 m	○ Extreme overbreak ○ Support must be installed to preserve stope access and continue operation

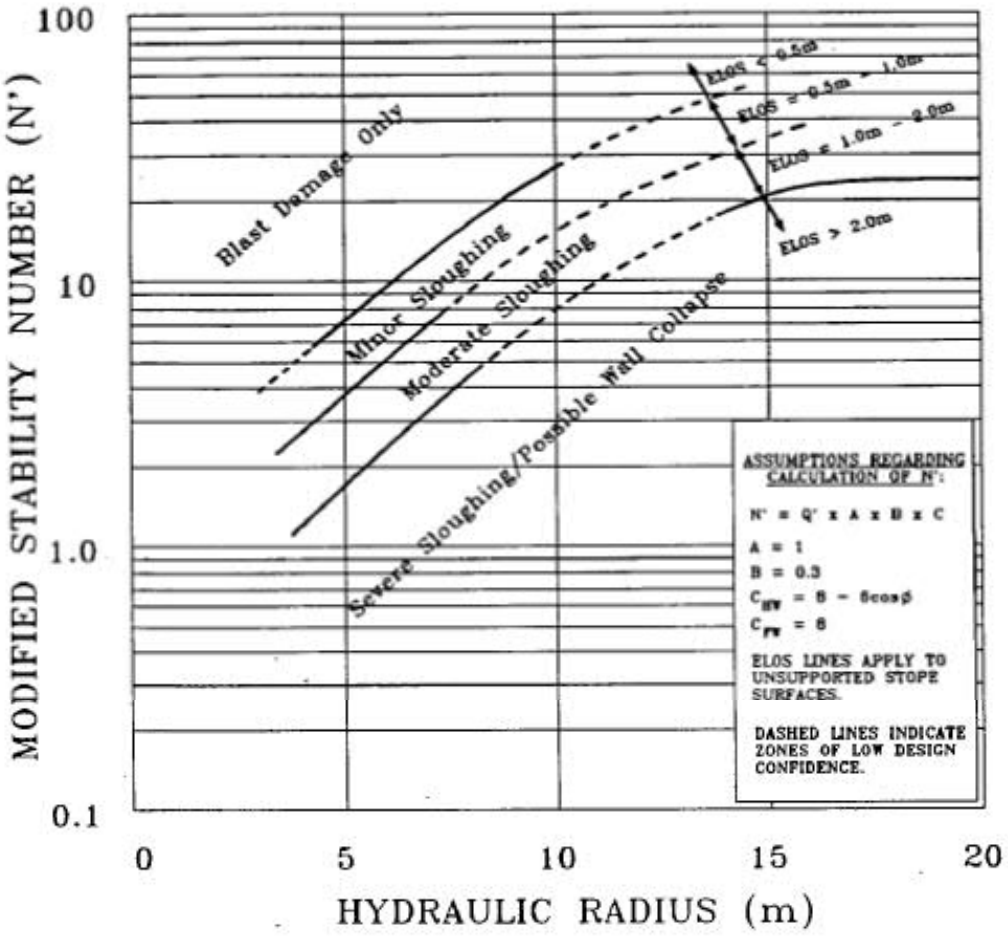

Figure 3.2: Dilution graph method (after Clark (1998))

4 Factors causing unplanned dilution

Mining operations are subject to increasing profitability if the mining process can be streamlined through maximizing ore recovery and minimizing dilution (Villaescusa, 1998; Henning & Mitri, 2008). Two main types of dilution exist which are planned and unplanned dilution. Planned dilution is inherently connected to the mine planning procedure. Trevor (1991) and Elbrond (1994) proposed that planned dilution is caused due to the orebody geometry and the selection of the mining method as well as drilling and blasting equipment.

The occurrence and severity of unplanned dilution greatly steer the profitability of mining operations (Henning & Mitri, 2007). Longhole open stoping is associated with relatively low mining costs and great sensitivity towards dilution (Stewart & Trueman, 2008). Scoble and Moss (1994) concluded that sloughing of abutted backfill material, waste overbreak from stope walls and blast-induced overbreak are considered primary causes for unplanned dilution. Due to its impact on the economy of longhole mining operations, many studies researched and determined further factors provoking unplanned dilution (Jang, 2014; Henning & Mitri, 2007; Villaescusa, 1998; Suorineni, 1998).

This chapter introduces to factors that are known to contribute to unplanned dilution. It will explain geological factors with primary focus on the exploration and the ore zone boundaries. A brief explanation of drilling and blasting factors follows accordingly. The major part of this chapter is devoted to the stope design.

4.1 Geological factors

Many studies were conducted to identify geological factors contributing to unplanned dilution as for example work from Suorineni (1998), Villaescusa (1998) and Potvin (1988). The exploration of an ore deposit and its resource modelling has a great impact on the performance of underground mine operations (Clark, 1998). Correct and thorough assessment of rock mass properties as well as accurate and precise interpretation of ore boundaries are vital for proper equipment selection and stope planning. A satisfying geological interpretation is achieved with but not limited to core logging, potential use of geophysical application and underground sampling of free faces (Villaescusa, 2004).

Stope planning and the drift development heavily rely on correctly interpreted geological data. Good practice is achieved when drifts remain in ore material and avoid close contact to or undercutting of hanging and footwall (Clark, 1998). Any misinterpretation due to missing or insufficiently examined samples can feature unplanned dilution (Villaescusa, 1998). Clark (1998) and Suorineni (1998) found that geological features tend to affect the stope performance and are directly linked to overbreak occurrence. Other geological and geotechnical factors are rock mass properties, stress environments (Henning & Mitri, 2007) and joint settings (Potvin, 1988).

4.2 Drilling and blasting factors

Missing geological data can cause insufficient orebody interpretation that lead to unplanned dilution. It can affect the stope efficiency as well as drilling and blasting performance (Villaescusa, 2004). Blasting causes ore to ideally break into homogenously sized particles with thorough ore fragmentation over the entire stope. No disturbances are conveyed into

adjacent waste rock mass and no instability is provoked. These objectives are found to contradict one another in reality which results in unplanned dilution (Wang, 2004). Blasting is mainly affected by a series of mostly operational parameters that can define over accurate or poor performance (Clark, 1998). A schematic overview of the factors to influence blasting can be seen in Figure 4.1.

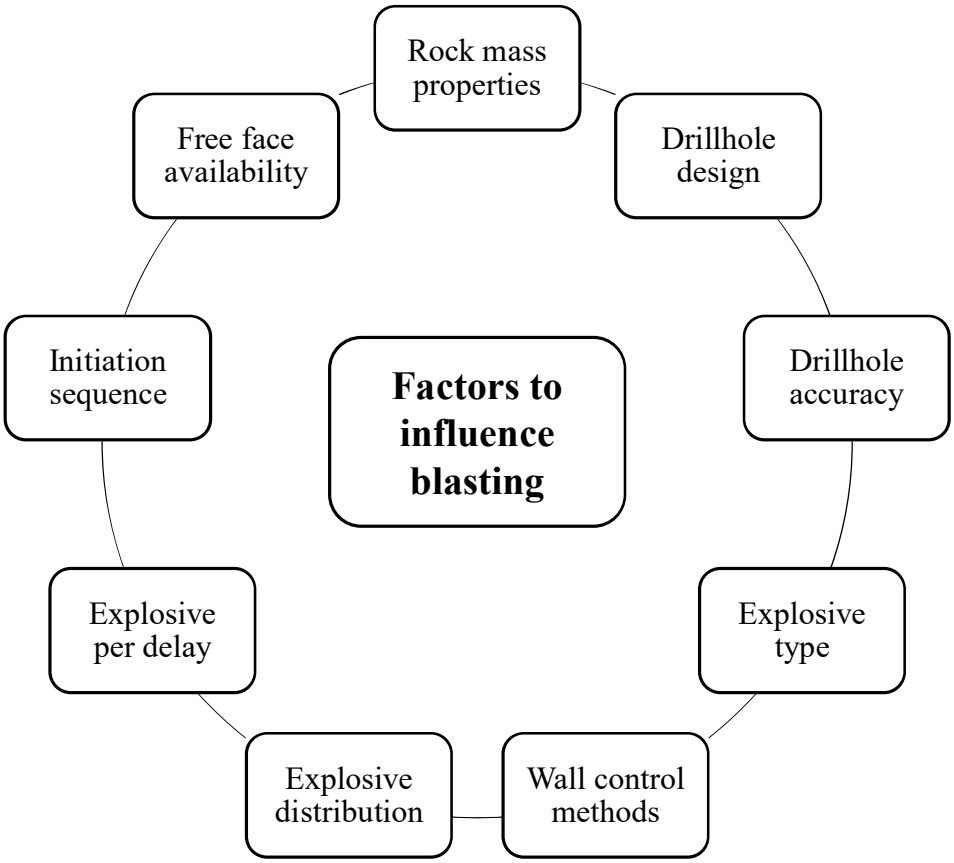

Figure 4.1: Factors to influence blasting (after Wang (2004), modified by Latta)

The key parameters in blasting operations are the drillhole design, the drillhole accuracy and the explosive types. The drillhole design is composed of factors such as drillhole length, diameter as well as spacing and burden (Wang, 2004). They mostly dictate the spatial fragmentation and general stope fragmentation success (Clark, 1998). The drillhole accuracy is highly dependent on the drillhole trajectory (Hendricks, et al., 1994) and the collar indication (Clark, 1998). Deviation in any of these accounts for drillhole inaccuracy. The drilling in and blasting of cemented rock fill or waste backfill is only one potential consequence. Other factors concern the explosive distribution and the explosive type. The explosive distribution of the blast is determined by the powder factor (Wang, 2004). The ideal powder factor aims for an adequate ratio of used explosives compared to fragmented rock (Lusk & Worsey, 2011). Another factor to influence blasting is the selection of proper explosive types such as ammonium nitrate and fuel oil (ANFO) (Lusk & Worsey, 2011). Because the provided stope data lacks sufficient information on these factors, the study does not focus on drilling and blasting parameters.

4.3 Stope design

The third category to have an influence on the stope performance is known as stope design. Many studies investigated how different geometries, mining sequences and stress states affect the individual stope performance (Heidarzadeh, et al., 2019). The main emphasis is put on the stope dimensioning first and follows with the stress sensitivity. The impact of mining sequence, different stopes types and undercutting concludes this chapter.

4.3.1 Stope height and length

As the span of most stope walls does increase when stope height is increased, the degree of instability will develop analogously. Perron (1996) analysed transverse stopes that were initially designed as 60 metres in height and 20 metres in width. The stopes had to be significantly shortened to reduce overbreak due to the unexpected surge of instability in the stope walls. The size reduction led to 30 metres tall and 20 metres wide longitudinal stopes instead.

The stope strike length is an additional parameter which is considered to cause overbreak. El Mouhabbis (2013) concluded that a strict correlation of increasing stope strike length and extra dilution is recognizable after investigating primary and secondary stopes in the Lapa Mine. Henning (2007) studied the effect of varying transverse stope strike length in different mining depths with rock mass having no tensile strength. The outcome of the study, shown in Figure 4.2, manifests a strong dependency on the stope strike length. The maximum difference in dilution density totals nearly one metre of overbreak within a size increment in length of 30 metres.

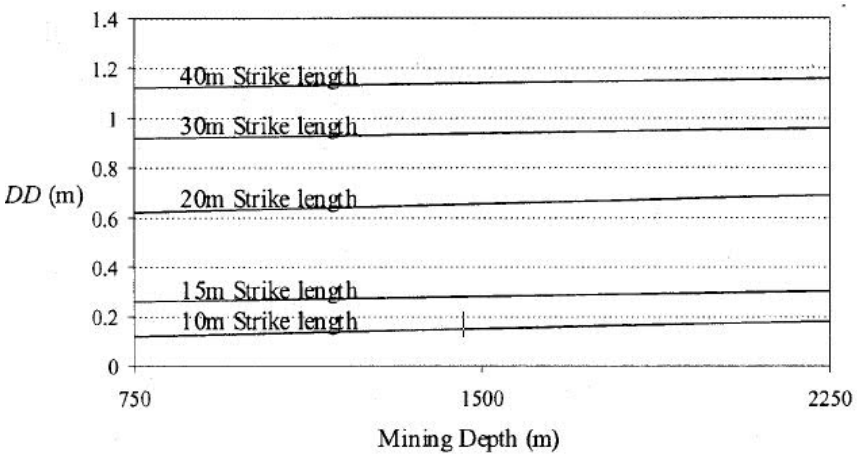

Figure 4.2: Anticipated dilution density (DD) for varying strike length and mining depths (after Henning (2007))

It is Henning and Mitri (2007) who studied the correlation of stope strike length and height for transverse stopes in blasthole stoping. Using numerical modelling, they found that the stopes which are shaped rectangular suffer less dilution compared to stopes with quadratic shapes (Figure 4.3). The stopes with the least length and greatest height are most favourable to produce little overbreak.

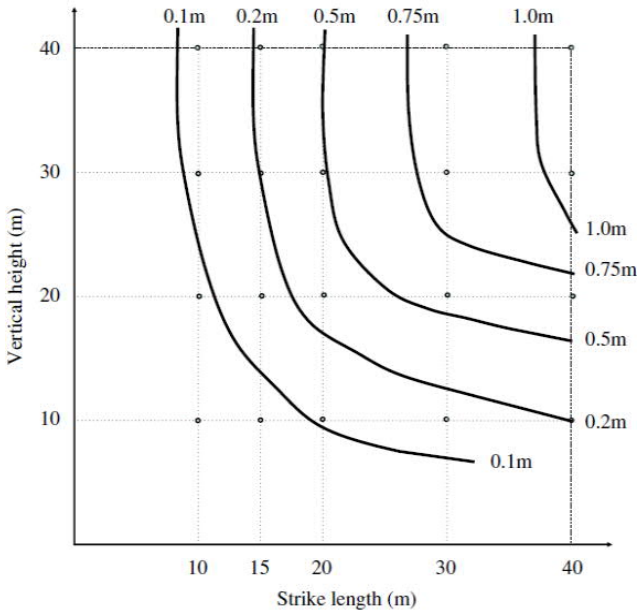

Figure 4.3: Dilution density prediction with varying stope height and strike length (after Henning & Mitri (2007))

It was again Henning and Mitri (2007) who analysed the correlation of stope overbreak and aspect ratio. The aspect ratio is the quotient of strike length and the true height of the stope. The result showed that tall stopes with short length or vice versa produce relatively little overbreak (Figure 4.4). Conversely, the greatest overbreak occurred in quadratic stopes.

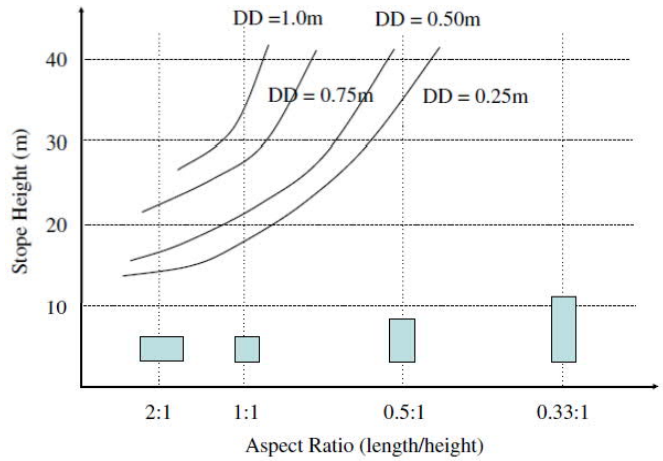

Figure 4.4: Anticipated dilution density regarding stope height and aspect ratio (after Henning & Mitri (2007))

4.3.2 Stope inclination

Similar to stope length and height, the stope inclination is of great importance regarding stability and minimisation of overbreak. The stope geometry dictates over favourable stress alignment and whether or not it will circumvent the opening. Yao et al. (1999) proposed that

stopes with near vertical geometry are less affected by external dilution compared to inclined stopes. The same tendency was proven by El Mouhabbis (2013) who found overbreak to increase by 33 % if the hanging wall dip is declined from 90 to 80 degrees. Stresses are redirected due to the shallower dip and gravity facilitates the release of displacements which causes overbreak.

Henning and Mitri (2007) examined occurring overbreak of various hanging wall angles under consideration of different stope strike lengths and heights. The study showed two distinct behaviours. The first result supports Yao et al. (1999) in their assumption that more overbreak is generated with a declining hanging wall angle. The second outcome has proven the strong correlation of hanging wall overbreak towards increasing stope strike length and height (Figure 4.5). The differences in dip angles become most apparent when exceeding the stope strike length of 20 metres. Interesting remains that the dip angle has an extensively larger influence on dilution in larger stope dimensions.

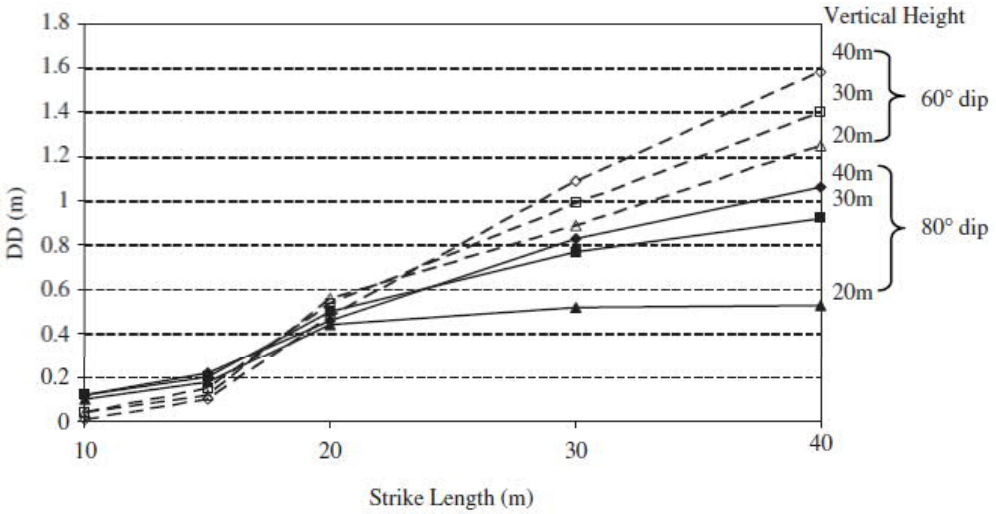

Figure 4.5: Hanging wall angle sensitivity on overbreak (after Henning & Mitri (2007))

4.3.3 Hydraulic radius

The hydraulic radius is described as the quotient of exposed surface area divided by its circumference. In combination with the modified stability number N', it is used when designing stopes with respect to their stability. In stopes with low geometric complexity, the hydraulic radius is found appropriate to predict stope stability (Stewart, 2005). However, the hydraulic radius becomes diminishingly important once the stope geometry becomes more complex. The complexity of a stope is predominantly dependent on the variation in hanging and footwall boundaries and the differences in dip angles (Henning, 2007). After comparing original plans with actual post-blast conditions, Germain et al. (1996) stated that the use of the hydraulic radius to indicate stope stability is inappropriate.

4.3.4 Stress state

Besides stope design parameters that allow adjustments, the stress conditions are a further decisive feature for stope planning. Dependent on the orientation of the in-situ stresses, the stopes can experience great relaxation zones in hanging and footwall. Relaxation zones are known as destressed zones (Clark, 1998). It was Clark (1998) and Wang (2004) who used

numerical modelling to investigate the relationship between the depth of relaxation zones, the associated overbreak and the hydraulic radius (Figure 4.6 and Figure 4.7).

The results were made on the assumption after Arjang (1991) that the major principal stress σ_1, the intermediate stress σ_2, and the minor stress σ_3, are set perpendicular to stope walls, in line with the stope strike, and parallel to dip, respectively. Potvin (1988) already concluded greater relaxation zones to happen along hanging and footwall if the major in-situ stress σ_1 is directed perpendicular to the stope walls. Both results underline the principal influence of hydraulic radius on relaxation zones as relaxation zones are major indicator for dilution (Clark, 1998; Wang, 2004). In particular, relaxation symptoms tend to increase with greater stress ratio K. The stress ratio is formulated in Equation (11) and expressed as the quotient of principal and intermediate stress. Wang (2004) has proven that larger stopes are more sensitive to greater relaxation zones and therefore, to dilution.

$$K = \frac{\sigma 1}{\sigma 2} = \frac{\sigma 1}{\sigma 3} \qquad \text{where } \sigma_2 = \sigma_3 \qquad (11)$$

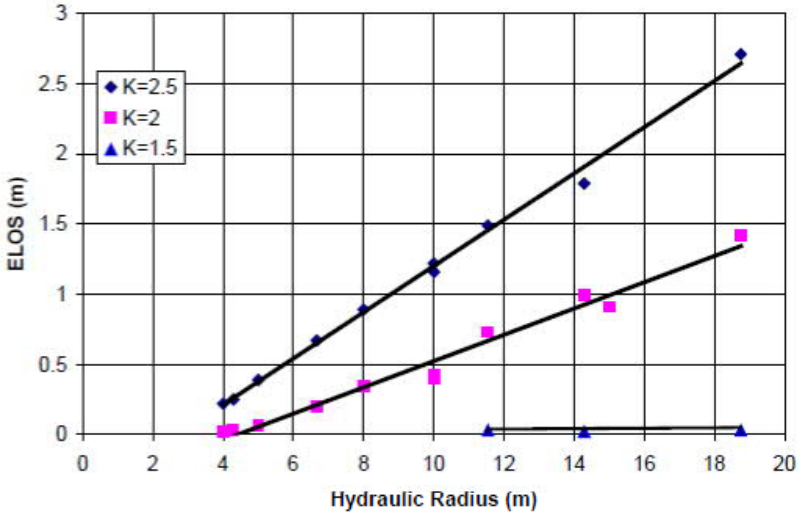

Figure 4.6: ELOS versus HR for different stress conditions K=1.5, K=2, K=2.5 (after Clark (1998,) from Wang (2004))

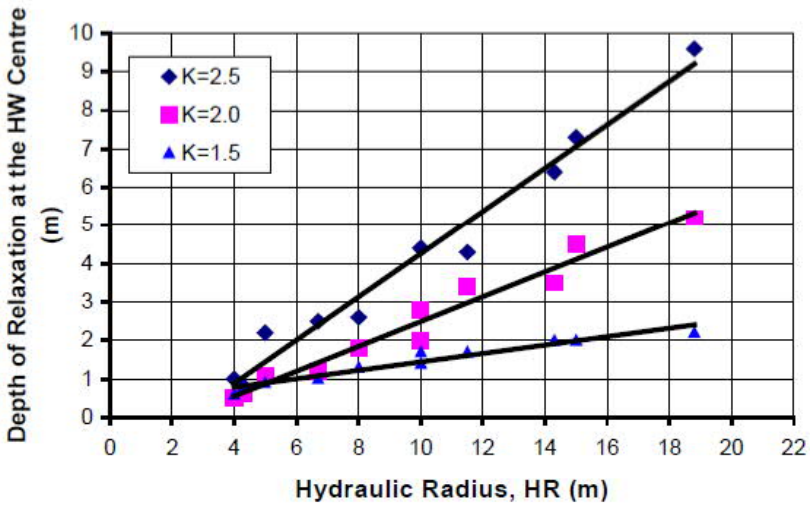

Figure 4.7: Relaxation depth versus HR with different stress ratio K (after Wang (2004))

Henning and Mitri (2007) conducted research on how pre-mining stresses affect stopes if σ_1 is oriented parallel or perpendicular to the sidewalls. Their research has shown that perpendicular stress alignments results in larger overbreak compared to parallel conditions (Figure 4.8). It was also observed that the impact of dip angle and stress conditions on overbreak are mainly associated in stopes which exceed 20 metres in length.

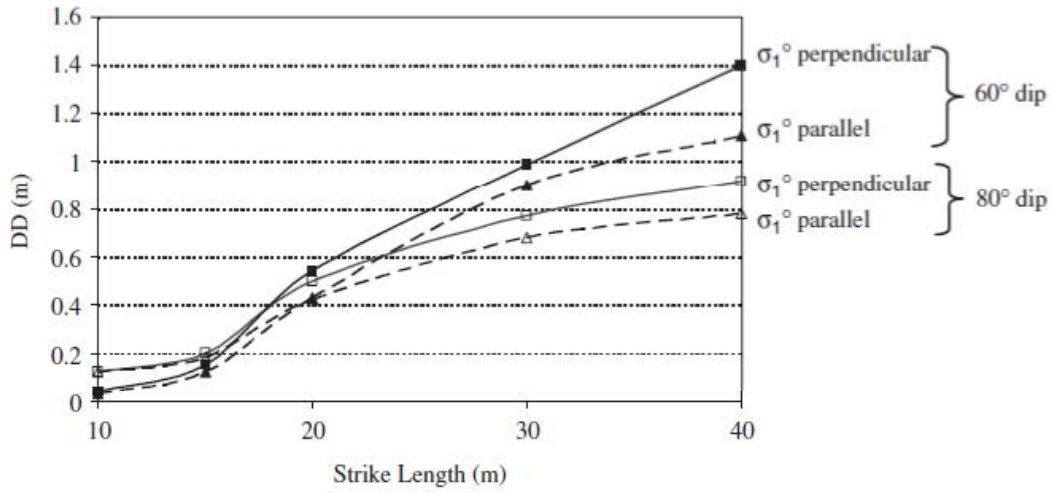

Figure 4.8: Impact of major principal stress orientation on overbreak (after Henning & Mitri (2007))

4.3.5 Mining sequence and stope type

When creating openings underground, stress directions are subject to re-alignment procedures (Villaescusa, 2004). The re-direction of stresses must be considered in the stoping sequence to prevent areas being mined which experience unfavourably concentrated stresses. Henning and Mitri (2007) have analysed the overbreak characteristic through a set of different transverse stopes with varying strike lengths (Figure 4.9). The stopes were

subdivided into three different primary stopes (P1, P2, P3) and two secondary stope types (S1, S2). The main difference between the primary and secondary stopes is the type of abutment adjacent to the stope walls. For primary stopes, ore or natural rock mass encapsulates the stope whereas for secondary stopes, the rock mass is partially or entirely replaced by backfill.

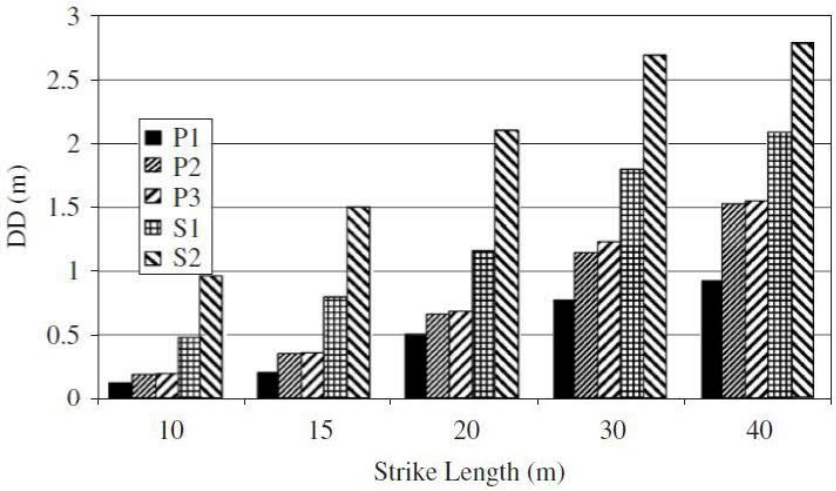

Figure 4.9: Overbreak associated with different stope types (after Henning & Mitri (2007))

The outcome of the numerical simulation concludes that primary stopes typically produce less overbreak than secondary stopes (Henning, 2007). In particular, the first sequentially extracted stope P1 showed the least overbreak whereas P2 and P3 showed great deviation from P1 but not amongst each other. Opposed to that, secondary stopes sustain more than twice the amount of overbreak than primary stopes. The secondary stopes showed overall the greatest overbreak potential with S2 being the stope in least competent conditions.

4.3.6 Undercutting

The stope undercutting is another factor that is known for its effect on enlarged overbreak (Villaescusa, 1998). On the one hand, undercutting helps to facilitate ore recovery. On the other hand, correlated wall instability and a higher grade of dilution from particular sidewalls impair the extraction (Germain & Hadjigeogiou, 1997). Wang (2004) states in his research that the degree of undercutting is directly linked to increments of relaxation zones in adjacent rock mass.

The Figure 4.10 shows a schematic illustration on how undercutting provokes additional sloughing due to increased stope wall instability. The original outline of the planned stope is heavily undercut by the bottom drift on the hanging wall side. Undercutting generally appears on the bottom drift of the stope when exceeding the width of the planned stope. The dotted black line illustrates the expected unstable zone which potentially lead to overbreak because of the undercutting. The green line represents the relaxation zone that is inevitably generated by extracting the stope even without undercutting. This common phenomenon in underground mining is subject to stress relocations due to adjacent open voids. The dashed red line shows and summarizes to what extent undercutting increases the relaxation zones. The original starting points of the relaxation zone (green) are shifted by the extent of the unstable zone (black) which provokes excessive overbreak.

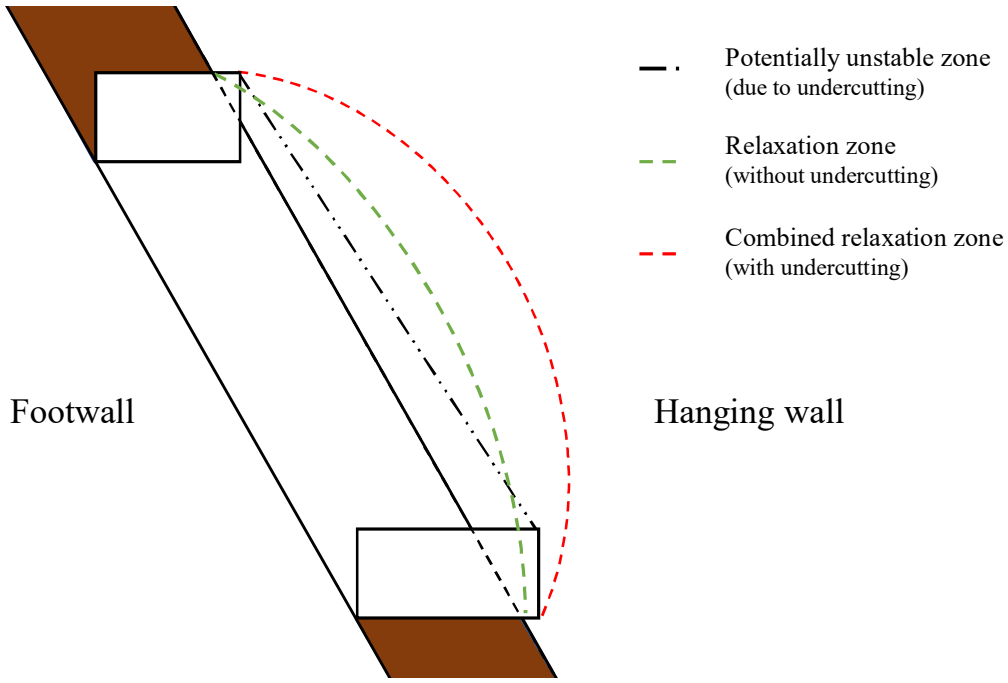

Figure 4.10: Illustrative scheme of undercutting effect on hanging wall stability (after Wang (2004), modified by Latta)

4.3.7 Others

Despite rock mass, stope design and blasting factors, few parameters such as the effect of time, backfill stability, fault intersections and cable bolting must be addressed as well. Suorineni (1998) examined the effect of fault zones crossing stope delineations in which multiple trends have been observed. Stopes that intersect fault zones behave more sensitive to unplanned dilution. This is due to the joint orientation and structural settings of the fault zone mass. The stopes show additionally greater overbreak if the fault zone is located in lower regions of the stope compared to fault zones intersecting near or close to roof areas.

The effect of time on the stability and dilution is also considered critical, especially for transverse stopes (Stewart, 2005). Clark (1998) used neural network analysis to prove the correlation of equivalent linear overbreak/sloughing (ELOS) and the stope life. Further, monthly scanning of open stopes proved that prolonged open space exposure is likely to promote dilution. The surveys observed progressive size increments in the stopes which are caused by gradual cavity of wall rock mass (Capes, 2009).

Another dilution potential is associated with backfill procedures. Backfill is typically deemed necessary in most open hole stoping operations due to its capability to prevent stope collapses. However, the backfilled stopes provide less strength properties compared to original rock mass (Abdellah & Ali, 2017). In general, backfill is subject to blast-induced and mining provoked stresses as well as overburden loading. Combined with unfavourable stope designs, an overload in stresses can lead to instability of backfill and increase the instability of stope walls (Badge, et al., 2011).

5 The Kylylahti mine

The Kylylahti operation is a multi-commodity underground mine bearing copper, gold, zinc as well as nickel and cobalt and to some extent silver. It is located in North Karelia in Eastern Finland and was discovered by Outokumpu Mining in 1984. In October 2014, Boliden acquired the operation from Altona Mining Ltd. and is operating the mine ever since. With a life of mine of 8.5 years, the production is going to cease in autumn this year. The mine is located in close proximity to the small village Polvijärvi and in reachable distance to the larger city Joensuu as shown in Figure 5.1. The corresponding processing plant is located roughly 40 km off-site in Luikonlahti. The processed concentrate is divisible into gravity gold, copper-gold as well as zinc and cobalt-nickel concentrate. Zinc is further processed in Kokkola with nickel and cobalt concentrates being transported to Kokkola harbour and shipped to external customer. The other concentrates are purified in Harjavalta.

Figure 5.1: Location of Kylylahti mine, processing plant and corresponding smelter (after DFAT (2020), modified by Latta)

The structure of this chapter is subdivided into three sections and starts with a brief explanation of the geological setting. Subsequently, the mineralisation is discussed with view on potentially interesting parameters for the later stope reconciliation. The description of the mining operation concludes this chapter with special emphasis on the mining method, the sequencing and the backfill procedure.

5.1 Regional setting

The Kylylahti mineral deposit is part of an agglomeration of deposits, known as Outokumpu mining camp. The agglomeration is situated in Eastern Finland and found amid the North Karelia Schist Belt (NKSB). The NKSB is predominantly encapsulated in the Paleoproterozoic domain originated after the Svecofennian orogeny in southwest direction whereas in contrast to that, the Archaean Karelian craton forms the borderline for the northeast region of the NKSB (Kontinen, 2005).

In general, the NKSB is argued to be distinguishable into two main tectonic stratigraphic units. The older units Sariola and Jatuli are understood to have formed approximately 2.5 – 2.0 Ga ago. Building upon Archaean gneissic regions, they mostly persist of metasedimentary deposits within cratonic to epicratonic characteristics (Kohonen & Marmo, 1992). The other unit, however, is known as Kaleva and is slightly younger dating back to 2.0 – 1.9 Ga ago. Further division can be made into upper and lower Kaleva, whereas Kylylahti is comprised of the upper Kaleva in all directions (Lahtinen, et al., 2010). Generally, the Kaleva domain is represented as sequential deep water turbidite deposits. The main difference between upper and lower Kaleva is conceived to be the origin of mass, namely allochthonous and autochthonous, respectively (Lahtinen, et al., 2010).

5.2 Local setting

The Kylylahti deposit is a multi-metal bearing deposit located in Eastern Finland. The deposit is located near the Kylylahti ultramafic domain, which is also considered a mostly serpentinite containing assembly (Kontinen, 2005). The orebody extends to approximately 1.5 km and consists of multiple lenses with strike into North-North-East (NNE) or South-South-West (SSW) vice versa (Malmberg & Svensson, 2019). The plunge of the deposit is mostly sub-vertical and adheres to the two different domains, called Wallaby and Wombat. Therefore, the plunge in the shallower region (Wallaby) is defined as roughly 25 degrees whereas the angle increases with depth resulting into 50 degrees for the Wombat orebody (Peskens, 2013).

As explained, Kylylahti is greatly comprised of the upper Kaleva formation. The hanging wall of Kylylahti, determined to be west from the orebody, is mostly made up of Outokumpu assemblage rocks. Typically, these rocks are originally metaperidotitic ophiolites of which serpentinite is a major component (Kontinen, 2005). Besides accumulating serpentinite assemblages, a remarkable quantity of rock alteration can be found such as quartz-sulphide, talc-carbonate and skarn rocks (Kontinen, 2005).

Moreover, the main rock mass of the deposit is considered mica gneiss and shown in the Figure 5.2. Other than the relatively competent material in the hanging wall, the footwall is extensively located in sharp contact to weak rock mass. Hence, graphite rich black schist with extensive folding in areas of the Gap region amounts for the largest quantity whereas foliated talc enriched rock mass intersects the black schist in lower levels (Kekki, 2020a).

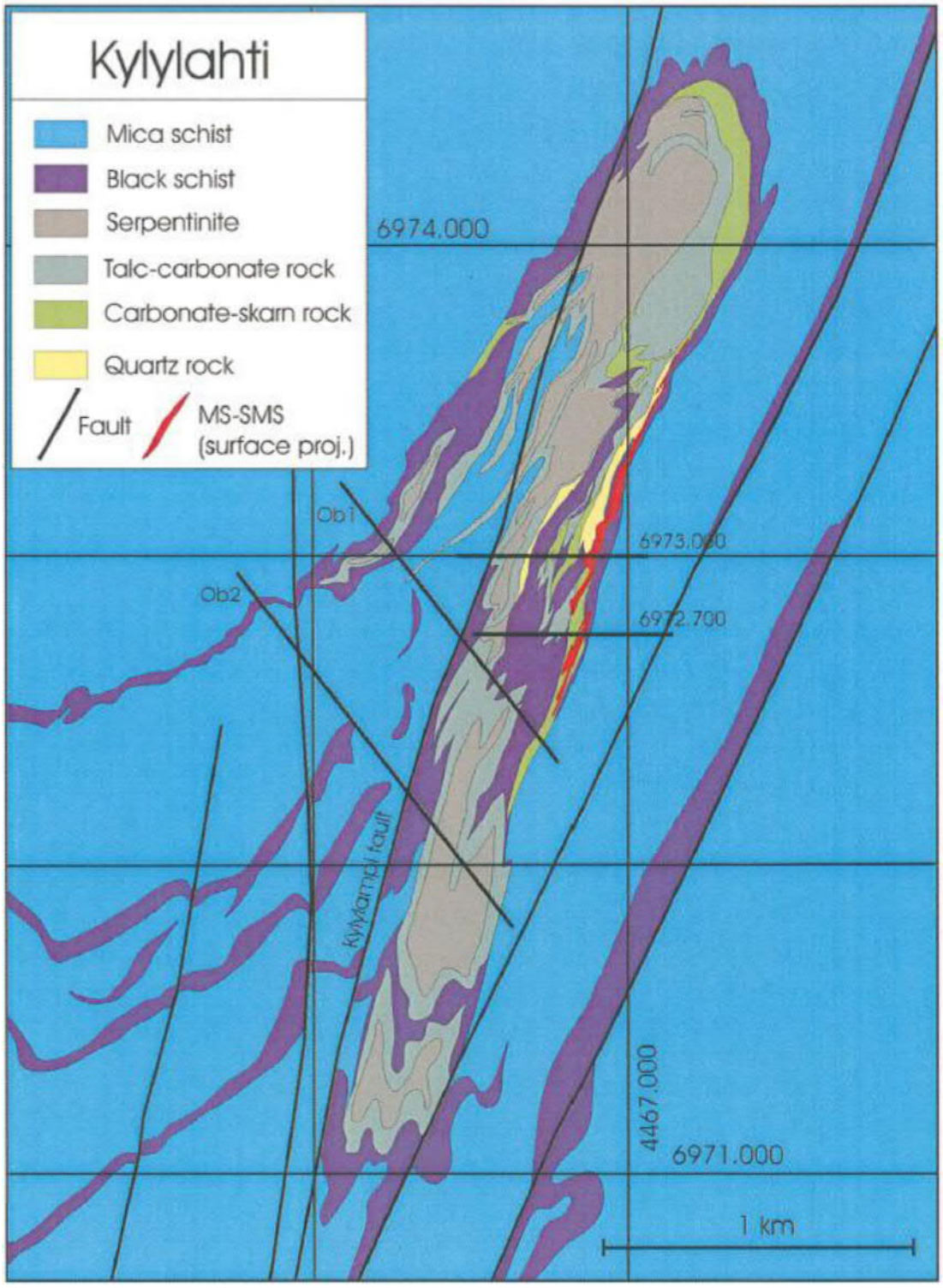

Figure 5.2: Kylylahti complex in cross-section view with local geological rock mass (after Kontinen (2005))

5.3 Mineralisation

This chapter discusses the general mineralisation. The deposit allows the distinction into upper and lower complexes, namely Wallaby and Wombat, respectively. The Gap zone was originally conceived to have a break between the two orebodies. More thorough exploration identified that the ore does transition continuously in this zone but to a lesser extent. Ever since, the Gap refers to all non-Wombat massive ore lenses below the level 300. The narrow transition zone from the Wallaby into the Wombat orebody is made visible in the Figure 5.3. Especially for stope design, the area is relatively challenging and demands for more complex stopes.

Because Kylylahti is part of the Outokumpu assemblage or the Outokumpu mining camp, it is mainly characterized by sulphide mineralisation. These types are typically known as copper-cobalt-zinc containing (Kontinen, 2005). The mineralisation is mainly interpreted as semi massive (SMS) and massive (MS) sulphide lenses and sulphide disseminations (DISS) (Peskens, 2013). The main difference in SMS and MS lenses is made concerning their sulphide content. Any ore with sulphide contents of 25 – 50 % is classified as SMS opposed to ore that is greater in sulphide content than 50 % which is categorized as MS. In contrast to SMS which are located east, the DISS lenses happen to be diversified across the hanging wall of the orebody complex (Kekki, 2020a).

Representing the three major sections which define the orebody structure, strike and plunge, the SMS mineralisation varies greatly in thickness ranging from five metres up to 50 metres (Malmberg & Svensson, 2019). The Figure 5.3 illustrates the SMS and MS lenses across Kylylahti applying different colours to indicate the allocation into either Wallaby or Wombat orebody. The gradually increasing thickness, similarly to the orebody complexity in the Gap, is considered another challenge for the mining method which is explained in chapter 5.5. The SMS and MS domains show overall sulphide contents of 25 % to 60 % with pyrrhotite, chalcopyrite and pyrite as main minerals. Additionally, pentlandite, sphalerite, cobaltite, linnaeite-polydymite and gold occur to a lesser extent. Interesting remains, that cobalt which accumulates in the lattice of SMS pyrite shows great economic potential in theory (Kekki, 2020a). Due to the current lack of cost-effective processing techniques, the recovered Co-Ni concentrate is stored and preserved at the Luikonlahti tailings pond for future treatment (Suominen, 2020).

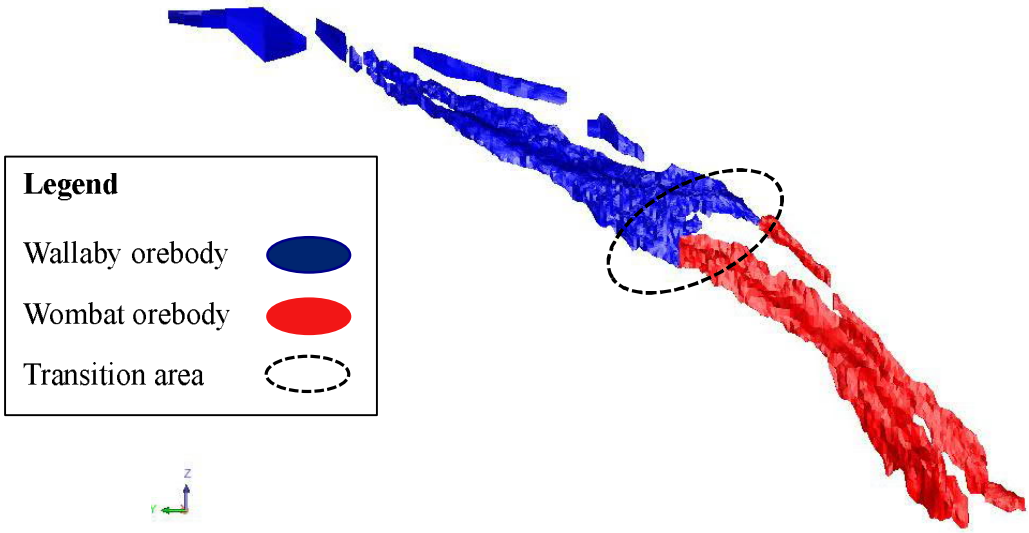

Figure 5.3: Semi-massive massive ore domains of the Kylylahti deposit (looking east) per orebody allocation

In comparison, the disseminated lenses show explicitly lesser sulphide content ranging from 5 % to 25 % only (Malmberg & Svensson, 2019). Among the DISS lenses, the categorisation into copper enriched and cobalt enriched dissemination is made. Both types are economically valuable regarding their gold containing lenses. Subsequently, the Figure 5.4 depicts the location of copper, cobalt and nickel disseminated lenses against the SMS and MS domains.

Figure 5.4: DISS mineralisation (left) and in contrast to the SMS-MS domains (brown) on the right

The major difference among SMS and DISS lenses remains in the economically feasible extraction and concentration of zinc over nickel and cobalt (Malmberg & Svensson, 2019). The Table 5.1 comprises the relevant information on ore types and correlating ore lenses. Generally, the ore types in Kylylahti are separated into three classification with room for further mineralogical interpretation (Kekki, 2020a). Unlike the SMS domain which contains mostly ore type M2, the DISS domains carry various ore types of which M4 and M5 are considered as tier one ore category. Another paramount ore type classifier is understood to be the sulphide content due to the explicit sensitivity of the processing stage to the sulphide grades and the pyrite content. M4 is the most beneficial ore type in terms of recovery. The sole occurrence of M4 per stope was relatively rare in the early production stage and the ore boundaries were difficult to estimate. Nowadays, the separation of M2 over M4 and M5 is typically sharp (Kekki, 2020a). Consequently, M4 is most abundantly found in a mixture with M5.

Table 5.1: Overview of ore type classification in Kylylahti (after Malmberg & Svenson (2019), modified by Latta)

Ore types in Kylylahti			
Category	**Classification**	**Concentrate produced**	**Specification**
M2	Semi-massive massive sulphides (SMS) and (MS)	- Cu concentrate, Cu-Au - Au-gravity concentrate - Zn concentrate	- Only Zn concentrate - Highest sulphide content
M4	Disseminated sulphides (DISS)	- Cu concentrate, Cu-Au - Au-gravity concentrate - Ni-Co concentrate	- Sulphide content < 10 % (Pyrite/Pyrrhotite ratio)
M5	Disseminated sulphides (DISS)	- Cu concentrate, Cu-Au - Au-gravity concentrate - Ni-Co concentrate	- Sulphide content > 10 % (Pyrite/Pyrrhotite ratio)

The Cu- and Co-enriched domains are particularly of interest as they are mined for their Ni-Co ore types. The Ni-Co ore types are mainly recovered from pentlandite and the relatively rarely occurring linnaeite-polydymite (Kekki, 2020a). In contrast to the moderately complex processing of cobalt and nickel from pyrite, the Ni-Co from disseminated zones is comparatively easy to process with conventional flotation (Suominen, 2020). For further illustration, the Figure 5.5 presents a mineral overview of the Kylylahti underground operation.

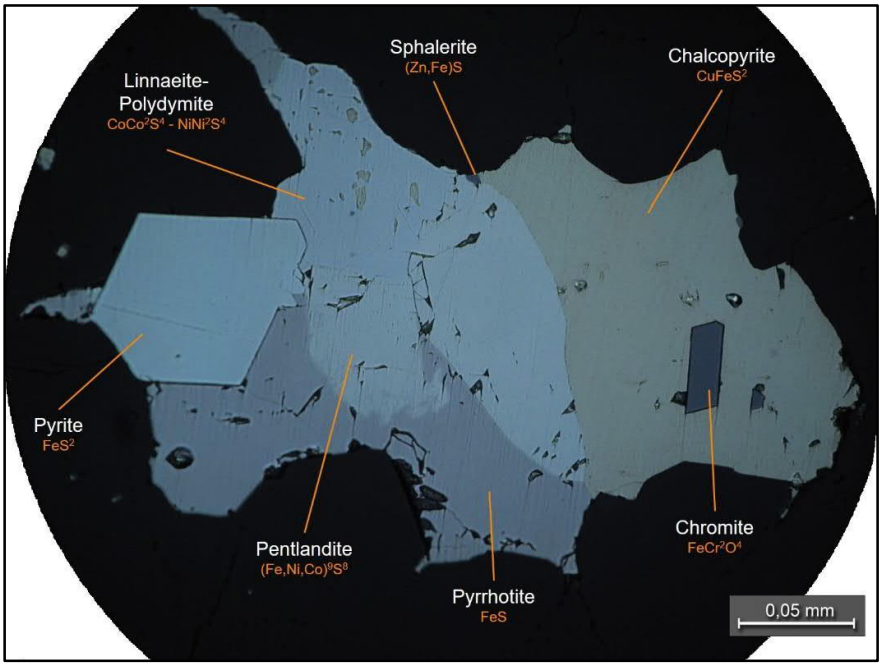

Figure 5.5: Single sulphide grain from Kylylahti consisting of multiple different minerals (after Kekki (2020b))

5.4 Geotechnical properties of rock mass

It must be noted that the footwall of SMS and MS domains is extensively bordered by black schist and in small areas by talc zones whereas the DISS zones are in relatively competent host rock such as quartz rocks, carbonite rocks and tremolite skarn (Peskens, 2013). The footwall in Kylylahti mainly consist of metasedimentary rocks such as black schist and mica schist (SRK Consulting, 2007). In contrast, the hanging wall comprises of ultramafics and cemented rocks which are shown in Table 5.2. The instability because of the black schist and talc zones is still prominent although the main rock types demonstrate fair to high intact rock strengths.

Table 5.2: General overview of rock mass properties in Kylylahti (after SRK Consulting (2007), modified by Latta)

General overview of rock mass properties in Kylylahti			
Main rock type	**Minor type**	**Intact rock strength [MPa]**	**Rock properties**
Sediments	- Black schist - Mica schist	> 120	- Generally high intact rock strength - Accommodates lots of structural features - Mostly graphitic bands
Ultramafics	- Serpentinite - Soapstone	115*	- Serpentinites are massive with few structures - Ranges from competent to extremely weak
Cemented rocks	- Carbonate - Skarn - Quartz-rock - Ore	> 100	- Massive with few structures - Ore zones comprise mixture of carbonate-skarn-quartz rock - Massive character of ore zone

Soapstone is inherently originated with talc schist and chlorite schists that are considered a concern. The intact rock strength for ultramafics accounts for the serpentinite only. Material such as talcose shows very weak intact rock strength with roughly 37 MPa. The contacts between black schist and ultramafic zones are a further concern to mining. Because these zones can be characterised as either relatively competent or very brittle, they demonstrate a certain unpredictability in rock mass behaviour. The cemented rocks incorporate the semi-massive (SMS) and massive (MS) sulphide lenses as well as the disseminated ore lenses. They have overall high intact rock strength and only low potential of structural formations which makes them the most competent material in Kylylahti. (SRK Consulting, 2007)

5.5 Mining method

Due to the rather tabular nature of the orebody and the sub-vertical inclination, the mining production commences with longhole open stoping (Malmberg & Svensson, 2019). The thickness of the orebody varies significantly over the strike direction which requires different mining approaches. The production results from 2019 (Table 5.3) have been achieved with a combination of longitudinal and transverse bench stoping. Longitudinal bench stoping has contributed the majority of the production with 16 completed stopes and three incomplete stopes transitioning into the year 2020. Only four transverse stopes were completed in the same timeframe. Nevertheless, transverse stopes make up for roughly a fifth of the production which is explainable by comparing stope dimensions.

Table 5.3: Production numbers of the Kylylahti operation from 2019 (after Malmberg & Svenson (2019))

Production 2019						
	Tonnage [kt]	**Cu [%]**	**Au [g/t]**	**Zn [%]**	**Ni [%]**	**Co [%]**
Mined	681	0.76	0.88	0.37	0.23	0.18
Milled	716	0.74	0.86	0.35	0.23	0.18

5.5.1 Longitudinal stoping

Longitudinal stopes account for the majority in the Wallaby orebody. But longitudinal stopes (LBS) find further application in narrow zones amid the Wombat domain which contains most of the transverse stopes. Longitudinal stopes are mined sequentially along the orebody on the respective production drift (Malmberg & Svensson, 2019). In contrast, the general mining sequence is understood to commence from the northern end of the domain upwards to assure stability and improve backfill handling. This minimises the need for horizontal ore pillars. The mining sequence can also start from the south towards north if ore pillars exist already (Malmberg, 2020a).

Kylylahti operates longhole drill rigs as drilling equipment with the option of upwards and downwards fan drilling (Peskens, 2013). Emulsion is used as explosive type in combination with electronic detonators. Impulse detonators are utilised in minor stopes or small stope blasts only (Malmberg, 2020a). The production drift is set to be five metres wide leaving possibilities to further increments if stope design requires larger drift dimensions. The main reasons for wider drifts are minimizing ore loss and additional support for upper drifts which results in increased safety and minimized overbreak (Malmberg, 2020a). Requirements for greater bottom sills are imposed by wider stope delineation or drilling equipment limitations. The bottom sill width for longitudinal stopes averages roughly eight metres and must provide sufficient spacing for loading equipment e.g. LHD loader to access the blasted stope (Malmberg, 2020a). The vertical drift spacing for longitudinal and transverse stoping is set to be 30 metres.

The Figure 5.6 depicts a typical mining sequence of longitudinal stopes with the corresponding backfill method. The stope number two is filled with waste rock only because it remains as the last stope on the particular level (Malmberg & Svensson, 2019). Commonly, 10 to 12 metres of the slot raise are initially blasted upwards to create open space to blast into (Malmberg, 2020a). The slot raise is highlighted in blue in stope number five. After blasting the first 10 to 12 metres upwards, the remaining metres are drilled downwards and blasted sequentially in five metres intervals. The last blast of the slot raise is then initiated with the surrounding blast rings to commence with the production blasting.

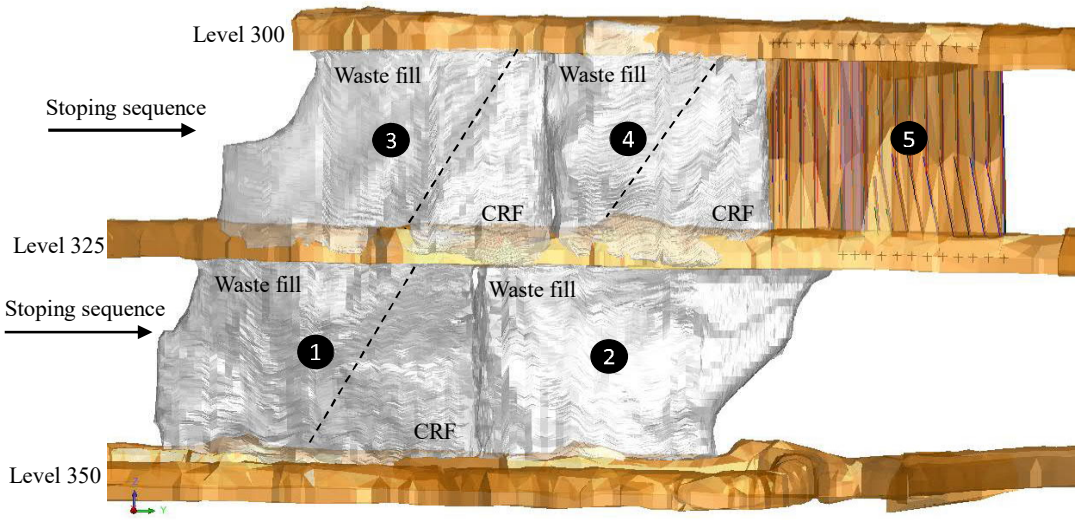

Figure 5.6: Schematic illustration of the longitudinal mining sequence (looking west) (after Malmberg & Svensson (2019), modified by Latta)

Once mucking of material is ceased, the stope is backfilled using a combination of unsorted waste and cemented rock fill (CRF). Dumping of backfill is executed from the upper sill of the respective stope. Due to safety obligations, trucks can only access the dumping area if the CMS survey proofs stable and secure ground conditions to drift and personnel (Lukkari, 2020). In closest vicinity to the adjacent stope, CRF is used to create sufficiently backfilled stope walls for the next stope blast as shown in Figure 5.6. The usual requirements for CRF regarding uniaxial compressive strength (UCS) is 2 MPa (Markström, 2019) which has never been properly tested and is rather taken as a suggestion (Malmberg, 2020a). The remaining void of the mucked-out stopes is then filled with unsorted waste rock.

5.5.2 Transverse stoping

Transverse bench stoping (TBS) is heavily applied as more than 50 % of the Wombat domain exceeds 20 metres in thickness (Peskens, 2013). The transverse stopes normally consist of primary and secondary stopes. The primary stopes are commonly designed to be 10 metres in width whereas secondary stopes are slightly wider with 15 metres to minimise costs from CRF (Malmberg & Svensson, 2019).

The production drifts are driven perpendicular towards the orebody with greater width for primary transverse stopes. Primary stopes are accessed by 10 metres wide production drifts which provide sufficient working space for longhole drill rigs to apply parallel drilling. The secondary production drifts are driven roughly five metres wide because fan-shaped drilling is required (Malmberg, 2020a). For primary and secondary stoping, upwards and downwards drilling is utilised using emulsion explosives ANFO and electronic detonators for blasting. The blasting sequence is analogous to longitudinal bench stoping. It includes the initial slot raise for creating open void and the consecutive blasting pattern starting at the slot raise with the surrounding blast rings.

When the primary stope has been drilled, blasted and mucked out, cemented rock fill (CRF) is used to fill up the open void in order to assure stability for adjacent secondary stopes. Secondary stopes are typically located between two CRF backfills. Due to the increased cost of CRF over waste rock fill and the larger dimensions of secondary stopes, it suffices to apply waste rock fill only in secondary stopes (Malmberg, 2020a).

Figure 5.7 illustrates how transverse bench stoping is conducted in Kylylahti. The numeration suggests the extraction sequence on the particular level only. However, the real mining sequence is illustrated later in Figure 5.9. The hardening time of the CRF can total up to a month for longitudinal and two month for transverse stopes before the CRF can be considered safe and stable (Markström, 2019).

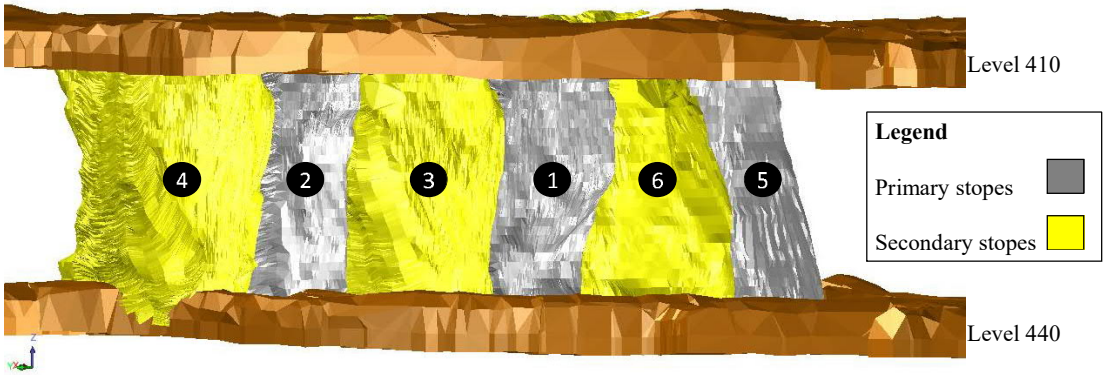

Figure 5.7: Transverse stoping sequence as per level (after Malmberg & Svensson (2019), modified by Latta)

Transverse stopes conform with the general mining sequence beginning in relative north of the production drift and do commence upwards. The generic 1-3-5 approach is used for transverse stoping and highlighted in the Figure 5.8. In this pattern, the primary stopes are determined to be 10 metres wide. Secondary stopes are defined 50 % wider resulting in 15 metres (Ghasemi, 2012). The universal trend of this sequence begins mid-centred and commences bottom-up until two primary stopes have been mined out. Stability assurance and proper stress handling are the main reasons for that. When the third step has been achieved, the stope sequence evolves lateral across the orebody with primary stopes only. As soon as the newly developed pillars have reached two stacked up stopes, the first secondary stopes in between the primary stopes can be mined out. In the meantime, CRF backfill has hardened and provides sufficient strength. Simultaneously, the next primary pillars to the horizontal left and right are mined analogously.

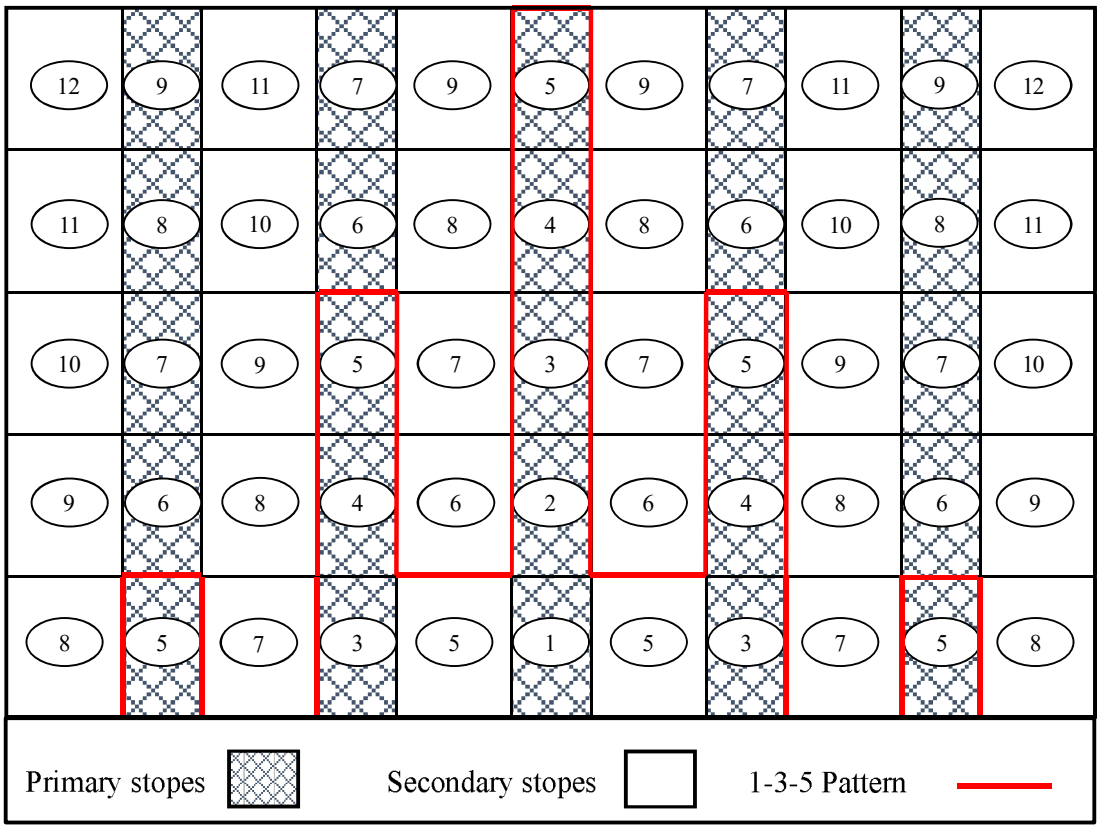

Figure 5.8: Typical 1-3-5 pattern in transverse open stoping (after Ghasemi (2012))

The 1-3-5 sequence assumes a tabular orebody with no dipping in the specific section. However, stoping is yet closely related to drift development and mill requirements which may impose certain ore types to be mined first. This can lead to deviation from original mine plans. In case of the Kylylahti underground operation, the sequence does not entirely comply with the simplified 1-3-5 approach (Malmberg, 2020a). The Figure 5.9 depicts the first transverse stopes that are mined in the Wombat orebody beginning in level 410. The orebody delineation is shown in yellow. Additional longitudinal stopes in the north are used for relatively narrow ore abundances. Other stopes marked with X do not contribute to this pattern as they are planned to be mined far later in the operation process.

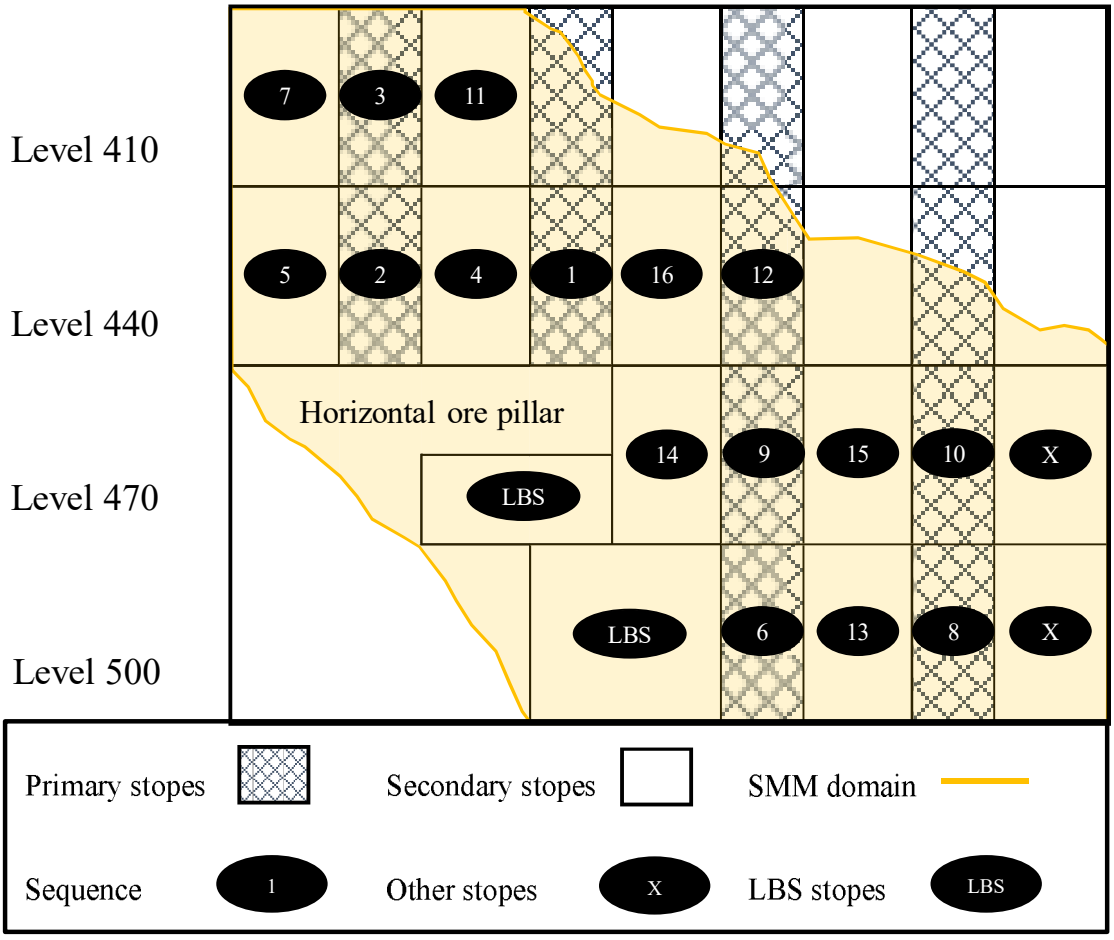

Figure 5.9: Mining sequence in upper Wombat orebody in Kylylahti

The stope sequencing emphasises to follow the 1-3-5 method as closely as applicable. But due to the plunge of almost 50 degrees, complications and deviations are inevitably. Another factor to consider whilst planning the sequence layout is the exposure of more than one secondary stope. Assuming the adjacent stopes 13 and 14 are both empty and not backfilled yet, the CRF backfills of the stopes 6 and 9 are likely to collapse into the open voids. If the stope number 16 and 7 are both open, the secondary stope in between acts as buffer and prevents any collapses of abutted CRF backfills. Greater deviations in sequence are found in the lower regions of the Wombat orebody because of stope design changes. Due to multiple ore lens intersections, the majority of stopes had to be split up into smaller fractions (Malmberg, 2020a). The result amounted for an augmented selectivity of different ore types but is followed by increasing operational complexity.

6 Database information

The mine production in Kylylahti is expected to end in Autumn 2020. Valuable data about the stope framework is gathered over the course of eight years of production. The main purpose of this chapter is to introduce the data information which the thesis is built upon. For the reason of ongoing production parallel to this study, the data encompasses mined stopes until the first quarter of 2020. The data is obtained by an assemblage of different methods. It includes information of the planning procedure and information of internal reports on host rock composition, structural interpretations and numerical stress modelling.

The comprehensive dataset is subdivided into three categories and includes the general stope settings, the design parameters and the performance attributes. Henning (2007) postulates a definition for stope datasets, which is found convenient to this study in a modified approach (Figure 6.1). The stope settings mainly focus on the stope location and environment. The location comprehends the orebody and drift level placement. The time of extraction and associated ore types complete the stope environment. Additional design parameters comprise, amongst others, the stope height, length, width and inclination. Stope performance attributes are defined as the dilution, ore loss and recovery as well as CRF intrusion.

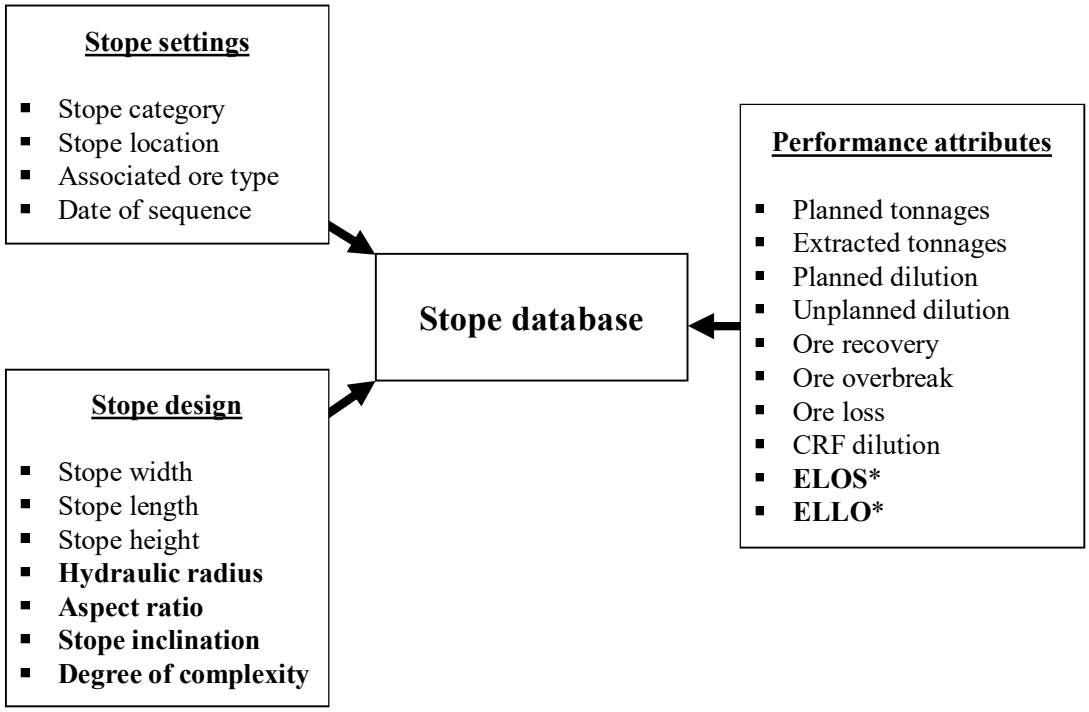

Figure 6.1: Stope database compilation (after Henning (2007), modified by Latta)

The attributes and factors highlighted bold have been independently gathered in close collaboration with the respective department. Data marked with additional symbols has been obtained by individual work with Surpac which subchapter 6.3 elaborates on.

6.1 General data overview

The stope framework of the Kylylahti underground operation comprises more than 170 stopes mined over the life of mine. In particular, 167 stopes have been analysed by using the Cavity Monitoring System (CMS). First mined stopes could not be examined due to lacking CMS application. Seven stopes were excluded from the set as they remain inappropriate for comparison due to individual issues. The analysed stopes are separated according to their settings as described in Figure 6.1. Further distinction is made between longitudinal and transverse stopes regarding their orebody location. The orebodies Wallaby and Wombat consists of 99 longitudinal stopes in total. As illustrated in Figure 6.2, the deeper Wombat orebody shows a greater population with 65 longitudinal stopes compared to 34 stopes in Wallaby.

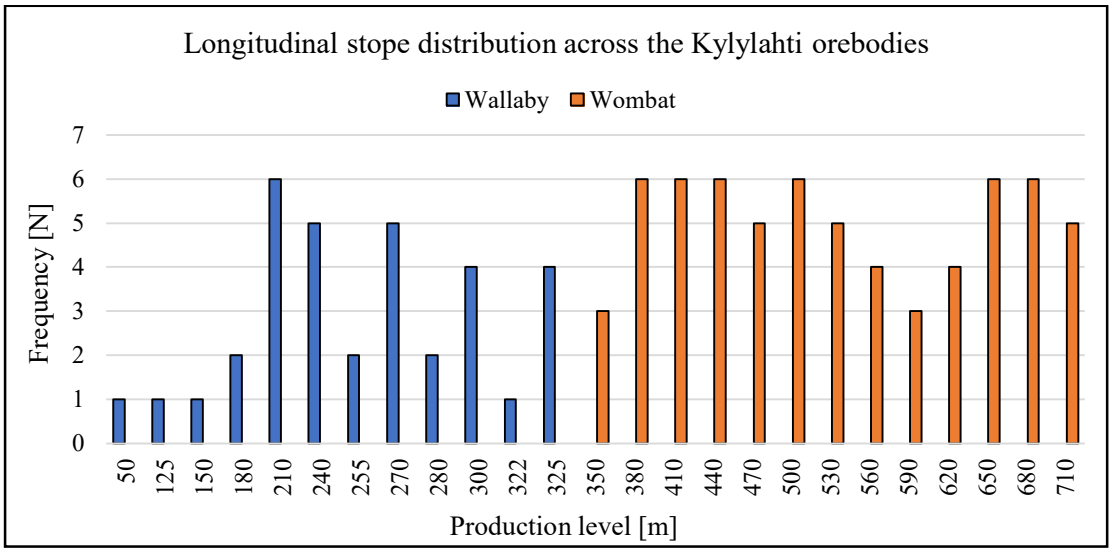

Figure 6.2: Longitudinal stope distribution across the Kylylahti orebodies

The data further consists of 68 transverse stopes of which 35 are considered primary and 33 are mined as secondary stopes. Transverse stopes are overly located within the Wombat orebody except for two stopes in level 210. The Figure 6.3 shows the frequency of transverse stopes per orebody. Because the orebody thickness reaches its peak in the levels 500 – 560, the greatest accumulation of transverse stopes is in the levels 500 – 560 as well.

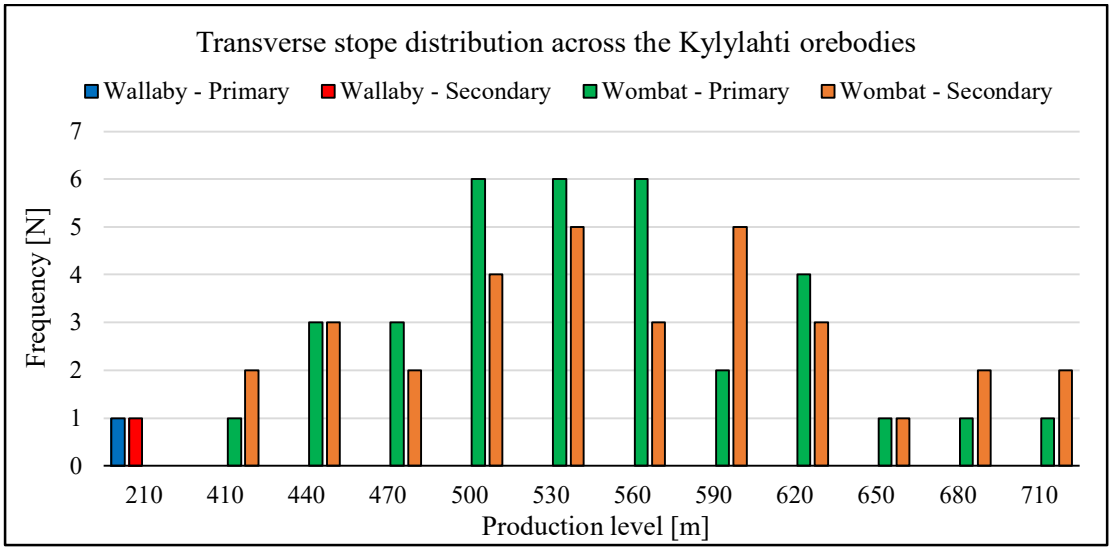

Figure 6.3: Transverse stope distribution across the Kylylahti orebodies

6.2 Stope geometry

One of the major sections of the database comprises geometrical features of the stopes in Kylylahti. The distinction is made into longitudinal and transverse stopes to account for both individually. Presented data comprehends the stope dimensions, the hydraulic radius and aspect ratio as well as the stope inclination and the degree of complexity.

6.2.1 Longitudinal stopes

Longitudinal stopes represent the majority of stopes in Kylylahti. As the Wallaby orebody remains relatively narrow and consists of longitudinal stopes only, a fair number of narrow stopes exists. As shown in Figure 6.4, the mode of longitudinal stope width is found to be six metres whereas the average and median values are eight and seven metres, respectively. The median and average value are comparative for the Wombat orebody despite the differences in orebody thickness.

Figure 6.4: Width frequency of longitudinal stopes

The length of the stopes is closely related to the prevalent ore domain characteristics because longitudinal stopes naturally extend along the orebody. The Figure 6.5 shows length variations ranging from 11 metres to over 50 metres at most. A bimodal distribution of stope lengths can be recognized with the mode in the 26 – 30 metres interval. The median length value in the Wombat orebody is 30 metres in comparison to 37 metres in Wallaby. Average values do not differ much. This is mainly due to longitudinal stopes which are used in short and narrow drift ends in Wombat.

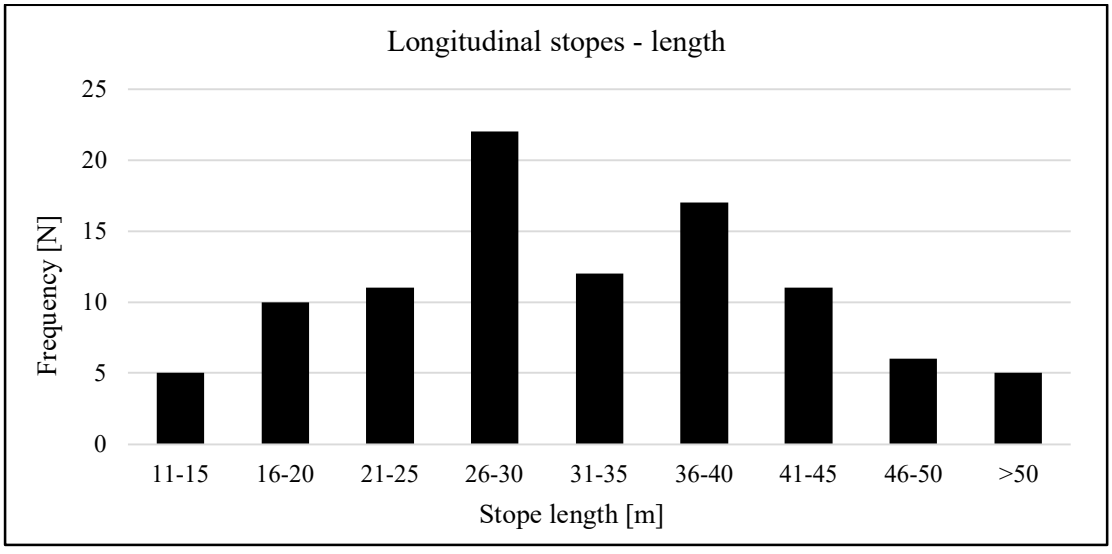

Figure 6.5: Length frequency of longitudinal stopes

The majority of the longitudinal stopes have heights that fall into the 21-25 metres interval (Figure 6.6). This is due to the 30 metres drift spacing and the deducted drift height of 5 metres. No differences in average and median values are found among the different

orebodies. The shorter stopes are mostly applied in tight drift ends which explains their reduced stope height. Other longitudinal stopes are operated as upper hand stopes only which explains the occurrence of stopes that are shorter than 20 metres.

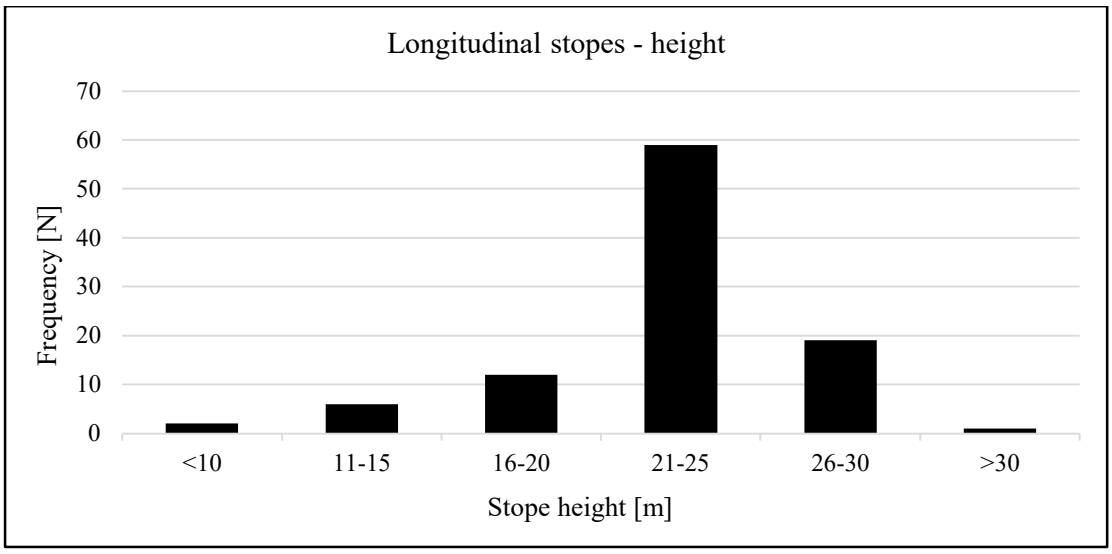

Figure 6.6: Height frequency of longitudinal stopes

For the stope inclination, the distinction is made between footwall (FW) and hanging wall (HW) dip. It is decided to classify dip angles into intervals of five degrees as shown in Figure 6.7. The histogram shows a normal distribution. The interval of 76 to 80 degrees is the most dominant for the footwall wall angle whereas the most prevalent hanging wall angle peaks in the 71 to 75 degrees interval. Out of 99 longitudinal stopes, 41 stopes have their hanging wall situated in the western sidewall. The western sidewall is also referred to as regional hanging wall. The distinction of western and eastern sidewall is useful because it helps to identify how certain rock types behave if they are located in the stope hanging or footwall. The properties of the rock types are explained in chapter 5.4. Of the 41 stopes, 16 stopes are located in Wallaby with 25 stopes situated in the Wombat orebody. Additional figures pertaining to the degree of complexity, the hydraulic radius and the aspect ratio are enclosed in Appendix 2.

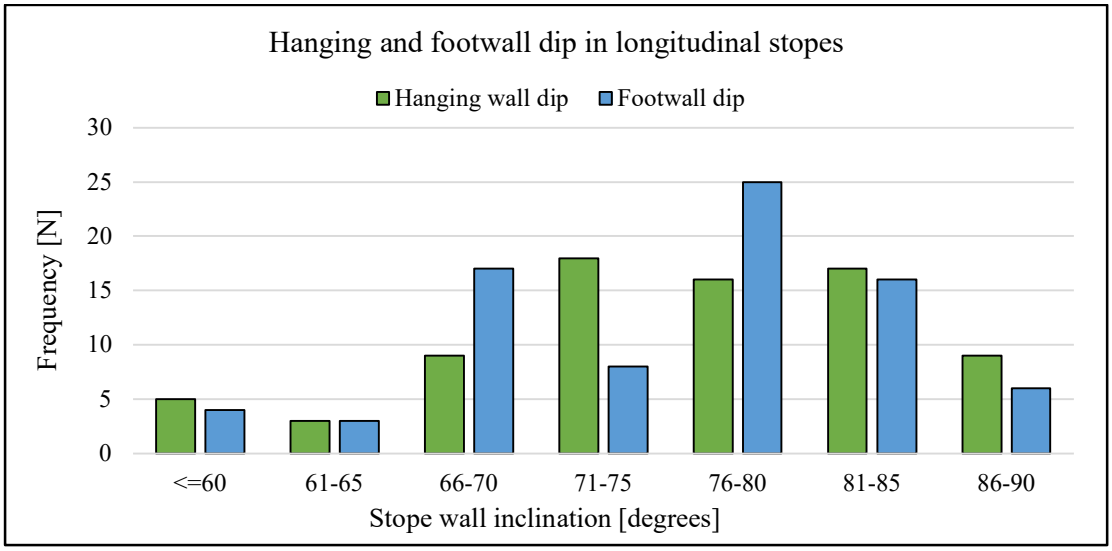

Figure 6.7: Hanging and footwall dip in longitudinal stopes

6.2.2 Transverse stopes

Transverse stopes are overly found in the Wombat orebody. As explained in chapter 5.5, primary and secondary stopes are set to be 10 and 15 metres wide, respectively. The width distribution is shown in the Figure 6.8. Some deviations in stope width are imposed by individual stress handling, stability assurance or orebody redirections. The majority of secondary stopes which exceeds the standardized 15 metres in width is located at the orebody edges. If the orebody changes sharply along the east-west axis, the secondary stopes are designed three to four metres wider to cover additional ore. This procedure is cheaper than applying extremely narrow primary stopes (Malmberg, 2020a).

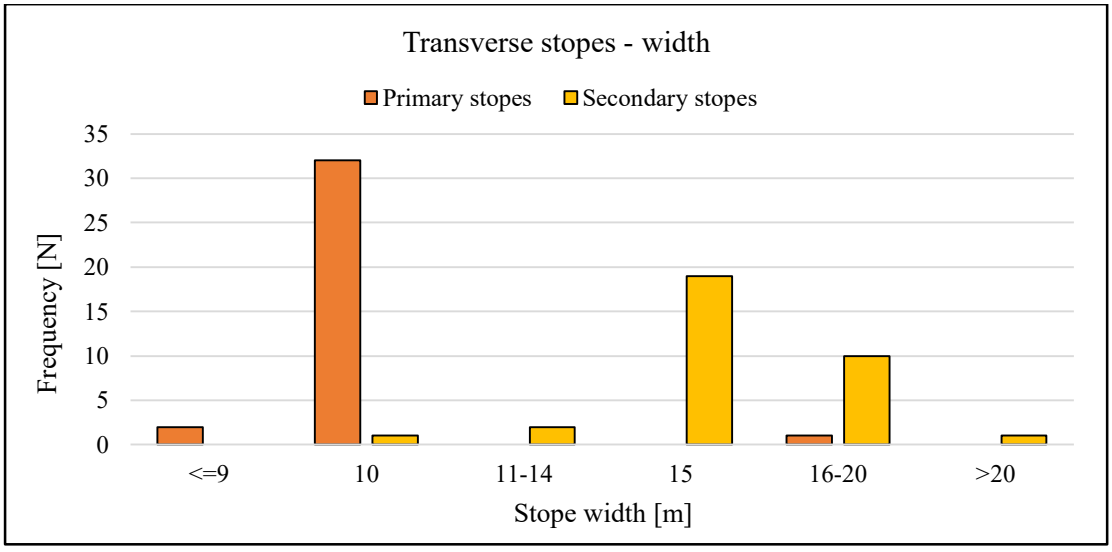

Figure 6.8: Width frequency of transverse stopes

The orebody thickness determines the strike length of the particular stope. Stope length variations range from less than 10 metres up to more than 40 metres (Figure 6.9). The stopes with greatest length are commonly accumulated in drifts around levels 530 to 620. The relatively short stopes represent partly a product of primary stopes splitting into several smaller stopes. For the levels 530, 560 and 590, the presence of a weak talc zone has had the planning department re-evaluating the stope design. Minimized stope exposure time was achieved as a result of the separation (Malmberg, 2020a). The average length of both stope types is found to be roughly 23 – 24 metres which is slightly below the average Wombat orebody thickness of 29 metres (Peskens, 2013).

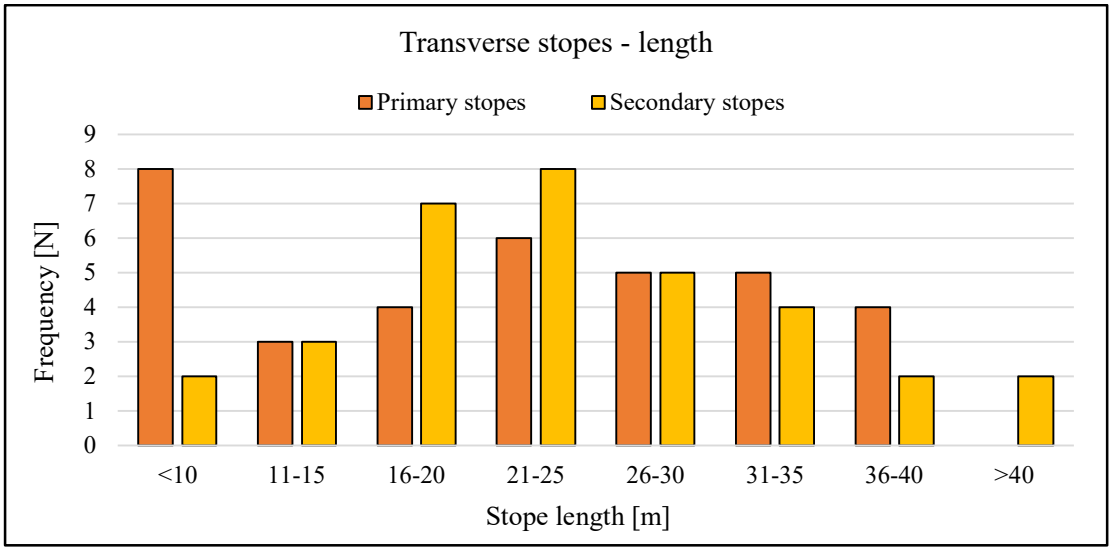

Figure 6.9: Length frequency of transverse stopes

The majority of transverse stope is found to be 25 metres tall. As the position of transverse stopes is usually mid-centred in the production drifts, discrepancies from ideal height profiles are rarely found (Figure 6.10). The standard deviation regarding stope height proves that transverse stopes deviate roughly 1.2 metres whereas longitudinal stopes deviate up to 4.3 metres from the mean.

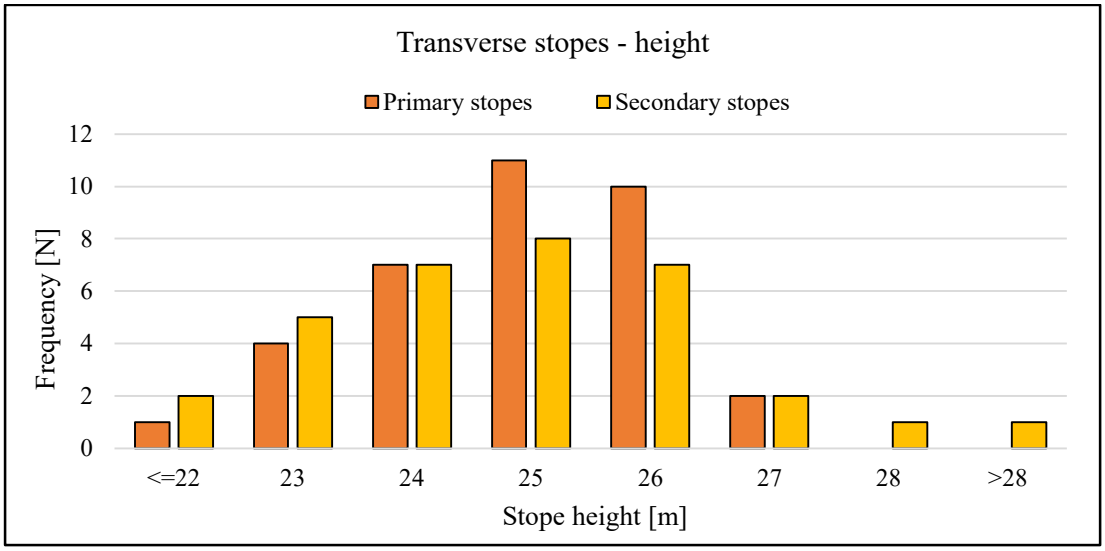

Figure 6.10: Height frequency of transverse stopes

Information on the hanging and footwall inclination of transverse stopes is plotted in the Figure 6.11. The distribution is overall left-skewed with a median inclination in the footwall of 77 degrees. This applies to primary and secondary stopes. Yet, the hanging wall inclination in primary stopes accounts for 80 degrees in contrast to 77 degrees for secondary stopes. A fairly large number of transverse stopes lack distinct hanging and footwall allocations. Most of the stopes are designed in trapezial shape resulting in two footwalls or two hanging walls. Other differences between longitudinal and transverse stopes are known to be the different interpretation of hanging and footwall. The hanging and footwall are represented as end walls in transverse stopes and as sidewalls in longitudinal stopes.

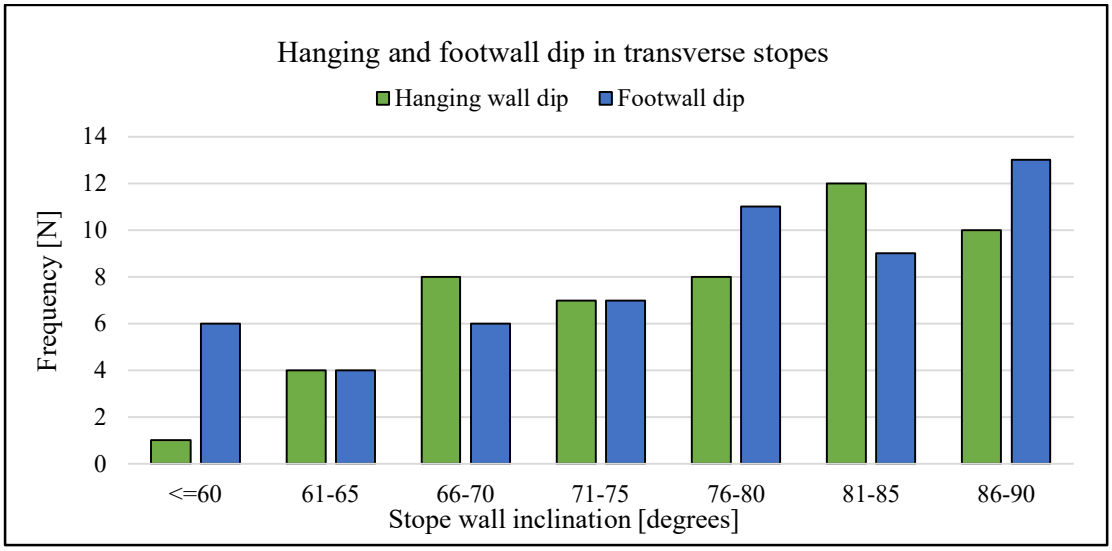

Figure 6.11: Hanging and footwall dip in transverse stopes

Out of 68 transverse stopes, 25 stopes have distinct hanging and footwalls. These stopes are particularly important because they provide information of how rock mass behaves if located

in hanging and footwall. Information on the degree of complexity, the hydraulic radius and the aspect ratio is provided in Appendix 2. A comprehensive summary of geometrical attributes per stope type is presented in the Table 6.1. It is decided to plot attributes accordingly to stope types and to use median values.

Table 6.1: Summary of stope geometry properties

Summary of stope geometry properties				
Database information		**Median values of stopes**		
Attributes	**Units**	**Longitudinal**	**Primary**	**Secondary**
Stope number	[N]	99	35	33
Stope width	[m]	7	10	15
Stope length	[m]	32	24	23
Stope height	[m]	25	25	25
HW dip angle	[degrees]	76	81	77
FW dip angle	[degrees]	77	78	76
Hydraulic radius	[m]	6.6	6.1	5.8
Aspect ratio	[L/H]	1.4	1	1

6.3 Macro application

The initial dataset provides information on the stope performance in terms of dilution, ore loss, ore recovery and ore overbreak. Further extension of the dataset is required in form of the earlier introduced equivalent linear overbreak/sloughing (ELOS) and equivalent linear lost ore (ELLO) methods which are useful when examining the stope performance. The ELOS and ELLO data is conceived to be the single-most important parameter to this study. The method does not only produce comparable data for longitudinal and transverse stopes but yields a more detailed analysis in particular.

The data acquisition is mainly done with information from planned stopes and actual CMS scans. The information is processed in the modelling software Surpac, version 6.8, which provides visualisation of the underground operation. Surpac deploys a so-called macro command that is custom built by the developer department of WSP Finland which represents Surpac in Finland. In order to deploy the macro correctly, actual and planned stope data must be existent with additional input such as ore solids, backfilled stopes and self-developed boxes. An example of how the macro interface is constructed is enclosed in Appendix 3.

The Figure 6.12 depicts how the input data looks like for longitudinal stopes. The planned stope, highlighted in brown, is plotted against the superimposed CMS scan in grey. Areas covered by the CMS profile express overbreak i.e. waste, ore or CRF overbreak. Zones which appear brown, exemplify ore loss zones which have not been successfully blasted. It must be mentioned that the stope scan only illustrates quantitative blast results. It does not consider if material is left behind. As a simplification, ore loss can be pictured as the orange zone in the Figure 6.12. If the CMS profile exceeds the planned stope file, it is automatically defined as overbreak. The type of overbreak depends on the material that exceeds the profile. It ultimately varies between ore, waste and CRF overbreak.

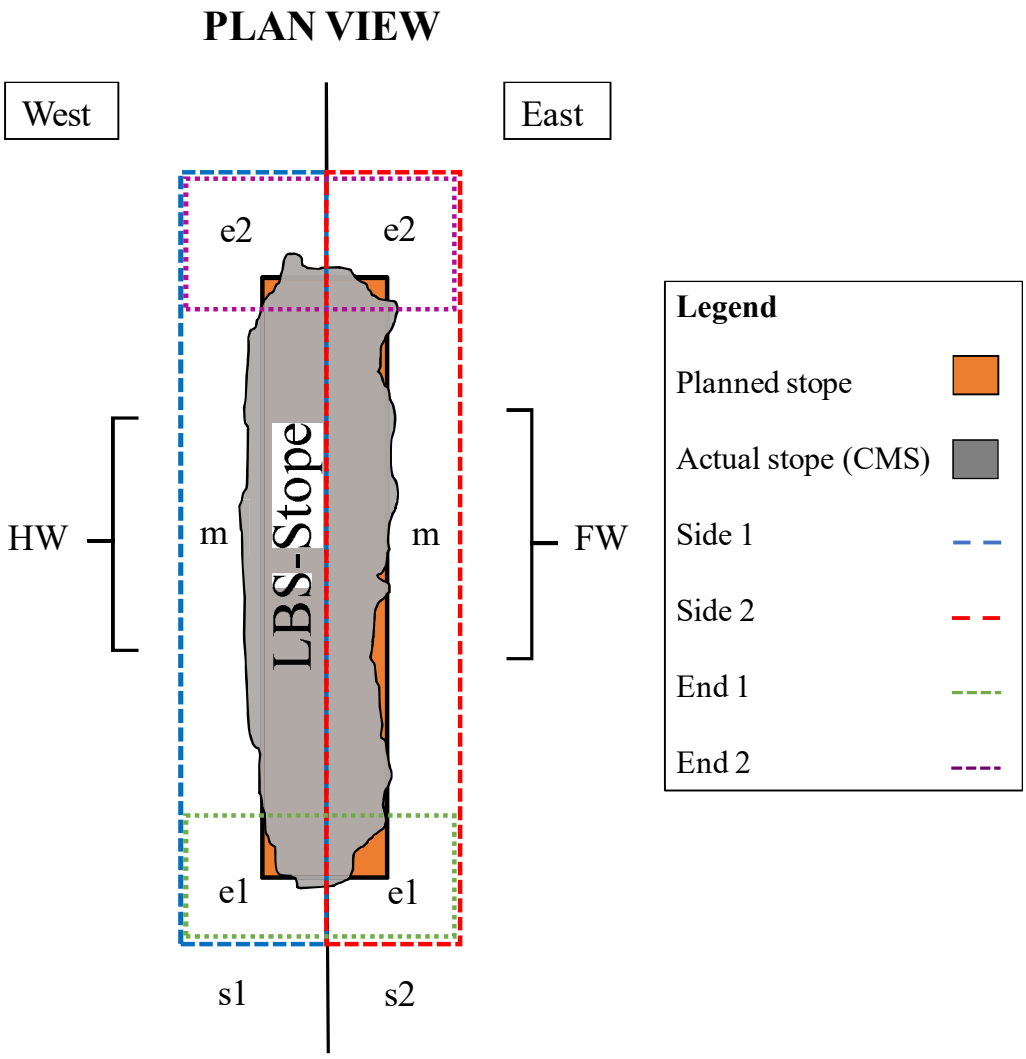

Figure 6.12: Scheme of a longitudinal stope with corresponding boxes in plan-view

The blue and red lines on the outer side represent the hanging wall and footwall of longitudinal stopes and sidewalls of transverse stopes, respectively. With the help of the four boxes, namely side 1, side 2, end 1 and end 2, the analysis allows to differentiate between in total six section if applied as explained. The consequence is an eventually more sophisticated and detailed overview of stope conditions. A schematic illustration of how the box design will change accordingly to the viewing perspective is presented in Appendix 3 as well as the figurative procedure for transverse stopes.

To enhance visualisation and to ensure proper explanation of the complex process, a video sequence is presented in Figure 6.13 in QR-Code format. Little by little is shown how the boxes are designed to cover the planned and the actual stope using a longitudinal stope in the Wallaby orebody as an example. Ore solids are visualised as an additional feature. The boxes correspond accordingly to the above described scheme and are coloured as predetermined in the Figure 6.12. Any identified ore loss and overbreak is then summarized

as volumetric units in a comprehensive output table. An exemplary output scheme is shown in Appendix 3.

Figure 6.13: QR-Code for illustration of macro input data

The degree of accuracy pertaining to the macro application is inherently linked to the computational process within the modelling software Surpac. Despite some minor differences, the macro application does work in a highly precise manner. The geometric complexity of either longitudinal or transverse stopes does not deteriorate the calculations. It must be noted that the precision and reliability of the macro output depends strongly on the input data as well. The input data comprises stope files, ore solids and the settings of boxes. Strict consistency must be applied when developing the box designs to achieve comparable results.

7 Results and key parameters of longitudinal stoping

To obtain a better understanding of how the stopes behave and what conditions forced them to perform as they do, the in-depth analysis attempts to reveal the most important parameters to affect stoping in Kylylahti. The results and the identification of the most influencing parameters are presented in this chapter. Statistics on ore loss and different overbreak occurrences are introduced first and followed by the key parameters that are found.

7.1 Ore loss and overbreak results

Experienced ore loss and overbreak in longitudinal stopes are used as the main objective to successfully assess stope efficiency and performance. Overbreak is categorized as either ore, waste or CRF material breaking or sloughing into the stope. The Figure 7.1 illustrates the average of stope efficiency attributes. The volumes of ore loss and overbreak which are calculated by means of the macro application are converted into an equivalent layer to allow reliable comparison among all longitudinal stopes. The conversion method is equal to the equivalent linear lost ore (ELLO) and equivalent linear overbreak/sloughing (ELOS) method. It is decided to split the data for longitudinal stopes into Wallaby and Wombat orebody. The presented results correspond to the ore loss and overbreak suffered from the sidewalls. CRF is not included in the illustration as there is no measurable CRF intrusion in the sidewalls for stopes in both orebodies.

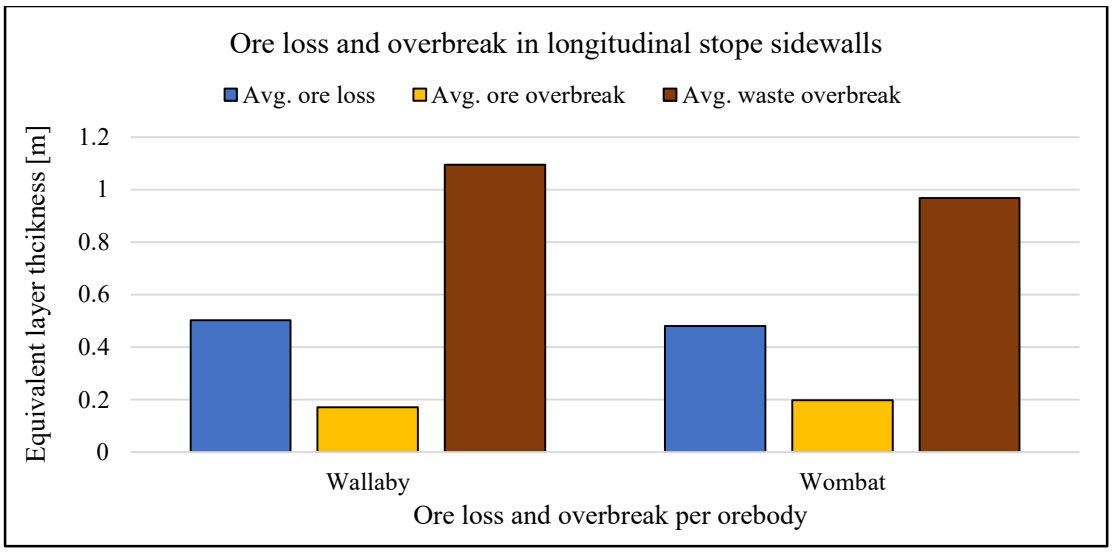

Figure 7.1: Ore loss and overbreak in longitudinal stope sidewalls

The stopes in Wombat are generally less regularly designed, yet the results for ore loss, ore and waste overbreak show almost identical numbers. The stopes sustain on average an ore loss layer of 0.5 metres projected along the surface area of the sidewalls. For the waste overbreak, the layer accounts for roughly 1.1 metres. The remarkable difference between ore and waste dilution is related to the longitudinal mining method. Stopes are mined along the orebody which leaves the sidewalls in most cases in waste rock. That explains why the sidewalls suffer mostly waste overbreak.

Comprehensive overviews of longitudinal stope performance in the Wallaby and Wombat orebody are presented in Table 7.1 and Table 7.2. Data on the stope end walls is further supplemented in both. The summaries comprise besides the average values for all stope efficiency attributes the 25 % and 75% - quartiles as well. The stope ends are always in close contact to CRF backfill instead waste rock fill due to stability assurance. The backfilling sequence can be read in chapter 5.5. However, the summaries demonstrate that CRF overbreak is almost non-existent in the end walls for Wallaby and Wombat stopes. The reason for this is further elaborated in the following chapter about key parameters.

Table 7.1: Statistical summary of longitudinal stopes in Wallaby

Statistical summary of longitudinal stopes in Wallaby				
Attribute	**Wall type**	**Average [m]**	**25 % - Quartile [m]**	**75 % - Quartile [m]**
Ore loss	Sidewalls	0.50	0.29	0.62
	End walls	1.51	0.63	2.28
Ore overbreak	Sidewalls	0.17	0.07	0.20
	End walls	0.49	0.10	0.65
Waste overbreak	Sidewalls	1.09	0.81	1.30
	End walls	0.59	0.18	0.61
CRF overbreak	Sidewalls	0.00	0.00	0.00
	End walls	0.09	0.00	0.01
Total overbreak	Sidewalls	1.27	0.97	1.41
	End walls	1.08	0.30	1.50

Table 7.2: Statistical summary of longitudinal stopes in Wombat

Statistical summary of longitudinal stopes in Wombat				
Attribute	**Wall type**	**Average [m]**	**25 % - Quartile [m]**	**75 % - Quartile [m]**
Ore loss	Sidewalls	0.48	0.28	0.58
	End walls	1.36	0.73	1.74
Ore overbreak	Sidewalls	0.20	0.08	0.25
	End walls	0.59	0.21	0.74
Waste overbreak	Sidewalls	0.97	0.68	1.29
	End walls	0.78	0.20	1.20
CRF overbreak	Sidewalls	0.00	0.00	0.00
	End walls	0.08	0.00	0.03
Total overbreak	Sidewalls	1.17	0.84	1.42
	End walls	1.44	0.71	1.91

It must be stressed that the comparison of end walls to sidewalls is not found appropriate. The reason is the enormous discrepancies of specific surface areas that are used to convert overbreak and ore loss volumes into equivalent layers. The sidewall area in longitudinal stopes is roughly the six-fold of the end walls. It is recommended to compare wall-specific data only.

7.2 Mining sequence and mining direction

The first key attribute to affect longitudinal stope performance is conceived to be the mining sequence. Particularly in the shallower Wallaby orebody, longitudinal stoping is the solitary mining method with the exception of two transverse stopes. It eases the visualisation of the correlation between stoping, mining sequence and performance. The impact of the mining direction on longitudinal stoping follows accordingly.

7.2.1 Mining sequence

The mining sequence nicely reveals the correlation of the mining direction on ore loss and overbreak. Due to the capability of the macro to allocate any form of ore loss or overbreak to specific stope walls, an evident trend can be conceptualised on the end walls. Figure 7.2 illustrates the average ore loss over the life of mine (LOM) in form of a stacked histogram. A consistent reduction of ore loss per operation year becomes apparent. The light surge in ore loss in the most recent years is presumably caused by the belated complexity of the drift system and their accessibility. The stopes mined between 2018 – 2020 are extracted in an almost totally separated part from the main orebody. The elevated ore loss results are most likely explained by inclined northern end walls. Continuous waste rock fill or residual pillar in between are the main backfill methods for these stopes which do not diminish the effect over the suggested improvement of CRF confidence (Malmberg, 2020c).

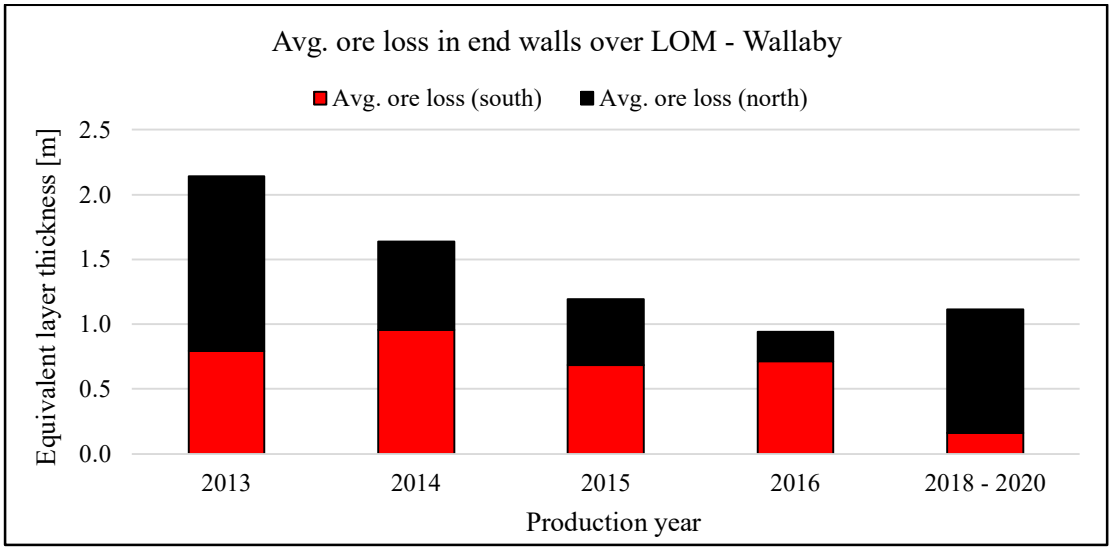

Figure 7.2: Ore loss in end walls over LOM in Wallaby

Since there are no significant improvements or major changes in stope details e.g. stope dimensions, changing design complexities or dip inclinations, the gradual improvement is most likely caused by operational factors. Another point supporting the hypothesis of improved satisfaction over backfill handling is the fact that a sufficient CRF composition has been found and applied relatively quickly in Kylylahti. The explanation yet holds as increased confidence in handling CRF stability in practice and creating a sufficient mixture for ideal CRF backfill took place in a relatively early phase of the operation. The theory is further supported by the visual representation of ore loss in northern and southern ends of the stopes in Figure 7.2. Over the course of the life of mine, a consistent decrease in ore loss is conceived which is predominantly driven by the ore loss reduction in northern ends. Since

the northern ends are mostly adjacent to CRF backfill because of the mining direction, it proofs that generally more confidence is achieved in backfill stability and blasting pattern.

Longitudinal stope drilling requires commonly a certain amount of space between CRF and borehole to not cause CRF instability. In Kylylahti, a security margin of approximately one metre on average is used. It seems that the safety margin supports the backfill stability as the buffer distance assures no drilling inside the CRF. But at the same time, ore loss is associated with the safety margin distance towards the CRF backfill because of insufficient fragmentation. A possible proof of this development is described earlier in Table 7.1 and Table 7.2 which shows that the occurrence of CRF overbreak is low to non-existent. Opposed to ore loss, longitudinal stopes regularly show tendency to ore overbreak into direction of mining. The end walls facing direct ore contacts are less restrictively mined than the end walls towards CRF backfill because ore overbreak is seen as little inconvenience only compared to backfill overbreak.

On the other hand, the Wombat orebody does not seem to be heavily dictated by the mining sequence nor does it steer towards a certain trend. The extraction sequence has no or only little impact on the Wombat longitudinal stopes as a variation of longitudinal and transverse stoping is applied. Because the longitudinal stopes are overly used to extract complex and narrow ore abundances in the drift ends, there is no clear procedure to follow through compared to the Wallaby drifts.

Another fact is the time span which is required to extract entire production levels. The Wallaby sequence started in the beginning of 2013 and has mainly ceased in the end of 2015. Only five more stopes have been mined ever since and overly in the past 9 months. The total duration to finish production levels in Wallaby is within roughly three years of consecutive operation. In contrast, the Wombat orebody started longitudinal stoping in early 2014 and applies it to date ever since which is about the doubled time span. Simulated stress modelling has been used to assess stress profiles in the Wombat orebody. The Finnish company Pöyry Finland Oy (2016) showed stress accumulation particularly in the northern and southern drift ends. The longitudinal stopes in Wombat are densely located in these critical zones. Given the fact that Wombat consists predominantly of transverse stopes, the assumption can be made that longitudinal stopes are exposed to stronger stress re-directions.

7.2.2 Mining direction

The analysis detected certain similarities pertaining to Wallaby and Wombat stopes. Ore loss and overbreak are even more pronounced in the Wombat orebody compared to Wallaby. The Figure 7.3 and Figure 7.4 depict the average ore loss and overbreak in the stope end walls. As the mining direction is generally considered north to south, it proves the assumption that northern end walls retrieve greater ore loss over southern ends. Firstly, the northern ends are located at the bottom of the orebody which automatically implies a declined end wall angle that promotes ore loss. And secondly, this might be due to the CRF being backfilled in the northern ends which requires the aforementioned safety margin between drillhole and backfill. The ore overbreak occurs overly in the opposite end wall towards direct ore contact. Main driver of this event is considered the mining direction. The mining direction is sometimes reversed beginning in south and commencing towards north. This causes some profiles in Figure 7.3 and Figure 7.4 to be elevated against the general trend. Examples are namely level 500, 680 and 710 in which the mining direction is switched and commences from south to north.

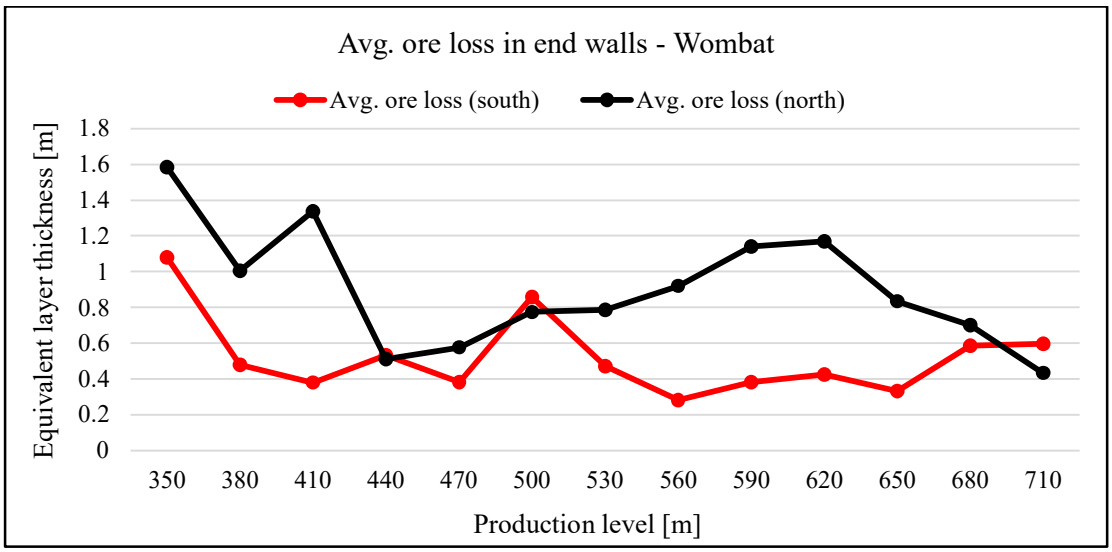

Figure 7.3: Avg. ore loss in the end walls of longitudinal stopes in Wombat

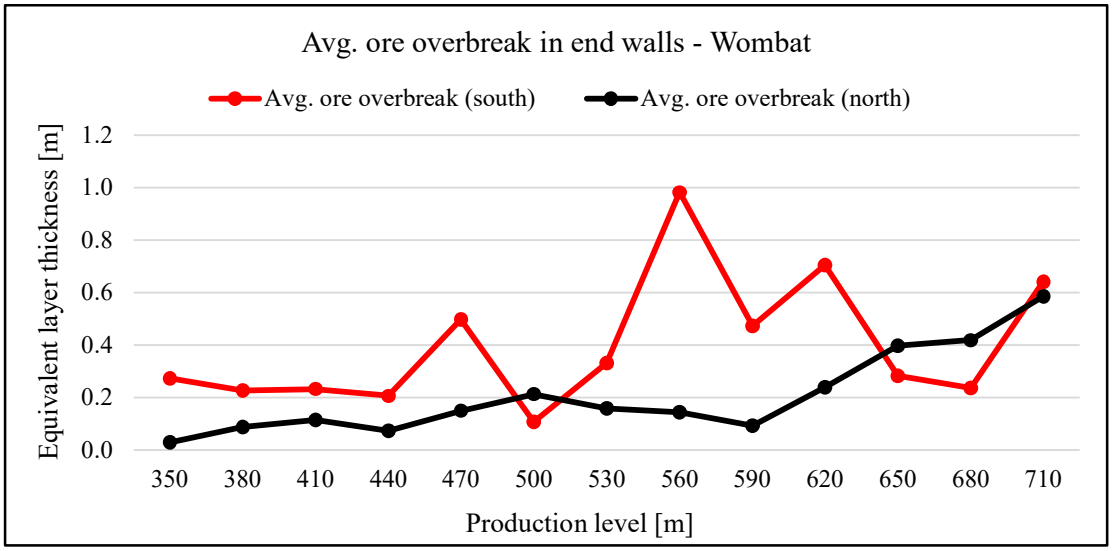

Figure 7.4: Avg. ore overbreak in the end walls of longitudinal stopes in Wombat

It can be concluded that the mining sequence is responsible for partially excessive ore overbreak and significant ore loss in the end walls of the longitudinal stopes. No distinction is hereby made among Wallaby or Wombat stopes. However, the sidewalls do not correlate with the mining sequence. The pending waste overbreak plots of the Wallaby and Wombat stopes are attached to Appendix 4.

7.3 Stope design

The stope design is considered essential to stope planning and is known to affect longitudinal stoping drastically. Because the design incorporates numerous factors, the chapter is subdivided into stope dimensioning, stope wall inclination and geometric complexity. The chapter structure is aligned accordingly.

7.3.1 Longitudinal stope dimensioning

The factors to define stope dimensions typically comprehend the stope width, height and length. Because the height is predetermined by the production drift spacing, only the width and length differences are investigated. Similar to the previous comparison, the following results of longitudinal stopes are discussed per orebody. It is decided to use ore loss and overbreak results of the stope sidewalls since they represent the largest area of the stope and thus, the most valuable information.

Regarding the stope strike length, the positive correlation between increased stope length and waste overbreak can be concluded by the Figure 7.5. The upwards regression slope supports the positive correlation factor of 0.41. The stopes in the Wallaby complex start with the length of approximately 20 metres and produce roughly 0.75 metres of overbreak. More overbreak is generated if the stope length increases. A certain degree of unpredictability is perceived in stopes that are roughly 40 metres long. A reasonable explanation is that stopes with increased length profiles naturally become more susceptible to unfavourable conditions due to the greater stope span. However, there is no correlation noticeable in ore overbreak which is mainly due to the inconsistent presence of additional ore outside of the stope boundaries.

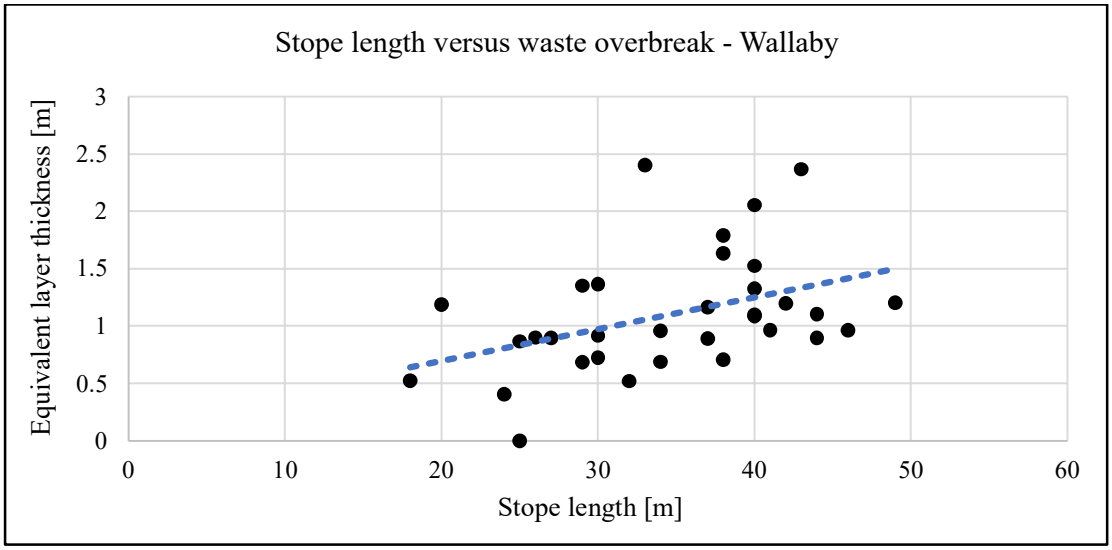

Figure 7.5: Scatter plot of stope length versus waste overbreak for Wallaby longitudinal stopes, r = 0.41

The Wombat analyse does not yield similar results when using a single parameter as input. Yet, the regression line slopes upwards when plotting stope dimensions and associated overbreak. Using the hydraulic radius, a measure to comprehend the entire span of a

sidewall, the Figure 7.6 depicts the results. The overall image suggests a positive yet lightly exponential trend which is remarkably less distinctive as in the Wallaby results. Below the illustrated regression line, the correlation is stronger compared to the data above the line. The two data points above the 2.5 metres of equivalent layer thickness represent the two stopes that are located in the Gap area. The geological importance for stoping is evaluated and discussed in chapter 7.4. It can be concluded from the two figures, that even in entirely different environments, the increased stope dimensions are likely to cause enlarged overbreak.

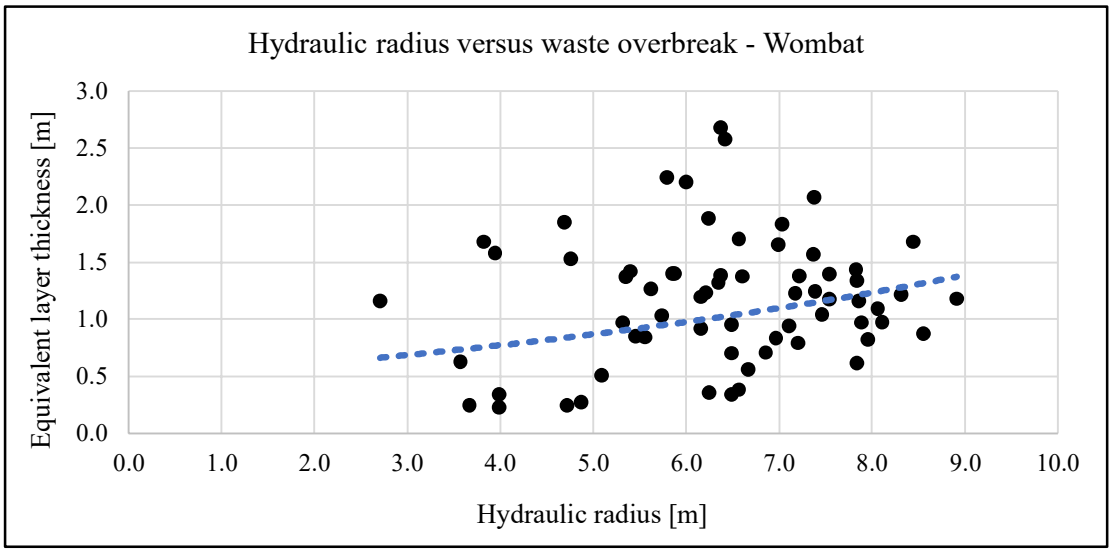

Figure 7.6: Scatter plot of waste overbreak versus hydraulic radius for longitudinal stopes in Wombat, r = 0.15

7.3.2 Hanging wall inclination

The analysis of overbreak in the hanging wall of the stope is an interesting and influencing parameter. Figure 7.7 shows the average hanging wall overbreak per sidewall and is separated after the Wallaby and Wombat orebody. The image clearly states that the sidewall in which the hanging wall is located sustains larger overbreak compared to the footwall side. If the hanging wall is located in the western sidewall, more overbreak is generally generated there. The behaviour for the scenario if the hanging wall is located in the eastern sidewall acts vice versa. From the Figure 7.7 can be concluded that the effect of the hanging wall has to be considered a main parameter of stoping in Kylylahti.

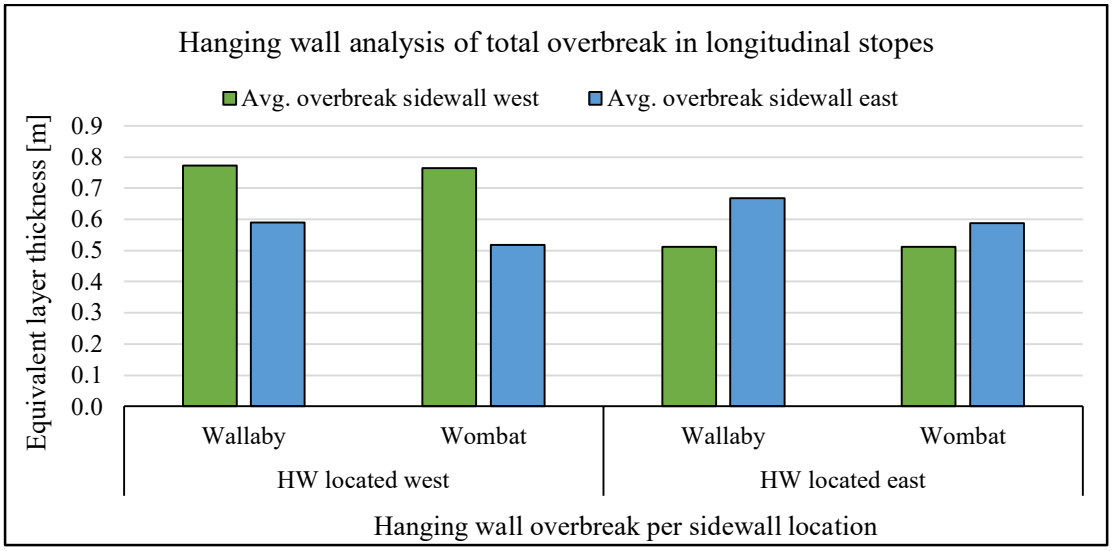

Figure 7.7: Hanging wall analysis of total overbreak in longitudinal stopes

An important aspect concerns the variation in dip angles of both hanging and footwall. Studying the different impacts of flatter inclinations starting from 90 degrees (vertical) down to a minimum of 60 degrees, only very little if any correlation could be attested towards increased overbreak and declining dip angle. The exclusive observation regarding varying stope wall inclinations is that a declined dip angle leads to greater fluctuation of overbreak in the respective stope wall.

7.3.3 Geometric complexity

When planning the stope design the ore delineation of the deposit dictates the shape and geometry of the stopes in width, length and height. It affects the stope inclination and requires in some cases highly complex designs. One reason for the greater degree in complexity is the below cut-off material which intersects the stope at the top or bottom drift. In this scenario, waste is preferably mined separately to decrease dilution. Another explanation is a sharp alteration of the orebody in height which requires the total stope height to follow closely.

The geometric complexity is a factor implemented in this study that mainly relies on preliminary stope assessment. The initially presented dataset is supplemented with different percentages on ore loss and shape dilution. The interpretation is made by the mine planning department in Kylylahti. It is an approach to account for any encountered irregularities and complexities. The following Table 7.3 shows the conversion of these percentages into categories to allow for stope clustering. Six different categories are established ranging from favourable designs to severe stope complexities. The greater the addition of percentages, the higher the degree of complexity becomes. The slicer column represents the mathematical threshold that defines the different intervals. Appendix 4 is supplemented with three illustrations which show typical examples of stope profiles that have basic, high and severe complexities.

Table 7.3: Geometric complexity classification

Geometric complexity classification		
Complexity	**Information on percentages**	**Slicer**
Favourable	Negative	< 0
Basic	No percentages assigned	= 0
Low	Ore loss AND/OR shape dilution	< 5
Medium	Ore loss AND/OR shape dilution	< 10
High	Ore loss AND shape dilution	< 15
Severe	Ore loss AND shape dilution	> 15

The cluster returns an overly accurate outcome of how stopes suffer overbreak. It is shown that overbreak excess correlates with increasing complexity of stopes. In Figure 7.8 the trend seems to build up progressively from low (~0.9 m) towards high (~1.5 m) in Wallaby. The illustrated intervals basic, low, medium and high conform with the Table 7.3. Stopes which are considered basic have an unusually high overbreak average. The complexity corresponds firmly with the group assessment of the mine planning department. The utilization of an adjustment factor for ore loss and shape dilution has not been standardized from the beginning which explains the vast majority of basic stopes in the early state of the Kylylahti mining operation. The other categories were mainly mined after two to three years thereafter.

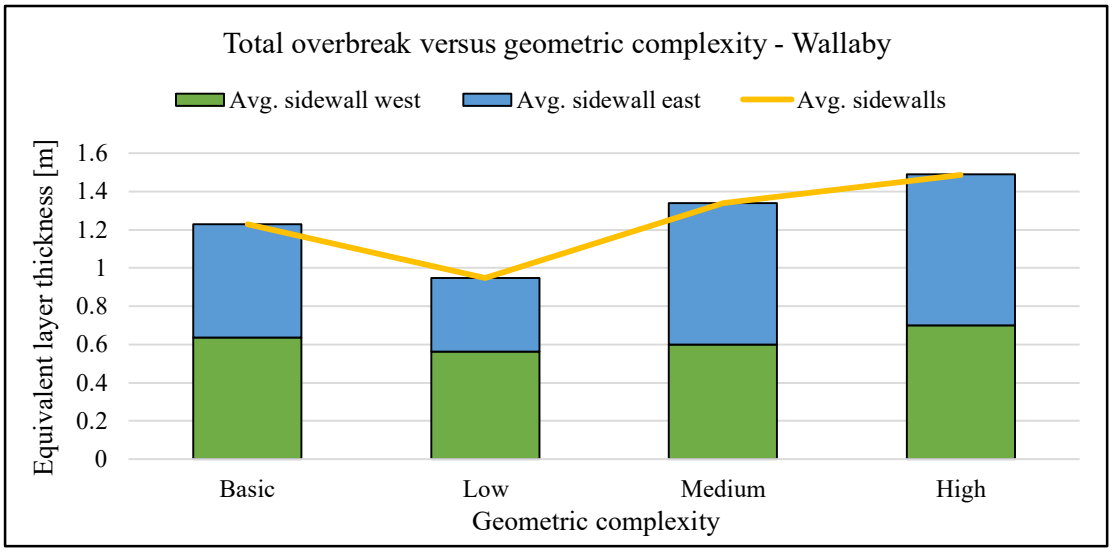

Figure 7.8: Total overbreak after newly introduced geometric complexity in Wallaby longitudinal stopes

A similar behaviour is found in the Wombat stopes as shown in the Figure 7.9. The stopes are supplemented further with the severe category. Since the stopes are situated either in front (north) or behind (south) the transverse stopes in Wombat, it is decided to plot the results after stope location and complexity. It appears, that the complexity represents a critical stoping parameter which is applicable independent of the location. The complexity proves suitable to predict distinctive overbreak quantities in the front and back of transverse stopes. However, medium and high results alongside the transverse stopes deviate from the trend. The challenging environment which the longitudinal stopes are located in presumably

causes these fluctuations. The majority of those stopes are found in the Gap area, a transition zone between Wallaby and Wombat which is known to be very challenging and demanding for stoping. The Gap zone is investigated more thoroughly in the following chapter.

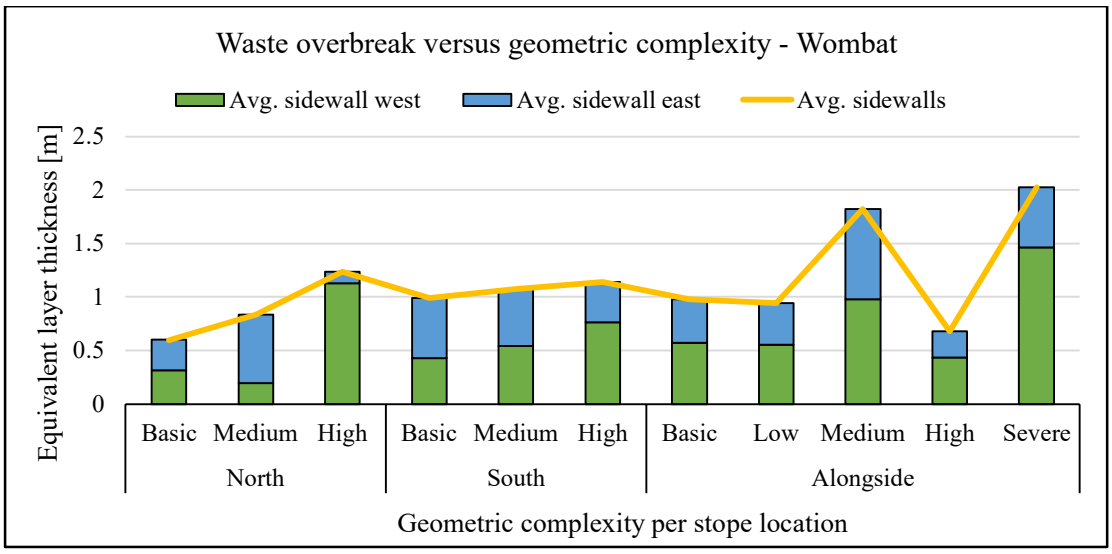

Figure 7.9: Waste overbreak after geometric complexity for longitudinal stopes in Wombat

Although the predictability is sufficiently shown, the same effect does not translate into ore loss prediction. In terms of ore loss predictability, it can be concluded that with more complex stopes ore loss tends to increase. As a matter of fact, large fluctuations deteriorate the application of the geometric complexity on ore loss. The geometric complexity does contribute significantly to the overbreak occurrence in longitudinal stoping. It can help with the production planning as it is strongly correlated to excessive overbreak in more complex stopes. Therefore, it is conceived as a critical parameter for longitudinal stoping on overbreak assessment.

7.4 Geological formations

Stopes located in geologically challenging environments is another key parameter that is emphasised. The presented results examine the impact of present structural formations as well as the impact of black schist in particular. The chapter structure follows accordingly.

7.4.1 Presence of structures

Plotting the longitudinal stope data against the depth to check for location dependencies, increasing overbreak peaks are noticeable in level 380, 410 and to some extent level 470. The average waste overbreak derived from the sidewalls in level 380 totals 2.0 metres as shown in Figure 7.10 whereas the average waste overbreak in Wombat accounts for 0.9 metres. The excessive overbreak is roughly twice as much which indicates that the area underlies drastic conditions. Elevated overbreak numbers are additionally retrieved for the production levels 410 until 470. The production drifts in deeper regions such as level 560, 620 and 680 also show deviated overbreak numbers from the average of 0.9 metres.

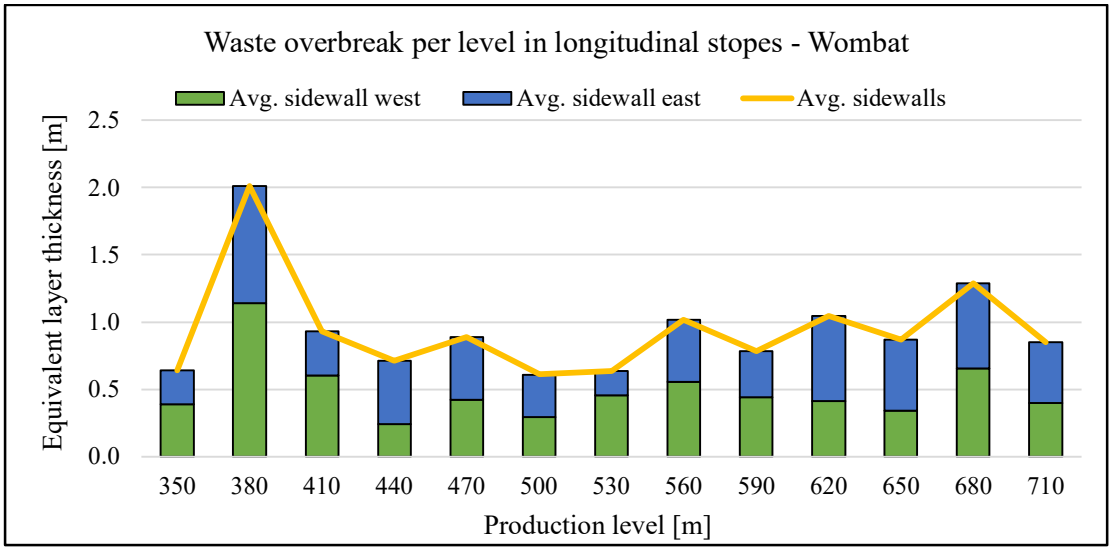

Figure 7.10: Waste overbreak per level in longitudinal stopes for the Wombat orebody

Level 380 is in particular challenging as there are two parallel massive ore lenses, Wombat and Gap, which have foliated black schist located in between (Malmberg, 2020c). The foliation in the Gap zone has such a great span, that stopes in the level 380 are partially with both sidewalls in the black schist material such as stope 380jpL2. In the Figure 7.11, the black schist is illustrated in the footwall of the Gap and on top of the Wombat massive sulphide lens in a cross-section view. The foliation mainly comprises level 380 to 410 and encapsulates the stope 380jpL2 from both sidewalls here.

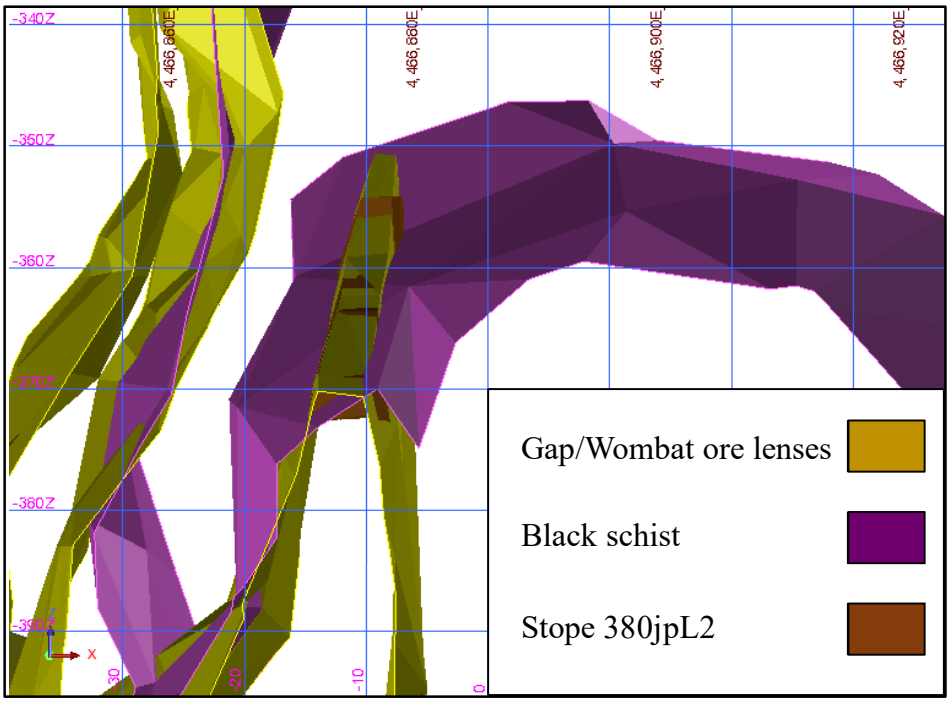

Figure 7.11: Black schist foliation next to the Gap and on top of the Wombat ore lens encapsulating stope 380jpL2

The attested foliation and structural changes in any direction are likely to cause overbreak and elevate the unpredictability of stoping behaviour. The graphite rich black schist can be described as extremely weak material and a potential threat to abutted stopes (Kekki, 2020a). The different rock mass properties are described in chapter 5.4. Black schist is considered a sedimentary rock type that accounts for a high intact rock strength (>120 MPa) but heavily accommodates structural graphitic bands (SRK Consulting, 2007). These layers are main causes for black schist to cave into the stopes. Even though the transition zones were considered in the stope planning, the stopes produced significant quantities of overbreak. Given the alarming overbreak results for the Gap zone, it can be concluded that the consideration of the geological formation is vital and of crucial importance to stope planning.

Despite the Gap area, which underlies a very dominant transition issue with additional black schist presence, the Figure 7.12 shows constantly elevated numbers for lower drifts such as level 560 and 620 as well as level 680. Especially in the level 680, the overbreak occurrence significantly exceeds the Wombat average of 0.9 metres by 0.4 metres. The prevalent characteristic is striking that southern regions of both, level 560 and 590, suffer large waste intrusion with level 620 incurring overbreak from the northern region. The potential structural anomaly is not associated to overbreak in level 680. The explanation for overbreak in level 680 is presumably black schist as the entire level is found to be next to the weak material (Malmberg, 2020c).

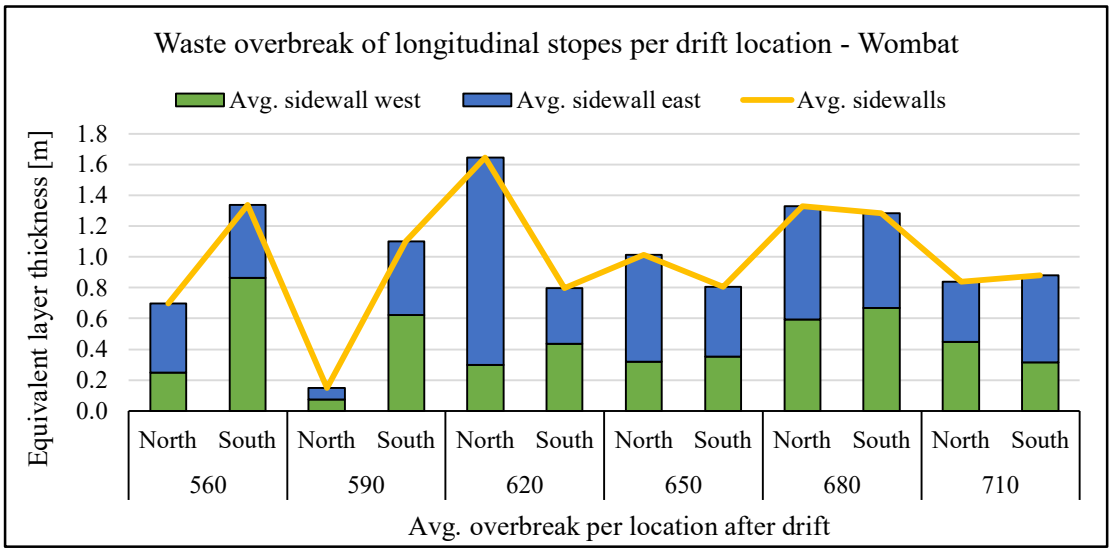

Figure 7.12: Waste overbreak of longitudinal stopes in the lower levels after drift location in Wombat

Concerning the transverse stope analysis, the presented issue is prevalent in primary and secondary stopes as well. The presumable explanation of one or multiple structural formations is further supported with the fact, that both stoping methods are affected in the same production drifts. It has been demonstrated that the presence of possible structural formations affects stoping performance and must be considered a key parameter.

7.4.2 Black schist zone

The formation of black schist along the Kylylahti domain on its eastern side is considered a weak zone (Kekki, 2020a). The black schist belt expands from the upper Wallaby orebody with few exceptions towards the lowermost drifts in 810 metres. Surprisingly, the results of the different sidewalls in Wallaby stopes state that the overbreak occurrence is almost equally distributed in western and eastern sidewall. The overbreak is not overly larger when the stope hanging wall is located inside the black schist layer compared to the western sidewall. In lower levels, the numerical results even suggest that the main overbreak happens opposed to the black schist contact. This can be presumably explained by the cautious drilling approach of the Kylylahti staff towards the black schist. Over drilling of 0.5 – 1.0 metre into non-ore material is normally applied whereas drilling is stopped at ore contact towards black schist (Malmberg, 2020c). Nevertheless, the black schist presence does not seem to cause a deterioration to the stopes with view on numerical statistics.

It must be stressed that any stope planning has been conducted with great consideration of the black schist zones. As explained before, over drilling is strictly avoided towards black schist as one practical measure (Malmberg, 2020c). The assumption holds, that if stope planning had been done less cautiously regarding the black schist belt, greater excess of overbreak had been generated. Prove that the black schist has a visual impact on stoping is presented in Figure 7.13. Although the overbreak in the particular stopes is numerically ordinary, the CMS scan clearly shows structural overbreak in the sidewalls of stopes in the level 240 and 270. The blasted stopes (grey) nicely retrieve the image of vertically directed layers breaking into the stope rather than irregular boulders or displacements. To compare how irregular sidewall overbreak behaves, a further figure is attached to the Appendix 4 with another example of layering in level 240.

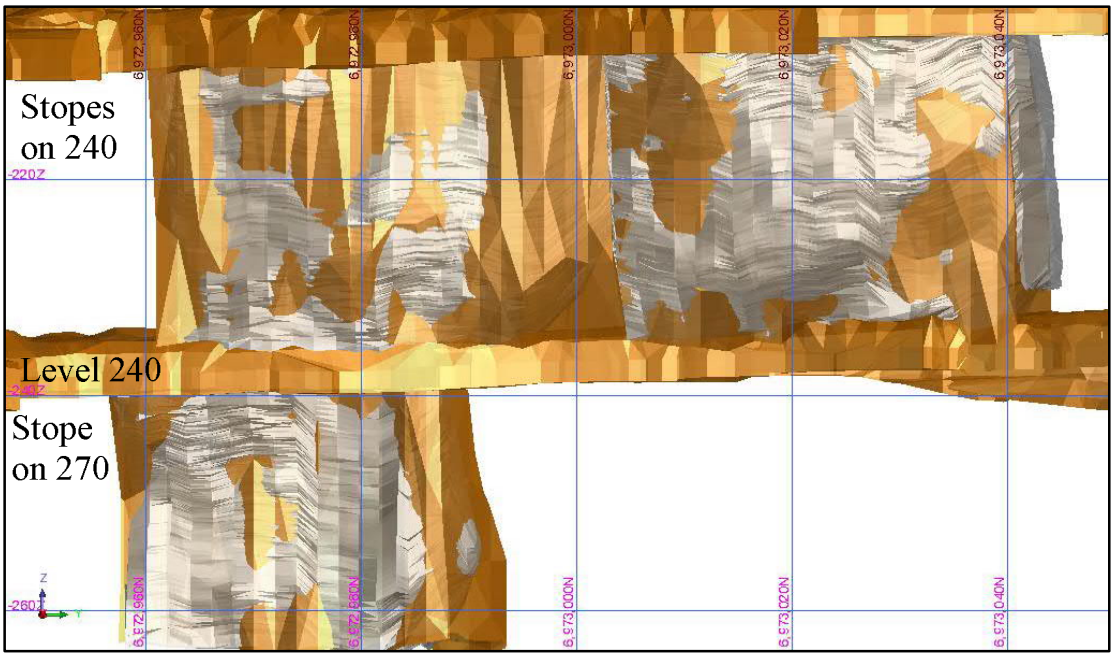

Figure 7.13: Visual layering of black schist overbreak in production levels 240 and 270 looking west

The Figure 7.14 helps to understand the black schist overbreak better. The stope 270L2 which is also visualised in the Figure 7.13, is displayed in a cross-section and looking north. The access drifts are visualised above and below the stope. A uniform vertical layer of overbreak that caves into the stope can be seen, especially in the right image. The footwall of the stope sustains overbreak in form of a consistent layer with a thickness of 1.0 metre.

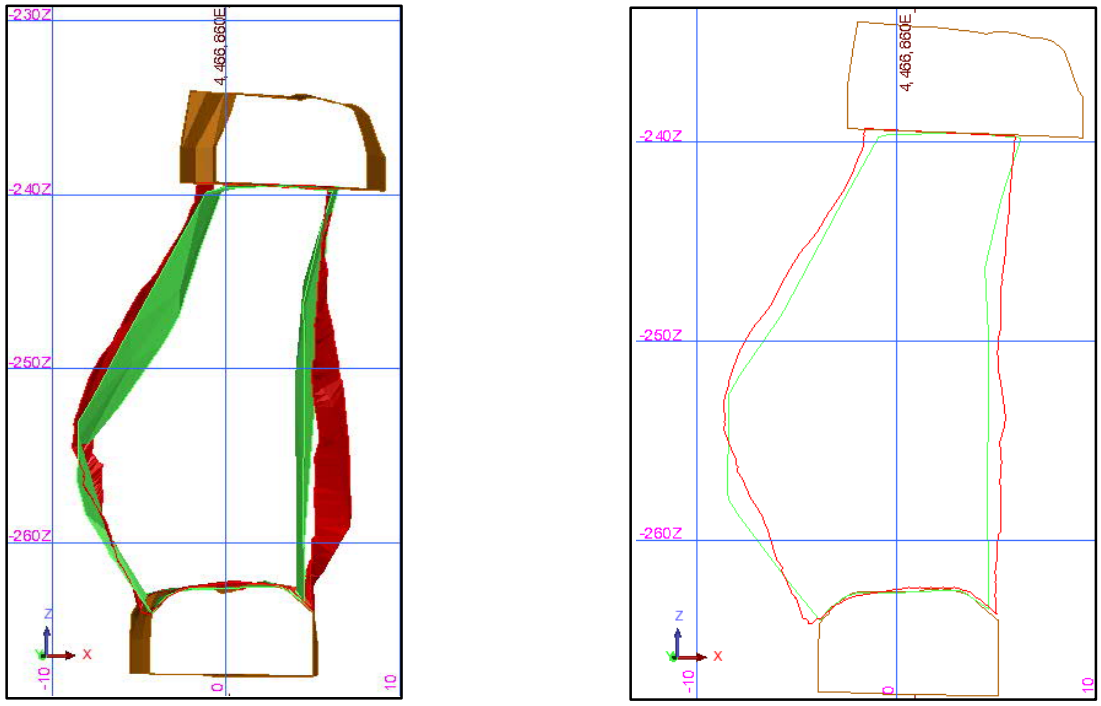

Figure 7.14: Cross-section illustration of the planned stope 270L2 (green) and its CMS scan (red) indicating uniform layer overbreak from black schist in the footwall (east)

Conclusively, black schist is a critical parameter to consider for stope planning. Although, it could not be proven numerically, the visual examination of the stopes that are affected by black schist shows clearly layered overbreak. This is presumably caused by caving graphite rich black schist layers.

8 Results and key parameters of transverse stoping

The identification of the most influencing parameters needs to be conducted on transverse stoping as well. The planning of transverse stopes is inherently different to longitudinal stoping which necessitates numerous other factors to be investigated. Those factors are considered to be the drift development, the backfilling technique and the stope type definition. Before introducing the identified key parameters of transverse stoping, the chapter shortly presents on overview of general ore loss and overbreak occurrence in the Kylylahti transverse stopes.

8.1 Ore loss and overbreak results

Because transverse stoping consists of primary and secondary stopes, the results of ore loss and overbreak are plotted for each stope type individually. The Figure 8.1 uses the equivalent linear lost ore (ELLO) and equivalent linear overbreak/sloughing (ELOS) method to convert obtained overbreak and ore loss volumes into an uniform layer. The hypothetical layer can be projected onto the total surface area of the stope sidewalls and helps to ease overbreak and ore loss understanding. A further benefit is the possibility to compare different stopes with each other.

Comparing the results, the equivalent layer of ore loss in secondary stopes is almost twice as thick as the primary stope layer. Adjacent CRF backfills in the sidewalls can be a reason for this. The CRF backfill requires drilling and blasting to operate further away from the backfill as in primary stopes to not diminish the backfill stability. Another reason for greater ore loss is that ore of secondary stopes adheres and sticks partially to the CRF backfill. Since CRF substitutes ore in the sidewalls of secondary stopes, the elevated CRF overbreak in these types seems reasonable. Primary stopes suffer conversely more ore overbreak due to direct ore contacts in the sidewalls. Any ore overbreak in secondary stopes is commonly non-existent since it is either waste or CRF backfill. The ore overbreak here is caused by upper level pillars breaking into the lower open voids and is conceived as a stope design issue (Malmberg, 2020c). The reason for excessive ore loss as well as the enlarged dilution in secondary stopes are addressed in the following chapters about key parameters.

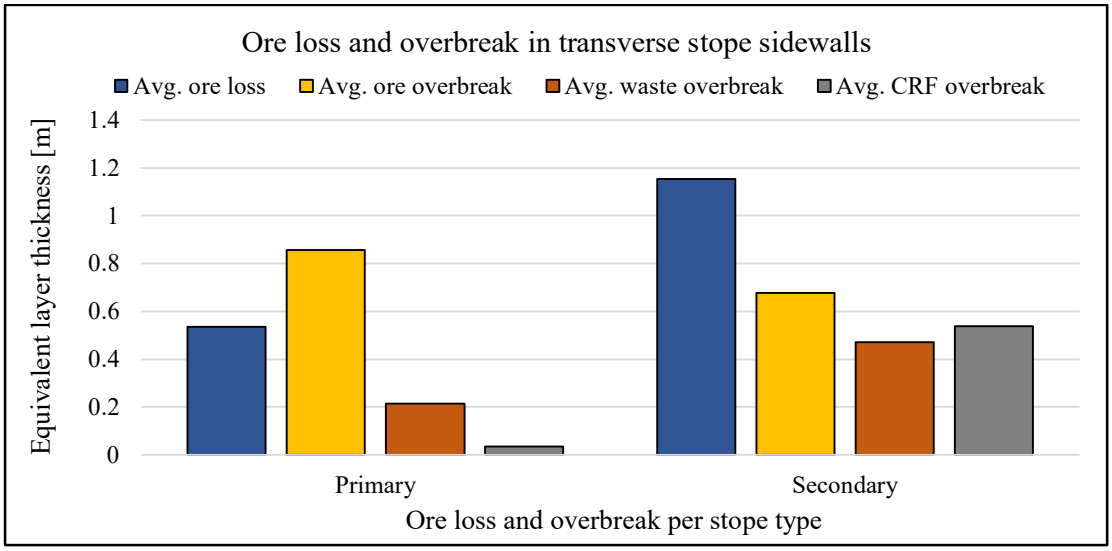

Figure 8.1: Ore loss and overbreak in transverse stope sidewalls

Further supplementation of statistical summaries is provided in Table 8.1 and Table 8.2. Attributes to evaluate stope efficiency i.e. ore loss and ore, waste and CRF overbreak are shown with included total overbreak. The total overbreak is defined as the addition of all overbreak types. Moreover, the tables include the 25 % and 75 % - quartiles. All numerical values have undergone the conversion after the ELLO and ELOS method. Whereas sidewall averages are already presented in Figure 8.1, the summaries provide results for transverse stope end walls as well. The apparent differences of enlarged overbreak and ore loss values in secondary stopes are only recognizable in the sidewalls. The end walls of both transverse stope types seem to behave almost identical with differences in the range of centimetres only. The comparison between sidewall and end wall is not recommended for the reason of vastly different surface areas that have been used for the conversion into ELOS and ELLO results. Only comparing values per each wall type provides reliable insights.

Table 8.1: Statistical summary of primary transverse stopes

Statistical summary of primary transverse stopes				
Attribute	**Wall type**	**Average [m]**	**25 % - Quartile [m]**	**75 % - Quartile [m]**
Ore loss	Sidewalls	0.39	0.20	0.47
	End walls	0.54	0.31	0.73
Ore overbreak	Sidewalls	0.86	0.43	1.12
	End walls	0.39	0.14	0.44
Waste overbreak	Sidewalls	0.21	0.03	0.27
	End walls	1.01	0.31	1.33
CRF overbreak	Sidewalls	0.04	0.00	0.00
	End walls	0.05	0.00	0.00
Total overbreak	Sidewalls	1.11	0.49	1.36
	End walls	1.45	0.59	1.75

Table 8.2: Statistical summary of secondary transverse stopes

Statistical summary of secondary transverse stopes				
Attribute	**Wall type**	**Average [m]**	**25 % - Quartile [m]**	**75 % - Quartile [m]**
Ore loss	Sidewalls	0.91	0.56	1.09
	End walls	1.15	0.58	1.46
Ore overbreak	Sidewalls	0.68	0.36	0.84
	End walls	0.34	0.11	0.49
Waste overbreak	Sidewalls	0.47	0.07	0.57
	End walls	1.04	0.30	1.43
CRF overbreak	Sidewalls	0.54	0.19	0.69
	End walls	0.12	0.02	0.10
Total overbreak	Sidewalls	1.67	1.09	1.99
	End walls	1.51	0.74	1.67

8.2 Mining sequence and stope types

The mining sequence determines the plan of stoping over the course of the entire production. When examining the longitudinal stoping sequence, a characteristic pertaining to ore loss has been made visual. The transverse stoping sequence is mainly driven by the sequence between primary and secondary stopes. The key parameter identification in this chapter emphasises the vertical location of primary and secondary stopes according to the extraction sequence.

The Figure 8.2 explains the different stope types that are found in Kylylahti. Transverse stopes typically consist of primary and secondary stopes. The difference in a further type distinction is made per level. The bottom stope is defined as the first and lowermost stope of the vertical sequence. Subsequently, the middle stope follows on top of the bottom stope with the third stope on the uppermost level. Three stopes are stacked upon each other at maximum in Kylylahti. Because stoping commences not strictly vertical but expands horizontally too, the explicit time of extraction is not relevant at this point. This is a main difference compared to the mining sequence analysis in longitudinal stoping.

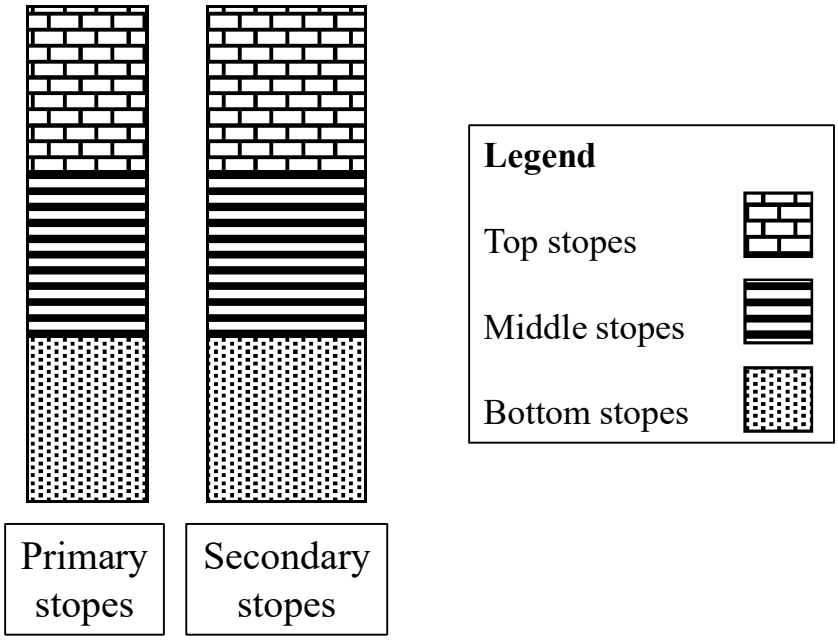

Figure 8.2: Schematic overview of stope type classification after vertical extraction

The Figure 8.3 shows the development of average total overbreak in transverse sidewalls. More specifically, the transverse stopes are classified into primary and secondary stopes with further division into the newly introduced bottom, middle and top stopes. The average overbreak layer of primary stopes which are classified as bottom stopes is the least (0.8 m). Stopes which are located in the middle sustain increased overbreak (1.3 m) with the largest overbreak (1.44 m) in top primary stopes. The discrepancy appears to be remarkably large between bottom stopes compared to the other two types. When comparing middle and top stopes only, the differences are comparatively low.

For secondary stopes, the trend behaves almost identical except for the middle stopes which sustain similar quantities of overbreak compared to the top stopes. Middle stopes suffer comparatively large quantities in contrast to bottom secondary stopes. Yet, both stope types generate significantly more overbreak on average than the equivalent primary stopes. It is recognizable that the differences between similar primary and secondary stopes decline with higher vertical location. Expressed in numbers, the discrepancies account nearly 0.6 m for bottom stopes and start to recline into 0.5 m for middle stopes and 0.4 metres for top stopes.

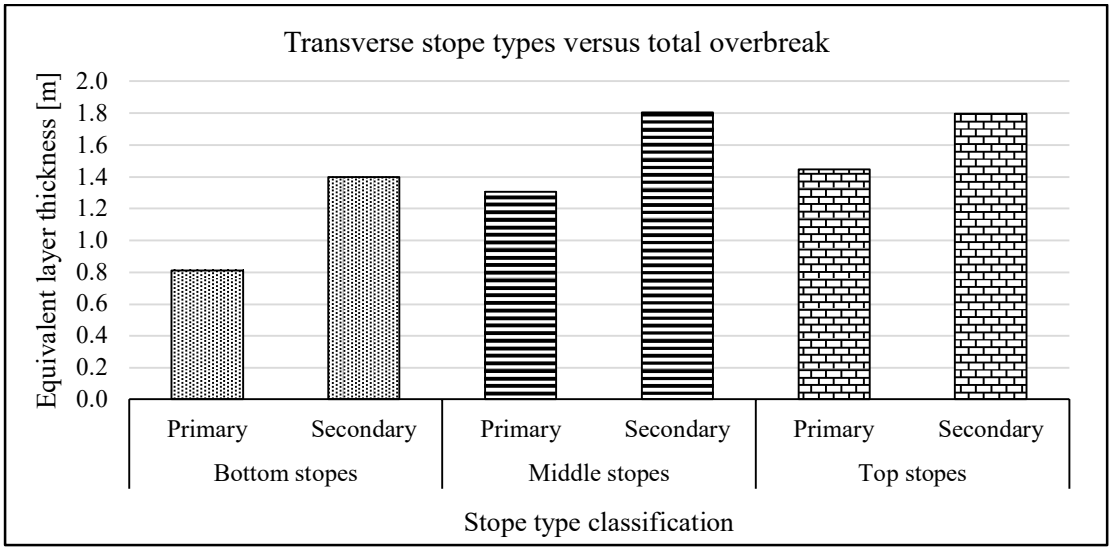

Figure 8.3: Transverse stope types versus total overbreak

It is demonstrated that the stope type after vertical extraction is a critical parameter to consider. When stacking the stopes, overbreak and stope stability are heavily deteriorated. This behavioural pattern of secondary stopes generating more overbreak in the sidewalls is mainly caused by conditions that have happened after primary stope extraction. CRF backfilling or shape differences from original stope plans are examples for post-mining conditions of primary stopes.

8.3 Stope design

The stope design has shown to affect longitudinal stoping with regard to the dimensioning and geometric complexity. Transverse stopes are less likely to undergo changes in their dimensions because the assignment into primary and secondary stopes already fixes preliminary designs. The width is overly 10 and 15 metres for primary and secondary stopes, respectively with predetermined stope heights of 30 metres. The stope strike length is limited to the Wombat orebody thickness and constrained by stability requirements. The analysis of the stope dimensions principally focuses on the stope strike length, the hydraulic radius and the aspect ratio which is defined as the ratio between stope length and height. The importance of hanging and footwall inclination on overbreak and ore loss concludes the chapter.

8.3.1 Transverse stope dimensioning

Transverse stoping is applied in areas of the deposit in which the orebody width becomes too large for longitudinal stoping. The stope strike length is the ultimate factor that can be subject to drastic changes because it is inherently linked to the orebody width. It is due to the mine planning department of the underground operation to assess the costs of drift development, additional slot raising and different ore tonnages when planning the total length of the stope (Malmberg, 2020a).

An apparent positive correlation of increasing stope strike length and increased overbreak is shown in Figure 8.4. The correlation becomes most distinctive when examining the total overbreak in the sidewalls of secondary stopes. The correlation coefficient is calculated as 0.6. The illustrated regression line slopes clearly upwards. Potential overbreak is

increased by roughly 0.3 – 0.4 metres with every increment of 10 metres in stope strike length. Further observations found a low negative correlation towards increasing stope strike length and reduced ore loss in the sidewalls. The development has been observed by the Kylylahti mining department as well which assumes that ore which is stuck to the sidewalls caves into the stope after longer exposure time with increasing stope length (Malmberg, 2020c).

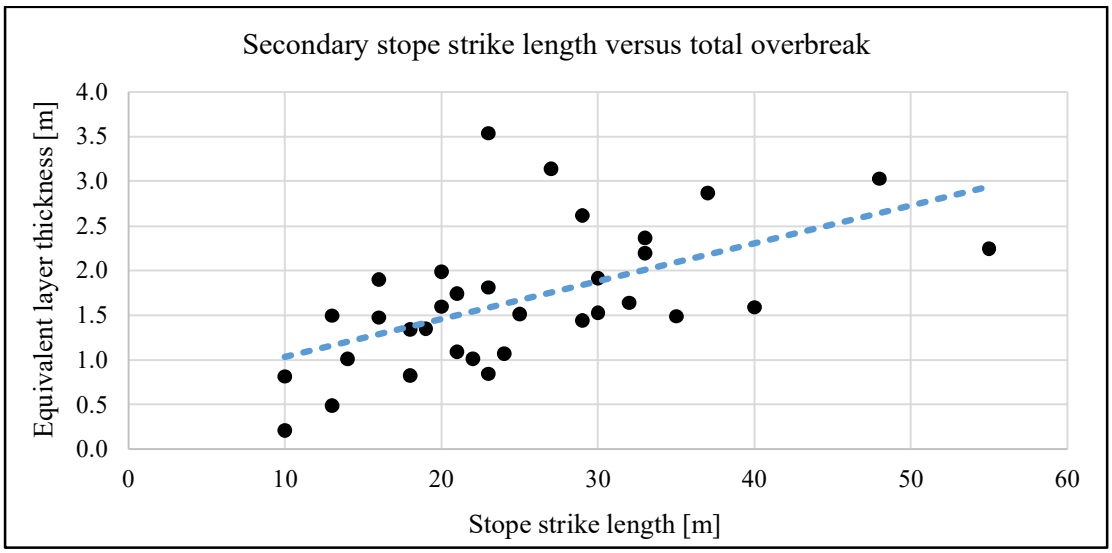

Figure 8.4: Secondary stope strike length versus total overbreak results in the sidewalls, r = 0.6

An additional correlation of overbreak and increased stope span is apparent when plotting the hydraulic radius against the total overbreak generated along the sidewalls of secondary stopes. Figure 8.5 displays a clear correlation of progressive overbreak and increased hydraulic radius. The positive correlation is indicated by the correlation factor of 0.6. Similar correlation is obtained for the impact of the aspect ratio on total overbreak. The hydraulic radius and the aspect ratio, which is the ratio of stope length and height, correspond directly to the stope length. As the stope length shows correlation to overbreak, so does the hydraulic radius and aspect ratio.

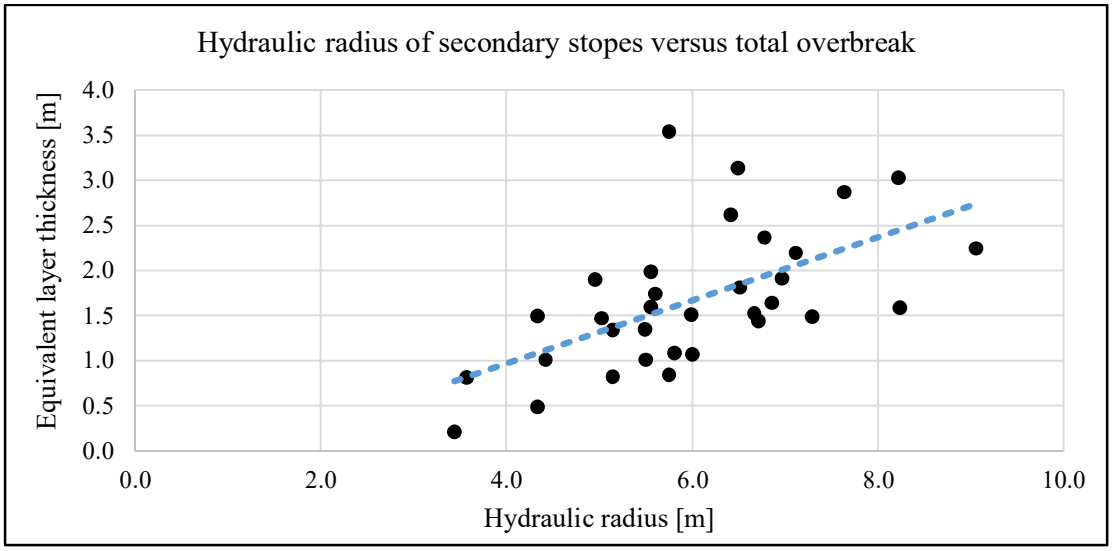

Figure 8.5: Hydraulic radius of secondary stopes versus total overbreak results in the sidewalls, r = 0.6

Primary stopes appear to be correlated less distinct to the stope length, hydraulic radius and aspect ratio increase. However, a high level of unpredictability in primary stopes is found in the scatter plots of length and hydraulic radius both plotted against total overbreak. The figures are enclosed in Appendix 5. As for the hydraulic radius, the threshold is defined as 6.0 metres after which stopes begin to fluctuate heavily in sustained overbreak. The critical threshold in terms of length is conceived to be 25 metres. Stopes show almost no correlation to length or hydraulic radius increments until they exceed the specific margin. Beyond the critical point, the range of sustained overbreak varies in an interval of almost 2.5 metres.

8.3.2 Effects of dip inclination

With varying length layouts, the stope dimensions are proven to affect transverse stoping. Another key parameter in transverse stoping is found to be the hanging and footwall inclination. The data that is used relies on the stopes that possess a distinct hanging and footwall. Figure 8.6 plots the results of hanging wall overbreak and footwall ore loss.

It becomes noticeable that with decreasing dip angle, the overbreak increases significantly. When the dip angle is straight vertical, the hanging wall suffers roughly 0.3 – 0.4 metres of overbreak. If the angle declines to 75 degrees, the amount of overbreak becomes twice as much. The identified correlation is found negative with a correlation factor of -0.64. Almost identical development is found when analysing the footwall angle according to sustained ore loss. It becomes obvious, that ore loss is promoted if the footwall angle flattens. Further proof is presented in form of the correlation coefficient of -0.76. It is attested that increased overbreak is commonly associated with shallower dips. Regarding the ore loss it is to conclude that shallower footwall angles promote ore loss. The suggestion can be made based upon the results that if the hanging or footwall angle declines 15 degrees, the amount of associated overbreak for the hanging wall and the ore loss for the footwall becomes twice as much.

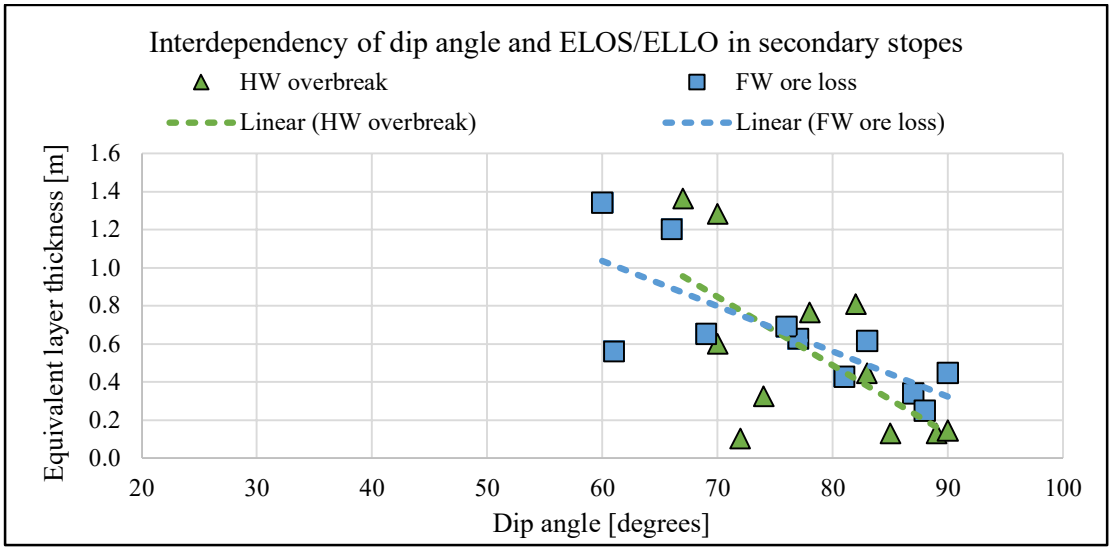

Figure 8.6: Dip angles of hanging/footwall in secondary stopes versus overbreak/ore loss, r_{HW} = -0.64 and r_{FW} = -0.76

The same characteristics cannot be duplicated with primary stopes. No distinct behaviour or pattern is noticeable when examining the numerical outcomes. A reasonable explanation emphasises the location of the primary stopes that have strict hanging and footwall. These stopes are mostly located in production levels 500 – 560. Primary stopes are split into many smaller primary stopes in those areas. Left waste rock pillars which are used to enhance stability also make proper interpretations of hanging and footwall more complex and less reliable.

8.4 Stope sub-type and environment

The geometric design has shown to heavily affect transverse stoping. Increasing stope sizes, especially in length, are associated with larger quantities of overbreak. The dimensions among primary and secondary stopes contain various sets of shorter and longer stopes. Mostly primary stopes have been split into multiple smaller stopes in the levels 500 – 590. The division into several smaller stopes has been utilised on secondary stopes as well. There are two reasons for the splitting which are nearby weak zones and intersecting waste rocks. The splitting of stopes allowed the first small stope to be mined and backfilled extremely quick. Short exposure time with fast backfill secured production and provided sufficient support towards the weak talc zone (Malmberg, 2020c). Other stopes were divided because of intersecting waste rock which is shown in Figure 8.7 as empty spot between stope 560ppL14/3 and 560ppL14/2. The green, blue and red stopes are planned designs with brown areas indicating the actual stope design after using the CMS scan. Visible red, blue and green spots automatically represent ore loss with brown areas indicating overbreak.

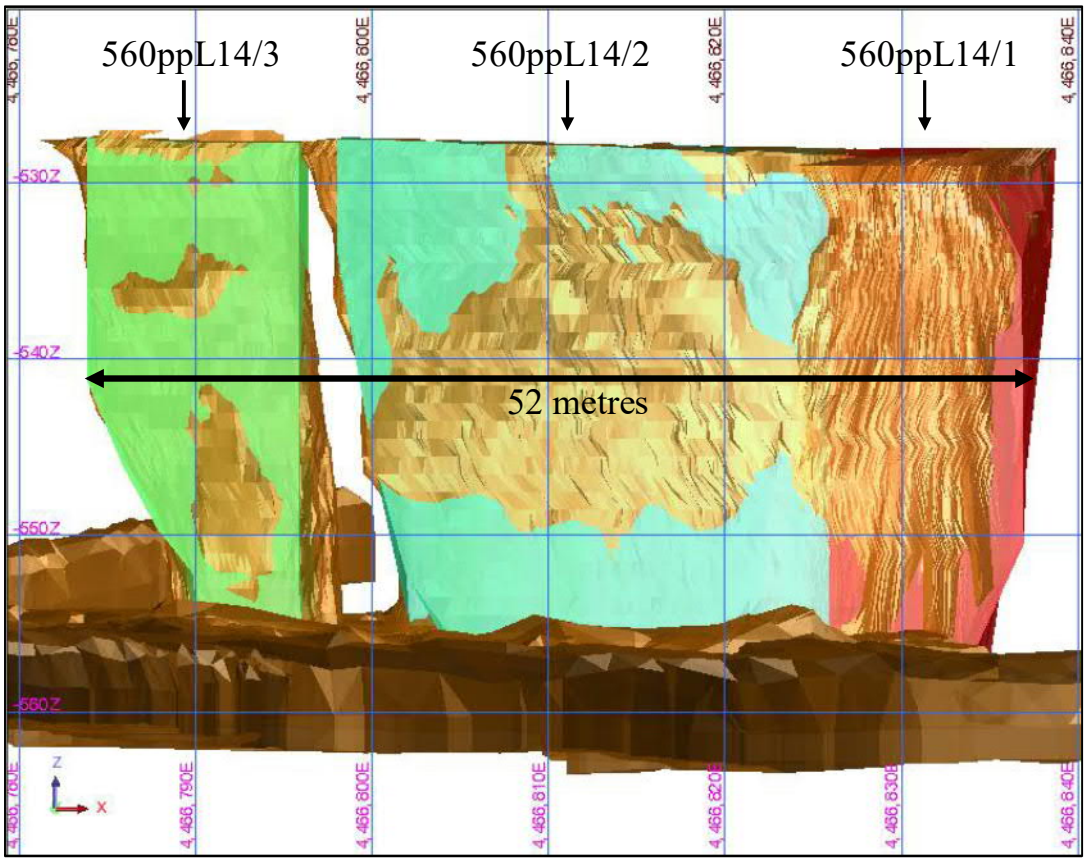

Figure 8.7: Sequential stope splitting shown for stope 560ppL14/1,2 and 3

The Table 8.3 comprises six different types of which type 1, 1.1 and 1.2 refer to primary stopes. The remaining types 2, 2.1 and 2.2 describe the secondary stopes. Further supplemented with the average total overbreak of the sidewalls, the stope environment explains the different conditions in which the sidewalls can be found. Ore comprises the sidewalls in almost all primary stope types whereas the end walls have direct contact to either ore, waste or CRF. The sub-type 1.2 is special as it comprehends an example of an ordinary primary stope (type 1) which is located next to CRF backfill of a longitudinal stope. The CRF is here situated in close contact to the sidewall opposed to an end wall.

Table 8.3: Transverse sub-types with different side and end wall environments

Stope side- and end wall environment		
Type	**Stope environment**	**Avg. overbreak sidewalls [m]**
1	Sidewalls in ore	1.17
	End walls in waste	
1.1	Sidewalls in ore	0.84
	One end wall in waste	
	One end wall in ore	
1.2*	Sidewalls in ore	0.83
	One end wall in waste	
	One end wall in CRF	
2	Sidewalls in CRF	1.70
	End walls in waste	
2.1	Sidewalls in CRF	0.51
	One end wall in waste	
	One end wall in ore	
2.2	Sidewalls in CRF	1.25
	One end wall in waste	
	One end wall in CRF	

Stope sub-types 1.1 and 1.2 are designed smaller than usual for the reason of stability assurance and excessive overbreak prevention. The division into sub-types 1.1 and 1.2 proofs to provoke less overbreak than single primary stopes with greater dimensions. Overbreak is reduced by nearly 0.3 metres. When comparing sizes, the type 1.1 is on average 9 metres long whereas the stope type 1.2 average 21 metres in length. The stope sub-type 2.1 and 2.2 are designed similarly averaging 10 and 26 metres in length, respectively.

Ordinary primary stopes (type 1) and secondary stopes (type 2) suffer the largest overbreak whilst having the largest dimensions. The effect of increased length on overbreak has been proven already in chapter 8.3. Combining the length of stope types 1.1 and 1.2 or 2.1 and 2.2, the total combined stope length is larger compared to ordinary primary and secondary stope lengths. The stope sub-types show less overbreak if projected along the entire stope span despite having larger dimensions. Yet, attention must be drawn to low elevations in ore loss for smaller secondary stope types compared to full-sized ordinary types. The benefits in reducing almost 0.8 metres of overbreak seem to justify the mild elevations for ore loss. The full results of the stope comparison are shown in Table 8.4. The original stopes did require stope splitting to prevent major talc collapses in the levels 500 – 590 and were not reduced because of too large stope dimensions. However, it is demonstrated that overbreak potential is reduced by decreasing individual stope sizes. It is also proven, that the overbreak from the hypothetical combined stopes produces less overbreak than ordinarily sized transverse stopes.

Table 8.4: Combined stope sub-type results

Combined stope sub-type results			
Type	**Avg. stope length**	**Ore loss**	**Avg. total overbreak**
Units	[m]	[m]	[m]
1	23.5	0.39	1.17
1.1 + 1.2	27	0.33	0.8
2	26.5	0.80	1.84
2.1 + 2.2	36.5	1.07	1.05

Examining the total overbreak composition, large quantities of CRF and increased volume of ore accounts for the overbreak in secondary stopes. The Figure 8.8 depicts the overbreak composition which contains ore, waste and CRF overbreak. It displays the location of the stopes per orebody location. Any transverse stope located within the orebody is referred to as inside. The stopes at the edge of the orebody with almost one full sidewall in waste are considered outside.

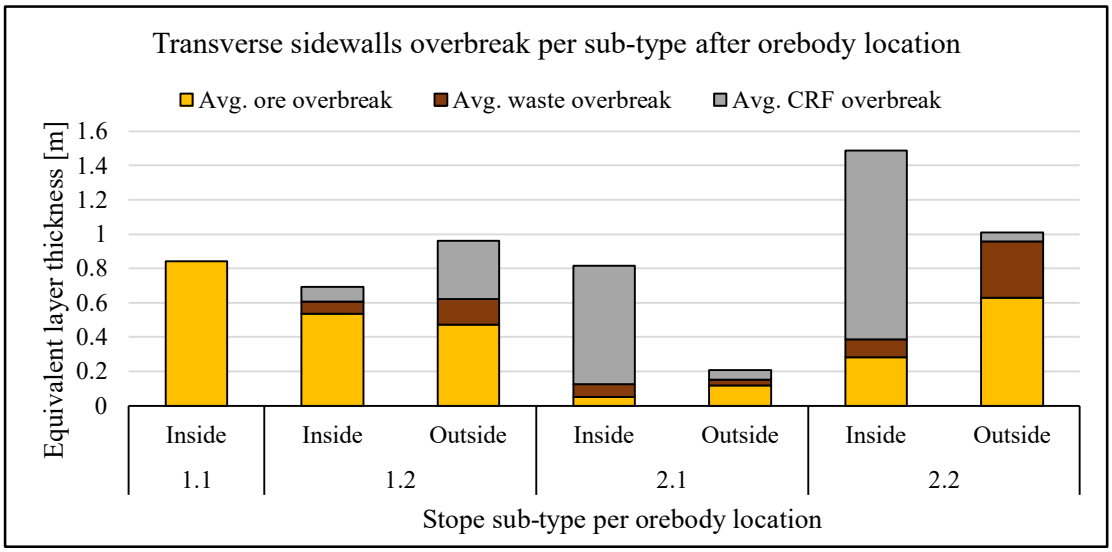

Figure 8.8: Transverse sidewalls overbreak per sub-type after orebody location

Pertaining to the primary stopes, ore overbreak contributes the most to excessive dilution with little CRF contribution in sub-type 1.2. Stopes that are classified as special type 1.2 are the cause for the unusual CRF contribution in primary stopes. Interesting is that secondary stope type 2.1 shows greater sidewall dilution if located inside the orebody compared to stopes located at the edges. The higher degree of instability is most prevalent in the type 2.2 which translates into excessive CRF overbreak if located inside the orebody. For stopes located at the orebody edge, the overbreak composition consists mainly of ore and waste rock. As the transition of the orebody boundary towards waste is rather gradual than sharp, ore is diluted with waste and causes ore overbreak excess in sub-type 2.2.

If the economic viability withstands the increased expenditures in form of additionally required backfill, more drilling and time delays, the division into multiple stope types is a practical tool for reducing large dilution and instability. The overbreak in standard primary

and secondary stopes exceeded the overbreak of the split stopes. For primary stopes and particularly secondary stopes, the location of the stope regarding the orebody is found to have a major impact on the overbreak composition but also on overall dilution occurrence.

8.5 Post-mining conditions of primary stopes

The subdivision of primary and secondary stopes has shown that different overbreak profiles are associated with respective sub-types. Another key parameter of transverse stoping is considered to be the post-mining conditions of primary stopes. Due to the overall mining sequence, secondary stopes are reliant on how primary stopes have performed. The main factors to influence secondary stope environments are but not limited to blast-induced damage to adjacent rock mass, post-mining shapes of primary stopes and CRF backfill. If primary stopes suffer large ore overbreak from the sidewalls, the general shape becomes less rectangular and more barrel shaped. The same characteristics have been found in longitudinal stopes which became relatively bulky amid the sidewalls but showed extended ore loss towards end wall corners. The shape also resembled a barrel to some extent.

The Figure 8.9 illustrates a practical example in which primary stopes (blue) sustain severe ore overbreak (brown) and become barrel shaped. The highlighted space in between the primary stopes indicates the area in which secondary stopes are planned. The issue of large ore overbreak in primary stopes is most prevalent in the levels 560 – 620. At the same time, the greatest abundance of ore loss in the secondary stope appears explicitly in the same levels as well.

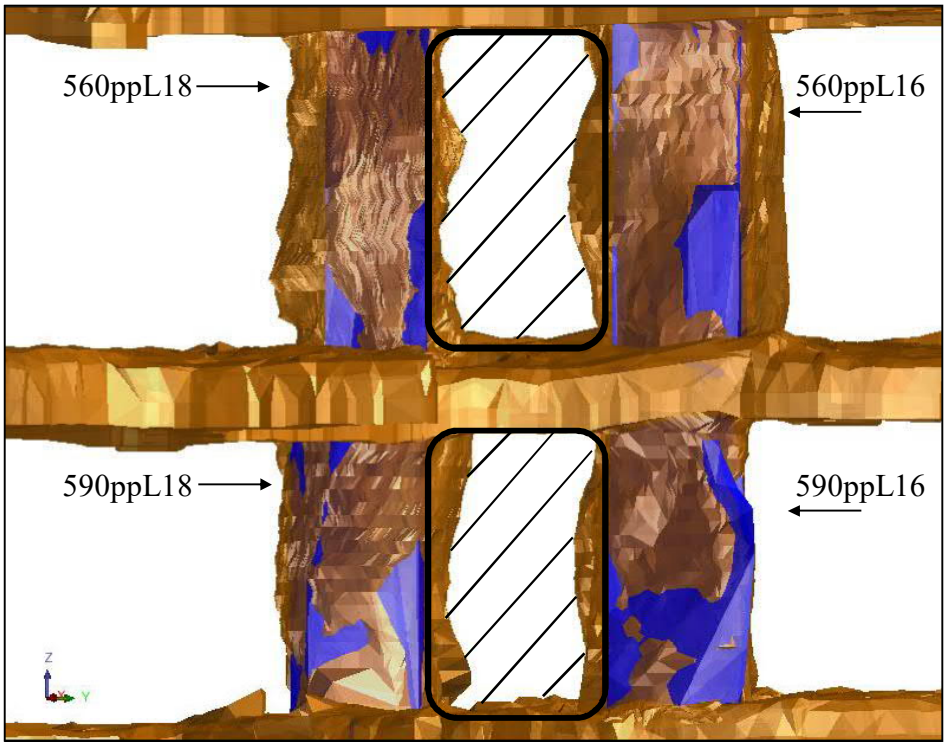

Figure 8.9: Post-mining issue in form of excessive primary stope ore overbreak

The distribution of ore overbreak in primary and ore loss in secondary stopes across the Wombat production drifts is plotted in Figure 8.10. Presented numerical results comprehend average ore overbreak and ore loss per level. The ore overbreak and ore loss total roughly 0.5 metres of equivalent layer thickness in the shallower levels. Besides a relatively low accumulation of ore overbreak and ore loss until level 530, a compelling increase in both is noticeable from level 560 onwards. Interesting is the correspondence of ore overbreak to ore loss and vice versa. If primary stopes suffer larger ore overbreak, secondary stopes incur similarly more ore loss. Note, that the deviation in level 590 is produced by one particular primary stope on the edge of the orebody. No ore loss can be associated with secondary stopes as the production drift closes with the primary stope.

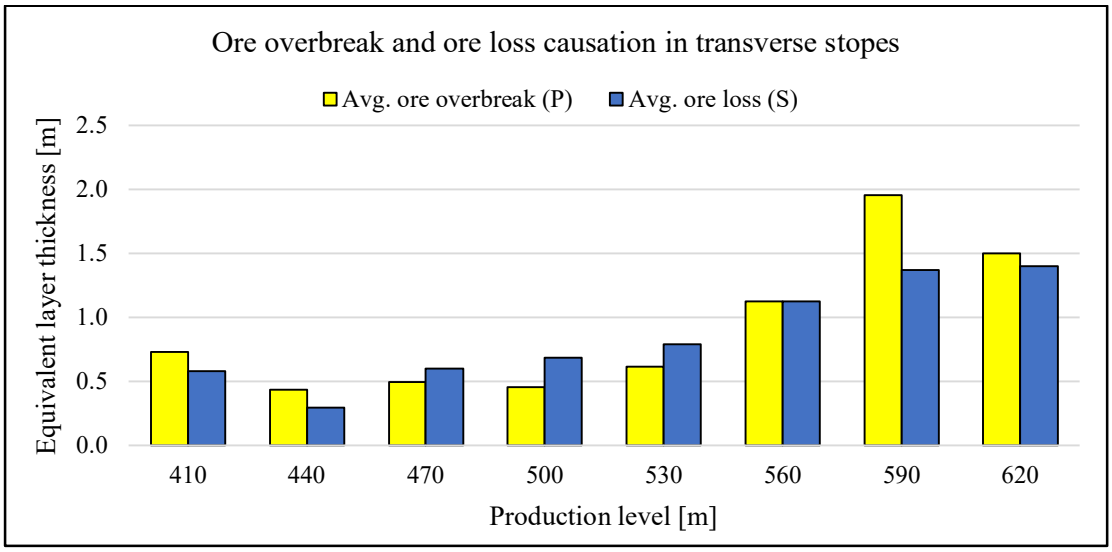

Figure 8.10: Ore overbreak and ore loss causation in transverse stopes

The correspondence of ore loss on ore overbreak is also found when checking explicitly for correlation. Concerning the Figure 8.10, the correlation factor is calculated as 0.91 which is close to maximum correlation. When comparing the results for ore overbreak and ore loss of the levels 410 – 530 to levels 560 – 620, the trend is even more prominent. With the ore overbreak and ore loss averaging 0.46 and 0.6 metres in the levels 410 – 530, the numbers total 1.33 and 1.35 metres in the lower levels, respectively. The correlation coefficient surges in maximum correlation of 1.0.

The reason for this development is mainly caused by the post-mining conditions of primary stopes. Since the primary stopes sustain overbreak in form of ore, the blasted stope shape differs from initial plans. The stopes become dilated and resemble eventually a barrel. When backfilling the stopes, the CRF adapts to the delineation of the blasted void. The different final shape raises problems concerning the secondary stopes which translates into operational limitations of the drilling equipment that causes ore loss. An attempt is made in the Figure 8.11 to visually explain the correlation of ore overbreak and ore loss. Primary stopes which have been mined and backfilled with CRF are coloured grey and are namely P1, P2 and P3. The remaining secondary stopes S1 and S2 are coloured in brown and have not been mined yet.

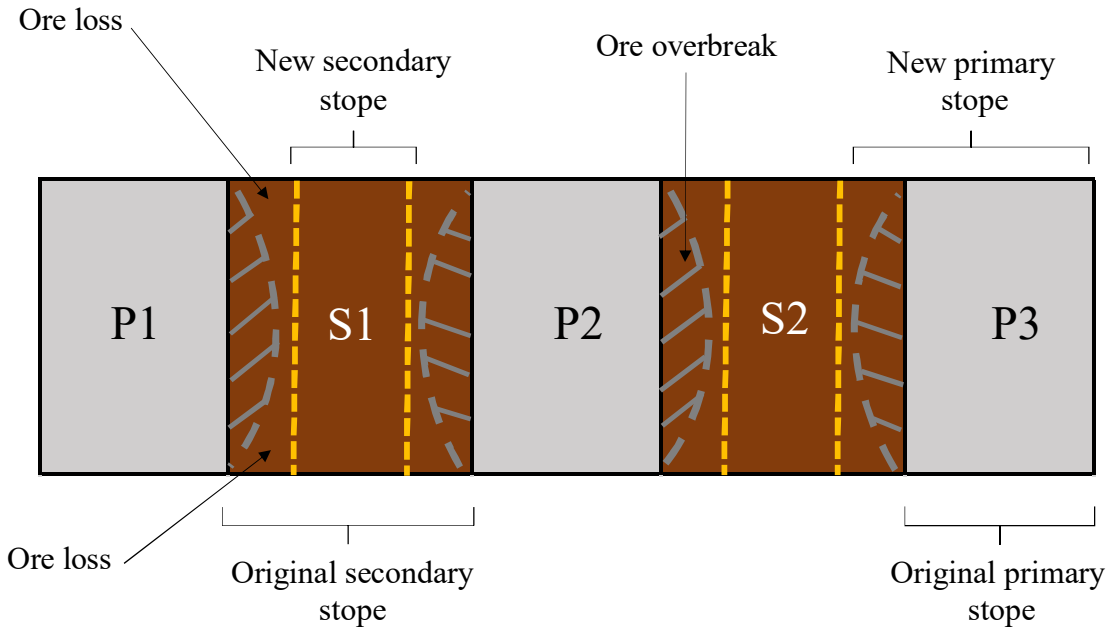

Figure 8.11: Schematic illustration of ore overbreak and ore loss correlation

Planned primary stopes are commonly designed rectangular and within standardized limits. Additional abutments along the sidewalls represent ore overbreak. The transition of the initial rectangular design into the barrel shape is highlighted. It must be stressed, that the illustration is not in scale and overbreak and ore loss are exaggerated for explanation purposes. A real case scenario is shown in the Figure 8.9. It has been decided that primary stopes sustain dilution on all sidewalls in this illustration. Ore overbreak can also occur only partially on one sidewall as the stope 590ppL16 in the Figure 8.9 shows.

In the Figure 8.11, the original secondary stopes are exaggerated in their perfect rectangular shape. In reality, secondary stopes S1 and S2 are designed more precisely with regard to the final layout of the mined primary stopes that became dilated. Blasthole drilling becomes increasingly complicated as a consequence. To retain CRF stability, the blastholes must be drilled with minimum safety distance of roughly one metres apart from the backfill (Malmberg, 2020a). Fan-drilling is typically used for blasthole drilling in secondary stopes. The drilling equipment is limited in its operational functionality and cannot access the entire ore in the stope sufficiently due to the elevated complexity of the CRF backfill shape. The secondary stopes that are eventually mined (yellow dashed line) are remarkably reduced in width. Both secondary stopes S1 and S2 loose significant quantities of ore in the corner on top and explicitly on the bottom because of insufficient fragmentation of ore.

It is demonstrated that the data of mined primary stopes can be utilised to approximate correlating ore loss for nearby secondary stopes. Further, it can be concluded that more primary ore overbreak translates into more ore loss in adjacent secondary stopes. On the other hand, ore loss will drop concurrently with decreasing ore overbreak. As opposed to the other parameters which have proven to impact transverse stoping actively, post-mining conditions is a parameter to consider prior the planning of primary stopes for more accurate production planning.

9 Best and bad practices for overbreak reduction

Besides the examination of key parameters, the study attempts to determine best and bad practices on how to reduce and control stope dilution and overbreak. Best practices are defined as methods that prove to restrain excessive overbreak and ore loss in stopes whereas bad practices promote overbreak and ore loss. The chapter starts with best practices first and follows accordingly with the explanation of bad practices and recommendations.

9.1 Best practices

Different factors such as varying stoping methods must be considered to prevent excessive dilution and ore loss. Longitudinal stoping differs in most aspects from transverse stoping. The adherence to a proper longitudinal mining sequence has shown to have a great impact on ore loss and overbreak in the Wallaby orebody. The results demonstrate that ore loss constantly shrunk with more years in operation as shown in Figure 7.2. The ore loss particularly towards CRF backfill was reduced significantly. This positive development is presumably due to increased confidence of how CRF backfill responds to nearby blasting.

A certain degree of stope instability is inherently accompanied when suffering overbreak. The backfill is found to have no negative impact on stope dilution. Because the CRF substitutes ore in the sidewalls of secondary transverse stopes, the consequence of increased CRF overbreak is reasonable. Non-existent CRF overbreak in longitudinal end walls proof the appropriate backfill mixture and application in Kylylahti. The overall sufficient performance of backfill and mixture has been observed.

The primary stopes in Kylylahti show a high level in unpredictability of overbreak if exceeding 25 metres in length. In chapter 8.3, a correlation effect is proven for overbreak to increase with larger stope dimensions. The sequential splitting divides ordinary transverse stopes into smaller stopes. Each of these smaller stopes is relatively short which translates into individual little overbreak. The correlation impact has been reduced remarkably as shown in Table 8.4. Standard primary and secondary stopes are on average 24 – 26 metres long and sustain overbreak of approximately 1.2 and 1.8 metres, respectively. The smaller stope sub-types 1.1 and 1.2 or 2.1 and 2.2 combined in one large theoretical stope average 27 and 36 metres with drastically reduced overbreak of 0.8 and 1.0 metres.

An additional operational advantage is that stope splitting offers the possibility to extract the first minor stope with unconventional longitudinal drift development. The establishment of the entire drift development for transverse stoping postpones the production severely. The possibility to extract small stopes already during production drift development is highly recommended from an economic perspective. Dependent on the distribution of high-grade ores, the drift development can be planned accordingly to be able to extract smaller high-grade stopes first during the development construction. Larger transverse stopes with mediocre grades can be mined after drift development completion (Malmberg, 2020c).

Other best practices require the stope design to be as simple as possible. In chapter 7.3 is demonstrated that increased overbreak is associated with more complex stope designs. Another contributing factor to overbreak is the inclination of stope walls. Declined stope walls are a decisive factor to provoke overbreak in the hanging and ore loss in the footwall.

The more vertical stopes walls are designed, the less potential towards overbreak and ore loss exists in the stopes. The summary of best practices is concluded as the following:

- Sufficient mixture and application of CRF backfill in longitudinal and transverse stoping
- Sequential stope splitting in transverse stopes which are extremely large or located near known weakness zones
- Aiming for simplified or basic stope designs with no sharp shape changes
- Aiming for steeply dipping stope sidewalls

9.2 Bad practices

Operating two mining method concurrently imposes rock mechanical concerns mostly on longitudinal stoping. In 2016, Pöyry Finland Oy (2016) conducted a rock mechanical study on how stresses are re-distributed over the life of mine (LOM) in Kylylahti. The numerical modelling showed enormous potential of damage to stoping and drifts development in the southern and northern ends of lower Wombat levels. The mid-centre of some lower production drifts also partially sustained high stress concentration because mining was done from north and south towards the middle. The stress peaks indicated magnitudes of more than 100 MPa. In most of these peak areas, longitudinal stopes are used as principal mining method to extract the remaining ore. The time of extraction is seen as critical aspect when operating two mining methods at once. The Wallaby stopes are relatively quickly extracted with most of the drifts being depleted within one year or less. The time to complete longitudinal stoping per drift in Wombat averages more than two years which is twice as much. Further stress modelling results are attached in Appendix 6.

The stope shape complexity is recommended to be as basic as possible. Higher levels in geometric complexity strongly correspond to larger dilution. Stopes that are determined to have high to severe complexity sustain significant overbreak. Very complex stopes usually contain separate waste solids which complicate mining severely. The issue can be resolved with selective mining of waste solids prior to ore. Complex stopes without intersecting waste solids are suggested to undergo a reduction in size or the split into smaller stopes to decrease overbreak potential. This applies to longitudinal and transverse stopes alike. Transverse stopes in particular can avoid unfavourable settings while being strictly perpendicular to the strike of the orebody. Concurrent emphasis must be laid on the stress directions that could modify the strict perpendicular settings of transverse stopes (Malmberg, 2020c).

Longitudinal stopes in the Wombat orebody are rather used as supplementary method for spot areas. The consequence is a lack of proper sequencing. The adverse effect of not operating with proper sequencing mixed with another mining method presumably deteriorates the identified stoping parameters. When comparing the correlation of stoping parameters, the factor of stope dimensioning is found to impact Wombat stopes less distinct than stopes in Wallaby. The results are stated in chapter 7.3.

9.3 Suggestions on precautions and improvements

The improvements towards less overbreak and ore loss happen to concern the geometric complexity, the stope dimensions and reinforcement methods. The difficulty in implementing any improvement is mostly driven by technical feasibility, economic viability and staff experiences. Especially concerning staff experience it is to say that there is no

professional staff in Kylylahti that supported the mine planning department with geotechnical data. Rock reinforcement and cable bolting are options that are commonly applied to stabilize development drifts. Without a rock mechanics department on-site, no proper rock mechanical investigations are made. Upper level drifts of each stope have cable bolts installed with some variation in bolting pattern over the past eight years (Malmberg, 2020a). Preventive actions regarding high dilution numbers comprise additional cable bolting in stope sidewalls. Because there has not been any rock mechanic engineer permanently on-site, the drifts were not designed for supporting the stope sidewalls with cable bolting. Single cases in Kylylahti have successfully used cable bolting to secure stope stability, which proofs that cable bolting could translate into improved stope sidewall stability. Dependent on the expenditures, cable bolting could offset the need for stope splitting when drifts are designed appropriately for the cable bolt use.

10 Discussion

The results of the in-depth analysis must be set into perspective as they can add valuable knowledge to the way stoping is planned. Yet, there is the need to critically assess the data acquisition by means of the custom-built macro. The chapter introduces to the advantages and drawbacks of the macro. An objective assessment and discussion on the meaningfulness of key parameters follows accordingly. The chapter concludes with an outlook which mainly concerns data interrelations and data that could not be used for the analysis.

10.1 Benefits and drawbacks of macro application

The equivalent linear overbreak/sloughing (ELOS) and equivalent linear lost ore (ELLO) methods have been key aspects in the determination of most influencing parameters for stoping. The CMS scan is paramount for evaluating stope performance to fully comprehend the blasted stope conditions. The macro has proven to be a reliable and an extremely helpful tool for the stope reconciliation. The greatest benefit of the macro application is understood as the high degree of freedom and flexibility for the user. It is up to the user's needs to define box sections. This allows to scrutinize stopes after their hanging and footwall, upper and lower stope areas, and spot analyses in the stope corners. The second biggest advantage is the traceability of overbreak from certain ore lenses or backfilled stopes. The localisation of critical spots in terms of CRF or ore overbreak in a distinct area can be conveniently assessed and helps to put the stope performance into a broader context.

Besides the overly positive characteristics of the macro, there are certain drawbacks and disadvantages to address. One of the two major drawbacks is the manual box creation which leads to increased biasedness and inaccuracy. The boxes must be drawn by the user and the success is defined over his or her experience and capability. The second disadvantage mainly concerns the lacking flexibility to follow hanging and footwall if they repetitively switch sides in a large longitudinal stope. Combined with overall complex stope designs, simplification steps must be applied, or the time consumption becomes almost exponentially larger. A full overview of benefits and disadvantages is presented in Table 10.1. Suggestions on improvement mainly emphasise to overcome the prevalent manual aspect of running the macro and develop boxes. This is likely to be accomplished with proper expertise in programming and coding by means of for example WSP Finland as in this study.

Table 10.1: Benefits and drawbacks of the macro utilisation when establishing the ELOS and ELLO database

Benefits and drawbacks of the macro utilisation	
Benefits	**Drawbacks**
Side-specific allocation of ore loss and overbreak in sidewalls and end walls	Self-development of boxes leaves room for human (user) error
Great traceability of certain ore types, ore lenses and backfill types per stope wall	Biased accuracy due to no absolute consistency in boxes (re)-creation
Possibility to check on properly blasted drillholes and resulting CRF (in)stability	Definition of sections must be determined universally and adhered to in each stope
Examination of ore loss and overbreak occurrence according to their origin	Lacking flexibility when following hanging and footwall in complex stopes
Exact localisation of ore loss in corners, end walls and sidewalls possible	Highly time-consuming due to limitations in computational capacity
Reconciliation tool for safety distance factor pertaining to drillhole distance towards CRF	New cut-off on pre-defined ore lenses results in ore overbreak instead of waste overbreak

The fundament of the macro application is mainly built upon the CMS scan as post-mining information. Any mistake or inaccuracy in the CMS scan eventually diminishes the macro results and ultimately, the stope reconciliation (Malmberg, 2020b). The key aspects to consider when working with the CMS scan data as primary input are listed as the following:

- **Semi-mobile nature**
  The CMS device is dependent on the maximum range of the telescopic stick that it is attached to (limitations in very long stopes)
- **Possibility of blind spots**
  Because the laser cannot see behind outcropping boulders in the stope walls, some area projections can be incorrect
- **Rock type distinction**
  CMS laser can only see if material is left in stope but cannot identify whether it is ore, waste or CRF backfill
- **Measurement frequency**
  The CMS is applied once the stope is mucked empty, no time-to-time measurements document the stope condition development

10.2 Critical assessment of key parameter results

The objective of this study is to identify the most important parameters to longhole open stoping in the Kylylahti underground mine. The data has shown various correlations amongst different parameters such as the stope dimension and the geological formations over to the mining sequence and the post-mining conditions.

- Key factors of longitudinal stoping

The identified key parameters on longitudinal stoping have shown to affect longitudinal stopes in both orebodies similarly. Correlations have been found on the mining sequence, the effect of mining directions, changing stope dimensions and geological dependencies. Throughout the examination of longitudinal stoping data, the reduced effects of identified parameters are found on stopes which are located in the Wombat orebody. The separation of stopes into both orebodies, Wallaby and Wombat, is considered important as they differ heavily in their regional environments. No uniform mining sequence and mining direction can be attested to the Wombat stopes.

The key parameters regarding longitudinal stoping have further shown to impact the Wallaby orebody the most. It is understood that the operation of two stoping method deteriorate the effect of key parameters on longitudinal stoping to a certain extent which complicates the overbreak predictability. All parameters are yet proven to have an impact on Wombat stopes despite the unfavourable settings imposed by transverse stoping. Conclusively, the results withstand the influence of transverse stoping in most cases. The parameters which have been identified are considered valid and proven to influence longitudinal stoping.

- Key factors of transverse stoping

Transverse stoping is affected by numerous parameters as demonstrated in this study. Besides the vertical mining sequence, the stope design is a factor that influences stoping. The correlation between increased stope strike length and increased overbreak is attested. Similar correlation is found pertaining to aspect ratio, which is defined as the length to height ratio, and the hydraulic radius since they both correspond directly to the stope strike length. Although the overbreak occurrence in primary and secondary stopes coincide with varying stope dimensions, the identified factors show less distinct development in primary stopes.

A high degree of overbreak unpredictability is found when primary stopes exceed 25 metres. The fluctuation in overbreak ranges from less than 0.5 metres to more than 3.0 metres amongst stopes that are longer than 25 metres. Similar behavioural development is retrieved for primary stopes when exceeding the hydraulic radius of 6.0 metres. Yet, secondary stopes do not show sensitivity to any unpredictability when exceeding certain stope lengths. The database does not provide more information to conclude why primary stopes start developing a high level of unpredictability from 25 metres length onwards. Similar trends were found in research of Henning and Mitri (2007). They found that primary stopes gain significantly larger susceptibility towards unfavourable conditions such as relaxation zones and stress redistribution when exceeding 20 metres in stope strike length. The final interpretation of this characteristic is not explainable with the limited data and must be addressed to further research projects.

Another parameter affecting transverse stoping is defined as hanging and footwall inclination. It is demonstrated that hanging wall overbreak and footwall ore loss increase when the respective dip angle declines. A suggestion is made that a dip decline of 15 degrees translates into twice as much overbreak and ore loss. The data used for the identification of the parameter comprises 16 stopes in total which corresponds to the little number of transverse stopes showing distinct hanging and footwalls. More data is required to establish

a comprehensive database although a first approach in the dip angle and overbreak/ore loss correlation is made.

Lacking sufficient data is a further concern regarding the sub-type analysis in chapter 8.4. It has been shown that smaller stope sizes result in reduced overbreak with stope sub-types 1.1, 1.2, 2.1 and 2.2 controlling overbreak better. However, the sample size of smaller transverse stope types is relatively small. Table 10.2 comprises the frequency of each stope that is found in Kylylahti. Type 1 and type 2 refer to ordinary primary and secondary stopes, respectively. The majority of transverse stopes in Kylylahti consist of these stopes.

Table 10.2: Frequency of transverse stope sub-types

Frequency of sub-types	
Sub-type	**Frequency**
Type 1	29
Type 1.1	1
Type 1.2	6
Type 2	24
Type 2.1	2
Type 2.2	3

Except for sub-type 1.2, the abundance of sub-types is very little. The database ideally contains at least 10 cases per type to fully examine their behaviour and their sensitivity towards overbreak and ore loss. The overall development yet demonstrates that smaller stope types preferably incur less overbreak than commonly sized transverse stopes.

10.3 Lack of interdependent influences

When checking for important factors that show an impact on stoping, the parameters that are found in this study have been examined exclusively. On the one hand, the results cannot be denied concerning their impact on stoping. On the other hand, stoping is a dynamic process which constantly underlies multiple factors and parameter concurrently. If only the length of a stope is extended, overbreak is likely to be increased as proven in this study. If other parameters such as blasting pattern, drillhole accuracy, rock mass or dip inclination are changed simultaneously with the length, the same stope presumably behaves differently than expected. The chances are high that overbreak is reduced because of more competent rock mass or because the dip inclination became steeper which is more favourable for stable sidewalls. The probability of overbreak being promoted is also given if blasting pattern are less accurately planned or the geometric complexity of the stope becomes more difficult.

The correlation of the stope length and overbreak is not necessarily obvious in the data because stoping underlies a certain dynamic and considers several parameters at once. The interdependency and in particular the weighting factor of such parameters has not been scrutinized in this study. In fact, the consideration of single factors and their effect on stoping is a prevalent issue to the mining industry and to research. It cannot be said with certainty that the stope length, width or height are acting more dominant in provoking overbreak than the dip inclination or geometric complexity. The issue of lacking information on the parameter interdependency in stoping is globally known but yet slowly picking up. An attempt is made by Heidarzadeh et al. (2019) who tackled the intercorrelation of stope dimensions and hanging wall inclination. By establishing a probability factor of failure, they

simulated over 400 scenarios with varying stope dimensions and hanging wall angles. They aimed for creating a predictive database that can be used for general predictions of how the input parameters are balanced against each other.

10.4 The multi-causation of stoping parameters

The multi-causation of different parameters on stoping is eminent important to fully understand. With better recognition of how factors offset, accumulate or diminish their impact, the stope planning becomes more manageable and pre-mining profitability calculations are more accurate (Malmberg, 2020c). The degree of correlation among these parameters is highly complex and requires more research (Heidarzadeh, et al., 2019). In the Kylylahti underground mine, a specific region has been identified that is not yet evaluated. The respective production levels nicely demonstrate the issue of multiple parameters affecting stoping simultaneously.

The production levels 560 – 620 gained attention in chapter 8.5 when examining the correlation of ore overbreak excess in primary stopes and secondary stope ore loss. The Figure 8.10 depicts the elevated profiles of ore overbreak for the critical levels 560 – 620. The analysis of total overbreak in the primary stopes (Figure 10.1) shows even greater dilution deviations amongst various drifts. The total overbreak for all primary stopes averages 0.7 metres excluding the levels 560 – 620. The excluded levels in particular contribute an average overbreak of 1.8 metres in comparison. In absolute numbers, the critical levels account for 300 % of the average overbreak in primary stopes in Wombat.

The different primary stopes are highlighted with respect to their location. Note, that levels 650 – 710 are not suitable for the level analysis as they lack density of data points. It becomes obvious that the critical levels underlie an anomaly as they differ vastly from other stopes. When aiming to find a reasonable explanation to the behaviour of these stopes, it is almost impossible due to the multi-dependency of parameters.

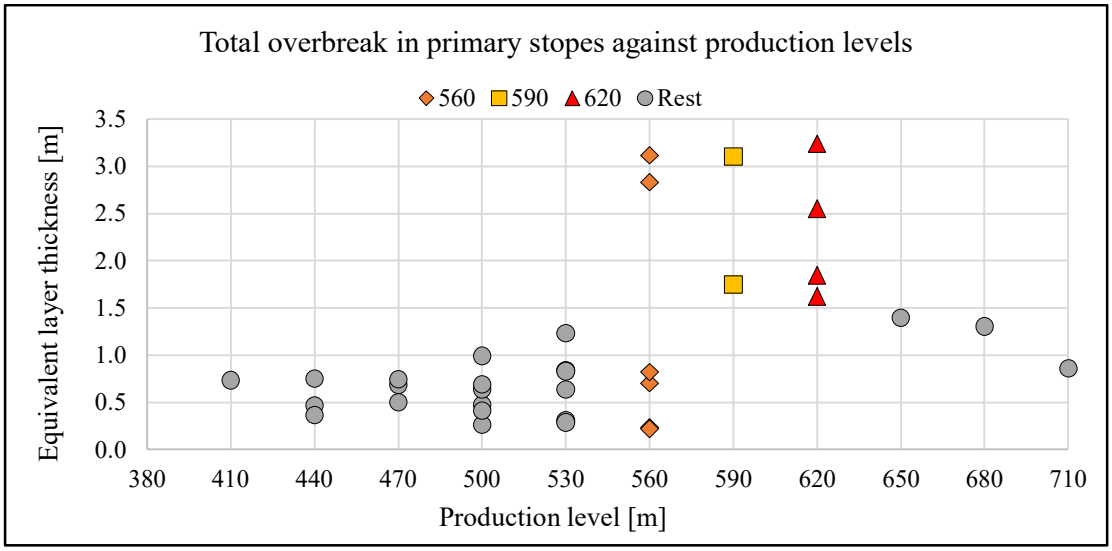

Figure 10.1: Total overbreak in primary stopes against production levels in Wombat

A variety of different plots has been established and evaluated to explain the presented overbreak issue. None of these led to a sufficient result. Parameters such as stope length, aspect ratio or hydraulic radius tend to fail their impact on the respective stopes. The stope sub-types and mining sequence also lack potential explanation as bottom stopes suffer as much overbreak as top stopes in these levels. With view on the geometric complexity it can be concluded that nearly every complexity is present which supports the assumption that not a single parameter but rather a multitude of parameters causes major overbreak in these levels.

The investigation of the levels 560 – 620 is conducted by means of numerical analysis and visual examination in Surpac. It is seen in all levels, that a selection of unfavourable settings and conditions is present that presumably explains the degree of overbreak excess for the stopes. The influencing factors are comprehended and noted as the following:

- Non-existent stope splitting

The successful utilisation of splitting stopes into smaller ones to prevent excessive overbreak has been proven in chapter 8.4. In the lower levels, stopes remain undivided and are mined sequentially as one unit. With view on the complexity of the drift design, the option is yet highly recommended. Level 560 serves as an example. In the production level 560, the subdivided stope 560ppL14 from Figure 8.7 is split and shows great results. The overbreak has been successfully reduced particularly in comparison to stopes in level 590 and 620 which do not apply this method.

- Complex drift design

The drift development for transverse stoping is built relatively uniform throughout the Wombat orebody. Compared to shallower production levels as for instance level 500, the access drifts are nearly six to seven metres wide. The drift width extends to roughly 13 metres on average in the levels 590 – 620 which is about twice as wide. The access drifts in level 590 and 620 are partially designed in curvy shape opposed to an almost rectangular drift development in level 500. Another issue to the stoping performance is associated with the more pronounced crosscut dimensions which can be found in deeper levels. The average crosscut area in level 500 totals roughly 49 m² whereas level 590 and 620 have 71 m² and 156 m², respectively. The crosscuts, especially in lower levels, have been known to be an issue to the drift openings already (Malmberg, 2020a). In combination with increased drift width, they are likely to impose great stress situations on the surrounding rock mass and provide undercutting potential. The stope 620ppL20 has shown numerically large overbreak towards the southern side where an enormous crosscut is found abutted to the stope.

- Aspect ratio

The aspect ratio, or length to height ratio, is found to have an impact on transverse stoping as it corresponds to any stope length increase. Whereas the aspect ratio is kept little in shallower drifts, mostly around 0.4 to 0.5, it tends to shift towards unfavourable ratios in deeper levels. Henning and Mitri (2007) studied the effect of aspect ratio and concluded that ratios of 1.0 or more are most unfavourable in terms of stability. Most of the stopes in the levels 590 and 620 have ratios of nearly 1.0 or above and suffer excessive overbreak.

- Inclined sidewalls

Although, the geometric complexity is less pronounced in transverse stoping, the geometry of the stope has a remarkable impact on the performance. Most of the overbreak in four explicit stopes that are located in the levels 590 and 620 results from one sidewall only. After visual examination, it can be concluded that nearly all overbreak is caused by inclined sidewalls. The effect of sidewall inclination is very distinct and conceived as main driver for dilution since transverse sidewalls are typically planned vertical instead.

- Ore types per stope

The Kylylahti deposit contains mostly semi-massive, massive ore lenses, so called M2 type, as well as gold rich ore lenses referred to as M4 and M5. The terms were described in chapter 5.3. The ore type M2 or M4/M5 are commonly found separately in transverse stopes. Few exemptions are overly located in the critical drifts in the levels 560 – 620. Elevated overbreak numbers suggest the assumption, that more ore lenses per stope promote instability of sidewalls as shown in Table 10.3. Stopes that bear only one ore type show remarkably reduced overbreak to stopes in the same level with multiple ore lenses. This is especially visible in critical levels 560 – 620. The ore type composition in transverse stopes is also conceived an influential factor for excessive overbreak in the levels 560 – 620.

Table 10.3: Total overbreak in transverse stopes per ore type (see chapter 5.3) summarized per production levels

Total sidewall overbreak per ore type						
Levels	**M2**	**M4**	**M5**	**M2/M4**	**M4/M5**	**M2/M4/M5**
Units	**[m]**	**[m]**	**[m]**	**[m]**	**[m]**	**[m]**
500	0.87	0.99			0.82	2.62
530	0.76		0.29		0.83	1.59
560	1.09	0.82			2.46	2.25
590	0.21				1.07	2.38
620	1.85				1.68	2.16
650						1.65
680		1.51		1.30		2.87

- Strike shifting

The curvy drift development in lower levels has been discussed already. Comparing the drift development of level 560 to level 620, the strike shift of the Wombat orebody becomes obvious as shown in Figure 10.2. In the shallower levels, represented by level 560, the direction of mining can be defined as roughly 19 degrees towards SSW. The orebody direction drastically pivots nearly 15 degrees towards west within only 60 metres in depth difference. No further pivoting of the orebody is noticeable in lower levels than 620. The

overall direction change of the orebody in lower levels presumably requires other approaches than standard procedures. Also, the stresses accelerate unusually quick towards very high values once mining started in level 620. An additional stress modelling results for the production level 620 is attached to Appendix 6.

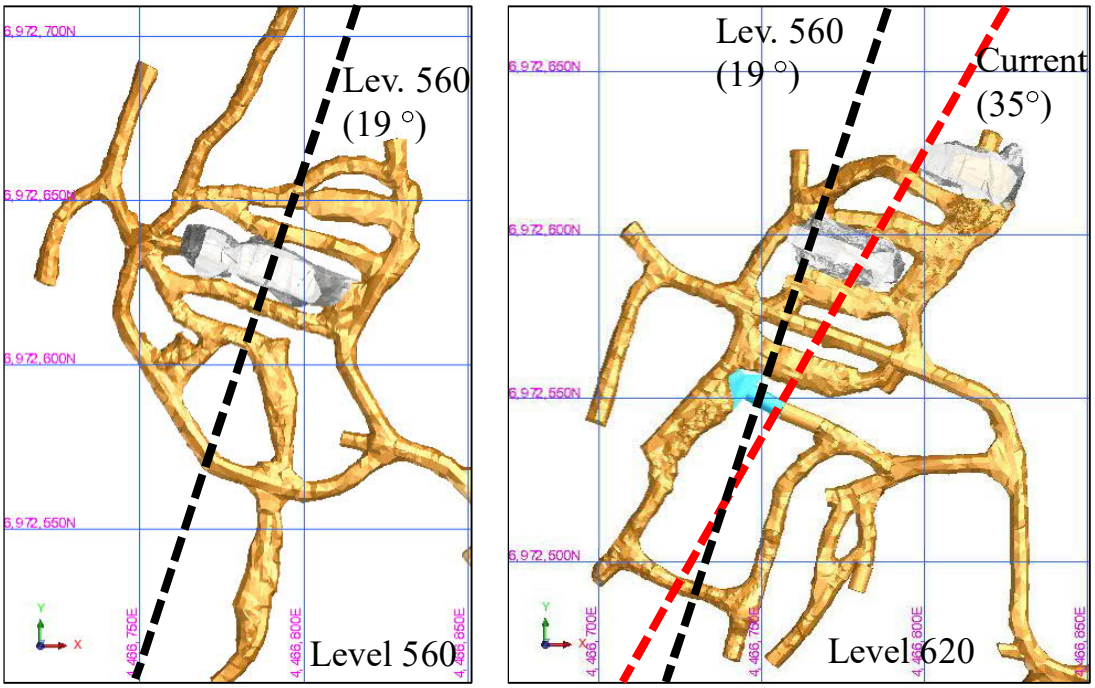

Figure 10.2: Comparison of drift design and mining direction in level 560 and 620 shows drastic strike shift in Wombat

- Inconvenient geological interpretation

Pertaining to insufficient exploration and geological interpretation of the orebody, the primary stope data retrieves indications of structural presence. The data states conditional overbreak of primary stopes. The presence of structural formation in the surrounding rock mass presumably caused primary stopes to sustain large overbreak. The assumption is further supported by the fact, that secondary stopes suffer the least overbreak in same production levels as shown in Figure 10.3. It appears that secondary stopes benefit from CRF backfilling which provides more stability compared to original rock mass. Missing updated stress modelling and investigation on geological properties are reasons to not conclude with certainty that structural presence caused or not caused stoping to perform accordingly.

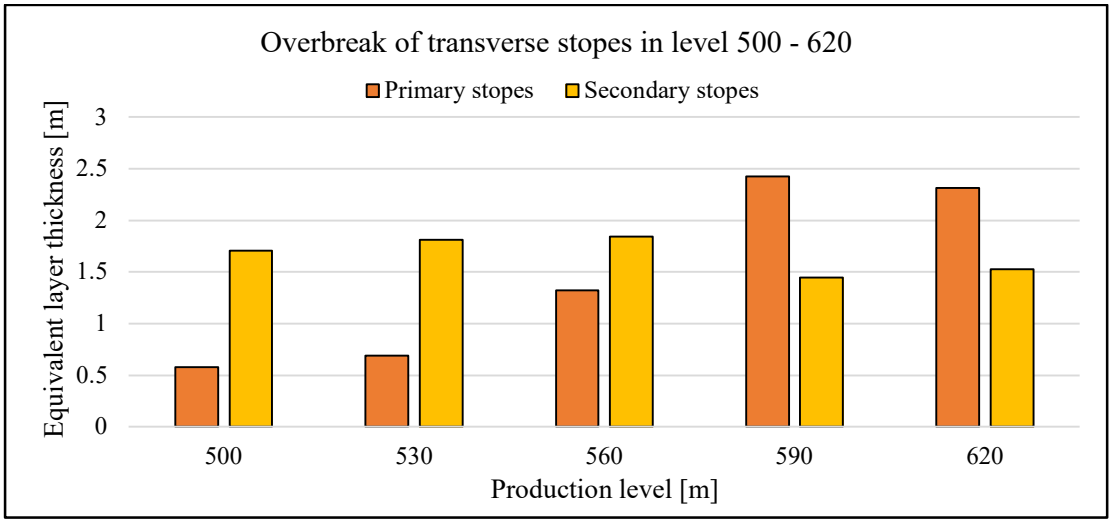

Figure 10.3: Overbreak in transverse stopes located in the levels 500 – 620

10.5 Missing and omitted parameters

This study determined various factors that must be consider with view on overbreak and ore loss. Most of the identified parameters correspond to stope design due to the dense information on stope planning in Kylylahti. A comprehensive examination has been conducted on stope design parameters that concluded interesting results. The examination had to omit certain stopes either because they were not suitable for comparison purposes or because it was not clear which information to use. Data from particularly the early stage of Kylylahti is missing. Lacking standardisation in stope design and uniform CMS scan development are considered the main reasons. Sometimes multiple CMS scans existed without a clear indication of the final version. The stope was then rather excluded than considered with the inappropriate or incorrect final version. Multiple planned stope designs existed similarly as well of which some versions included adjacent waste pillars, and some omitted the waste solids.

On the other hand, specific areas like drilling and blasting or thorough geological assessments on rock mass have been entirely omitted due to missing data. As mentioned in chapter 4, geological factors contribute significantly to stope performance as the geology dictates origin, composition and properties of the waste rock and ore. Improperly executed drilling and blasting, deviation and drillhole trajectory or inappropriate blast design heavily impact rock fragmentation. To fully comprehend the interrelationship among various parameters and how geology and blasting promote or avoid excessive overbreak, at least three more studies are recommended. One study each must emphasise on geological aspects and blasting parameters only with a third paper assessing the multi-causation of stope design, geology and blasting simultaneously.

11 Conclusion

This study is devoted to identifying the most influencing parameters on longhole open stoping in the Kylylahti underground mine. The stope efficiency is assessed with regard to overbreak and ore loss. Additional stope specific data has been obtained by computational means in Surpac. The chapter presents a concise summary of influencing parameters on stoping to address the study objective.

- Key factors for longitudinal stoping

The most influencing parameters on longitudinal stoping are found to be the mining sequence, stope dimensioning and geological formations. The mining sequence or mining direction has shown to remarkably affect the location of ore loss and ore overbreak. Longitudinal stope ends with close contact to CRF backfill sustain large ore loss quantities. The cemented rock fill requires mining to keep certain safety distances towards the backfill in order to properly handle stability. In contrast, ore overbreak is more pronounced in end walls facing towards direct ore contacts.

The stope dimensioning is another paramount factor to consider. Elevated overbreak volume is correlated to increasing stope length and hydraulic radius alike. A decisive parameter for increased overbreak is found to be the hanging wall. The hanging wall produces typically larger overbreak quantities compared to the footwall in Wallaby and Wombat stopes.

The geometric complexity is considered to have a tremendous impact on overbreak occurrence as well. A higher level of complexity promotes generally more overbreak. Geological formations represent the third category of influencing parameters on longitudinal stoping. Although numerically unobtrusive, visual examination showed the great impact of black schist layering as cause for excessive overbreak in Wallaby stopes. Also, geological formations in form of foliations or structures in general are understood and proven to have an impact on the stope efficiency.

- Key parameters for transverse stoping

The most crucial parameters for transverse stoping refer to the stope type classification, the stope design, the stope environment and post-primary stope conditions. The study discovered that the overbreak corresponds directly to the vertical location of stopes. Stopes located at the bottom of the vertical mining sequence showed the least overbreak with the ones located on top suffering the most overbreak. It is also found that each secondary stope sustained remarkably larger overbreak than primary stopes. Similar to longitudinal stopes, the design of transverse stopes is considered an influencing factor of overbreak and ore loss abundance. Increasing stope dimensions correlate directly with enlarged overbreak. Any inclination in the stope walls promotes not only excessive overbreak, but results in advanced ore loss if the footwall dip becomes declined. A development is recognized that a dip decline in the hanging or footwall of 15 degrees provokes twice as much overbreak or ore loss, respectively.

New insights are obtained regarding stope environment and post-primary stope conditions. It has been proven, that ordinary primary and secondary stopes commonly suffer less dilution if split into multiple smaller stopes. The reduction of overbreak in those stopes accounts for

up to 0.8 metres in total. An interesting development has been identified pertaining to post-primary stope conditions. It is demonstrated that ore overbreak from primary stopes translate proportionally into ore loss in secondary stopes. The increase or decrease of overbreak volume in primary stopes promotes increasing or decreasing ore loss in the secondary stopes, respectively. Limitations in the drilling equipment and the restraining CRF stability are seen as decisive factor for this effect.

- Best and bad practices

The best and bad practices concern methods or factors that prevent or provoke overbreak and ore loss in longhole open stoping. The CRF backfilling in Kylylahti is considered a best practice method. This applies to longitudinal and transverse stoping. It sufficiently provided stability as there are only two incidents regarding CRF instability. The stope analyses showed that CRF is yet a contributing factor to the overall overbreak composition. A further improved mixture of hydraulic backfill in combination with CRF could offset scattered cases of elevated CRF backfill segregation (Malmberg, 2020c). Another method to reduce overbreak effectively is considered the stope division. It must be noted that Kylylahti never saw the length of transverse stope as a critical issue but rather the near-by weakness zones and intersecting waste rock. But the observation with the numerical proof demonstrates that multiple smaller stopes result in improved performance over ordinary transverse stopes. Although, the total length of all smaller stopes exceeded the length of normal transverse stopes, the dilution has been significantly decreased.

Bad practices are methods or factors that need to be improved or changed as they impose unfavourable conditions for stoping. The issue of applying two mining methods at once in the Wombat orebody is found to deteriorate longitudinal stoping massively on multiple levels. Firstly, there is the prolonged extraction time that is needed for completion of longitudinal stopes per production level. The extraction time is increased by almost 1.5 years compared to Wallaby stopes. Secondly, the accumulation of stresses in the deeper Wombat orebody peaks in production drift ends in which longitudinal stoping is typically applied.

- Multi-causation

The eminent importance of different parameters on longhole open stoping has been attested throughout this study. Some factors are known to affect longitudinal and transverse stoping similarly. Other factors are considered to have impacts on specific stoping methods only. The influence of several factors and their interrelation is found to be an issue to the identification of those parameters. The issue of multi-parameters that affect stoping is more prevalent in transverse stoping. The reason is overly found to be the complex drift design. It cannot be assessed to what extent single stoping factors contribute to overbreak as a whole nor can be quantified what weighting factor applies to each parameter. On the one hand, the multi causation cannot be investigated because no convenient examination method exists to this date. On the other hand, the given data overly concerns stoping design parameters and omits geological information as well as drilling and blasting parameters to a great extent. The multi causation and the lack of interdependency of the stoping parameters is a principal topic for further research.

12 Recommendations

The effect of identified parameters on stoping has been successfully demonstrated. The main focus is hereby laid on the stope design, the stope setting as well as the extraction sequence. No emphasis has been put on geotechnical and blasting parameters. Recommendations pertaining to further research have been gathered and comprehend the following:

- Comprehensive database

The time spent on establishing a well-documented and sophisticated database is considered paramount for the success of this study. The gathering of data mostly has happened manually, required several weeks and needed the collaboration of various departments. As there is data regarding more than 160 stopes in total, further studies must be provided with suitable data up front to enable full emphasis on the analysis. An example of parameters that are best to provide prior to stope analysis is enclosed in Appendix 7.

- Geotechnical information

Only little information on geotechnical data is available to this study. That is due to a missing rock mechanical department on-site. Relatively old data of previous consulting works provided the solitary source of geotechnical data. Up to date stress modelling is conceived to allow advanced analyses and more detailed conclusions. Missing geotechnical expertise did not allow to utilize sophisticated cable bolting and stope support at most. The stope support is best evaluated exclusively in a study to comprehend the impact on stope performance. Additionally, an immersive analysis is required on different rock mass properties and how they act under influences of the found stope design parameters.

- Drilling and blasting

Some data has been provided on drilling and blasting such as the drillhole length and the powder factor. The impact of properly aligned drilling pattern and the blasting procedure have to be included in further studies. Drillhole trajectory deviations as well as the drillhole collar offset could not be assessed due to missing data. This refers to the need for a comprehensive database prior to the analysis as it is eminent important for the study success. Suggestions recommend identifying the most critical parameters of drilling and blasting on stoping first.

- Need for meta-analysis

The need for a meta-analysis is of great importance once the most influencing parameters from stope design, drilling and blasting as well as geotechnical parameters are determined. Stoping is not solely affected by one category of parameters but is rather influenced by a dynamic environment. Interrelations among the parameters need to be modelled with the aim to state a weighting factor for each parameter. Their interdependency is highly unexplored and could lead to great improvements in stope planning.

- Sequential stope splitting

It has been demonstrated that the division of ordinary transverse stopes into smaller stopes acts beneficial when aiming for reduced overbreak. The applicability of these division depends on technical feasibility and economic viability. Backfilling and drilling operations are increased with more stopes which inevitably increases expenditures. These costs have to be evaluated and compared against reduced operational costs i.e. less overbreak hauling and less cable bolting due to increased stability. The correlation of ore overbreak in primary stopes and ore loss in secondary stopes requires an economic analysis as well. The ore loss hereby must be addressed in particular when primary stopes suffer large ore overbreak volume.

Bibliography

Abdellah, W. R. & Ali, M. A. (2017) Stability Analysis of Vertical and Inclined Backfilled Stope. *Journal of Engineering Sciences,* Vol. 45. p. 70-79.

Arjang, B. (1991) Pre-mining Stresses at Some Hard Rock Mines in the Canadian Shield. In: *CIM-Bulletin*. Vol. 84.

Badge, M. N., Emad, M. Z., Mitir, H. & Thibodeau, D. (2011) Examining the influence of stope dimensions and mining sequence on backfill dilution: a review with case study. In: Pal, B. K. & Chatterjee, S. (eds.) *International Conference on Technological Challenges and Management Issues for Sustainability of Mining Industries.* Rourkela, India. p. 13-28.

Barton, N., Lien, R. & Lunde, J. (1974) Engineering Classification of Rock Masses for the Design of Tunnel Support. *Rock Mechanics.* Vol. 6(4). p. 189-239.

Bieniawski, Z. T. (1976) Rock Mass Classification in Rock Engineering. In: Bieniawski, Z.T. (ed.) *Symposium on Exploration for Rock Engineering.* Cape Town, South Africa. Balkema. p. 97-106.

Bieniawski, Z. T. (1989) *Engineering rock mass classifications.* New York: Wiley.

Brady, B. H. G. & Brown, E. T. (2005) *Rock Mechanics for Underground Mining.* 3rd ed. Dordrecht: Springer Science + Business Media, Inc..

Capes, G. W. (2009) *Open Stope Hangingwall Design Based On General And Detailed Data and Collection In Rock Masses With Unfavourable Hangingwall Conditions*. PhD. University of Saskatchewan, Department of Geological and Civil Engineering. Saskatoon, Saskatchewan, Canada.

Clark, L. (1998) *Minimizing dilution in open stope mining with a focus on stope design and narrow vein longhole blasting*. Master's thesis. The University of British Columbia, Department of Mining and Mineral Process Engineering. Vancouver, British Columbia, Canada.

Deere, D. U. & Deere, D. W. (1988) The rock quality designation (RQD) index in practice. *Rock classifications systems for engineering purposes.* Volume ASTM Special Publication 984. p. 91-101.

Deere, D. U., Hendron, A. J., Patton, F. D. & Cording, E. J. (1967) Design of surface and near surface construction in rock. In: Fairhust, C. (ed.) *Failure and breakage of rock, proceedings of 8th U.S. symp. rock mech.*. New York. p. 237-302.

DFAT, (2020) *Finland Travel Health Insurance - Country Review.* [Online] Available at: https://www.aardvarkcompare.com/blog/finland-travel-health-insurance [Accessed 16 June 2020].

Dunne, K. & Pakalnis, R. (1996) Dilution aspects of a sublevel retreat stope at Detour Lake Mine. In: Aubertin, M., Hassani, F., Mitri, H. (eds.) *Rock mechanics tool and techniques*. Rotterdam. A. A. Balkema. p. 305-313.

El Mouhabbis, H. Z. (2013) *Effect of stope construction parameters on ore dilution in narrow vein mining.* Master's thesis. McGill University, Department of Mining and Metals and Minerals Engineering. Montreal, Quebec, Canada.

Elbrond, J. (1994) Economic effects of ore losses and rock dilution. *CIM bulletin.* Vol. 87(978). p. 131-134.

Forsyth, W., Kleine, T. & Cameron, A. (1994) *Inaccurate blasthole drilling.* Golder Associates Ltd..

Germain, P. & Hadjigeogiou, J. (1997) Influence of Stope Geometry and Blasting Patterns on Recorded Overbreak. *International Journal of Rock Mechanics and Mining Sciences.* Vol. 34(3-4).

Germain, P., Hadjigeogiou, J. & Lessard, J. F. (1996) On the relationship between stability prediction and observed stope overbreak. In: Aubertin, M., Hassani, F., Mitri, H. (eds.) *Rock Mechanics.* Rotterdam. Balkema. p. 277-283.

Ghasemi, Y. (2012) *Numerical studies of mining geometry and extraction sequencing in Lappberget, Garpenberg.* Master's thesis. Luleå University of Technology, Department of Civil, Environmental and Natural Resources Engineering. Luleå, Sweden.

Heidarzadeh, S., Saeidi, A. & Rouleau, A. (2019) Evaluation of the effect of geometrical parameters on stope probability of failure in the open stoping method using numerical modeling. *International Journal of Mining Science and Technology.* Vol. 29(3). p. 399-408.

Hendricks, C., Scoble, M. & Boudreault, F. (1994) A Study of Blasthole Drilling Accuracy: Monitoring, Instrumentation and Practice. *CIM Bulletin.* Vol. 87.

Henning, J. G. (2007) *Evaluation of Long-Hole Mine Design Influences on Unplanned Ore Dilution.* PhD. McGill University, Department of Mining, Metals and Materials Engineering. Montreal, Canada.

Henning, J. G. & Mitri, H. (2007) Numerical modelling of ore dilution in blasthole stoping. *International Journal of Rock Mechanics and Mining Sciences.* Vol. 44. p. 692-703.

Henning, J. G. & Mitri, H. (2008) Assessment and Control of Ore Dilution in Long Hole Mining: Case Studies. *Geotechnical and Geological Engineering.* Vol. 26(4). p. 349-366.

Hoek, E. (ed.) (2007) *Practical Rock Engineering*. Vancouver, British Columbia, Canada: RocScience.

Hughes, R. (2011) *Factors influencing overbreak in narrow vein longitudinal retreat mining.* Master's thesis. McGill University, Department of Mining and Materials Engineering. Montreal, Québec, Canada.

Hutchinson, D. J. & Diederichs, M. S. (1996) *Cablebolting in Underground Mines.* Richmond: BiTech Publishers.

Jang, H. D. (2014) *Unplanned Dilution and Ore-Loss Optimisation in Underground Mines via Cooperative Neuro-Fuzzy Network.* PhD. Curtin University. Bentley, Australia.

Kekki, J.-M. (2020a) *Explanation of ore lenses and respective mineralogical settings.* [Interview] (March 2020).

Kekki, J.-M. (2020b) *Single sulphide grain from Kylylahti consisting of multiple different minerals.* [Interview plus picture supply] (June 2020).

Kohonen, J. & Marmo, J. (1992) Proterozoic lithostratigraphy and sedimentation of Sariola and Jatuli-type rocks in the Nunnanlathi-Koli-Kaltimo area, eastern Finland; implications for regional basin evolution models. *Geological Survey of Finland Bulletin.* Vol. 364. p. 67.

Kontinen, A. (2005) *Geology of the Kylylahti Cu-Co Deposit Finland.* Kuopio: Vulcan Resources Ltd.

Lahtinen, R. et al. (2010) New constraints for the source characteristics, deposition and age of the 2.1-1.9 Ga metasedimentary cover at the western margin of the Karelian Province. *Precambrian Research.* Vol. 176. p. 77-93.

Lukkari, A. (2020) *Determination of safe work environment with Cavity Monitoring System application.* [Interview] 2020.

Lusk, B. & Worsey, P. (2011) Explosives and Blasting. In: Darling, P. (ed.) *SME Mining Engineering Handbook.* United States of America: Society for Mining, Metallurgy, and Exploration, Inc.. p. 443-462.

Malmberg, M. (2020a) *Stope design and drift development.* [Interview] (March 2020).

Malmberg, M. (2020b) *Introduction and assessment of CMS scanning.* [Interview] (May 2020).

Malmberg, M. (2020c) *Disscusion about longitudinal & transverse stope performance results.* [Interview] (August 2020).

Malmberg, M. & Svensson, P. (2019) *Mineral Resources and Mineral Reserves 2019 - Kylylahti.* Kylylahti, Finland: Boliden Kylylahti Oy.

Markström, A. (2019) *Cemented rockfill at Kylylahti mine.* Sweden: Boliden AB.

Mathews, K., Hoek, E., Wyllie, D. C. & Stewart, S. B. C. (1981) *Prediction of stable excavations for mining at depths below 1000 metres in hard rock.* Ottawa, Canada.

Mitri, H. S., Hughes, R. & Lecomte, E. (2010) Factors Influencing Unplanned Ore Dilution in Narrow Vein Longitudinal Mining. In: *SME Annual Meeting*. Phoenix, Arizona.

Morrison, D. M. (1995) *Deep Hardrock Mining - The Future.* Halifax, Nova Scotia: CIM-AGM.

Nickson, S. D. (1992) *Cable support guidelines for underground hard rock mine operations.* Master's thesis. University of British Columbia, Department of Mining and Mineral Process Engineering. Vancouver, British Columbia, Canada.

Pakalnis, R. (1986) *Empirical Stope Design at the Ruttan Mine, Sherritt Gordon Mines Ltd.*. Vancouver, British Columbia, Canada.

Pakalnis, R., Poulin, R. & Hadjigeorgiou, J. (1995) Quantifying the cost of dilution in underground mines. *Mining Engineering,* Vol. 47(12). p. 1136-1141.

Perron, J. (1996) Simple solutions and employee's involvement reduced the operating cost and improved the productivity at Langlois mine. In: *14th CIM mine operator's conference.* Bathurst, New Brunswick.

Peskens, T. W. (2013) *Underground mining method selection and preliminary techno-economic mine design for the Wombat orebody, Kylylahti deposit, Finland.* Master's thesis. Delft University of Technology, Department of Geoscience & Engineering. Delft, The Netherlands.

Potvin, Y. (1988) *Empirical Open Stope Design in Canada.* PhD. University of British Columbia, Department of Mining and Mineral Process Engineering. Vancouver, British Columbia, Canada.

Pöyry Finland Oy (2016) *Rock mechanical simulation of the Kylylahti mine.* Boliden Kylylahti Oy.

Pöyry Finland Oy (2017) *Rock Mechanical Study - LOMP.* Boliden Kylylahti Oy.

Scoble, M. J. & Moss, A. (1994) Dilution in underground bulk mining: Implications for production management, mineral resource evaluation II, methods and case histories. *Geological Society Special Publications No.79.* p. 95-108.

SRK Consulting (2007) *Mining Geotechnical Feasibility Study Report.* Vulcan Resources Limited.

Stewart, P. (2005) *Minimising Dilution in Narrow-Vein Mine.* PhD. University of Queensland, Julius Kruttschnitt Mineral Research Centre. Brisbane, Queensland, Australia.

Stewart, P. C. & Trueman, R. (2008) Strategies for Minimising and Predicting Dilution in Narrow Vein Mines - The Narrow Vein Dilution Method. In: *Narrow Vein Mining Conference*. Ballarat, Australia. p. 153-164.

Suominen, T. (2020) *Introduction to the Luikonlahti mill and its products.* [Interview] (March 2020).

Suorineni, F. T. (1998) *Effects Of Stress And Faults On Open Stope Design.* PhD. University of Waterloo, Department of Earth Science. Waterloo, Ontario, Canada.

Trevor, S. (1991) Dilution control at Hudson Bay mining & smelting, Flin Flon operations. In: *Proceedings of the 93rd CIM annual general meeting.* Vancouver, British Columbia, Canada.

Villaescusa, E. (1998) Geotechnical design for dilution control in underground mining. *Mine Planning and Equipment Selection.* p. 141-149.

Villaescusa, E. (2004) Quantifying open stope performance. In: *MassMin 2004*. Santiago, Chile: Quebecor World Chile S.A..

Wang, J. (2004) *Influence Of Stress, Undercutting, Blasting And Time on Open Stope Stability And Dilution.* PhD. University of Sakatchewan, Department of Civil and Geological Engineering. Saskatoon, Saskatchewan, Canada.

Wright, E. A. (1983) Dilution and Mining Recovery - Review of the Fundamentals. *Erzmetall.* Vol. 36. p. 23-29.

Yao, X., Allen, G. & Willet, M. (1999) Dilution evaluation using Cavity Monitoring System at HBMS-Trout Lake Mine. In: *101st CIM annual general meeting*. Calgary, Alberta, Canada.

Appendix 1

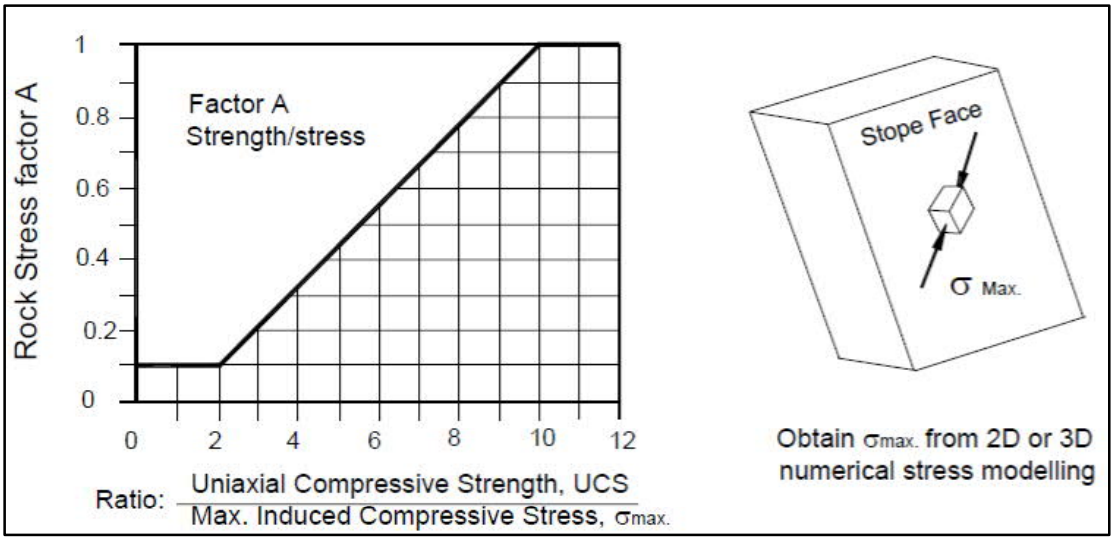

Figure A1.1: Determination of stress factor A (after Potvin (1988), from Hutchinson and Diederichs (1996))

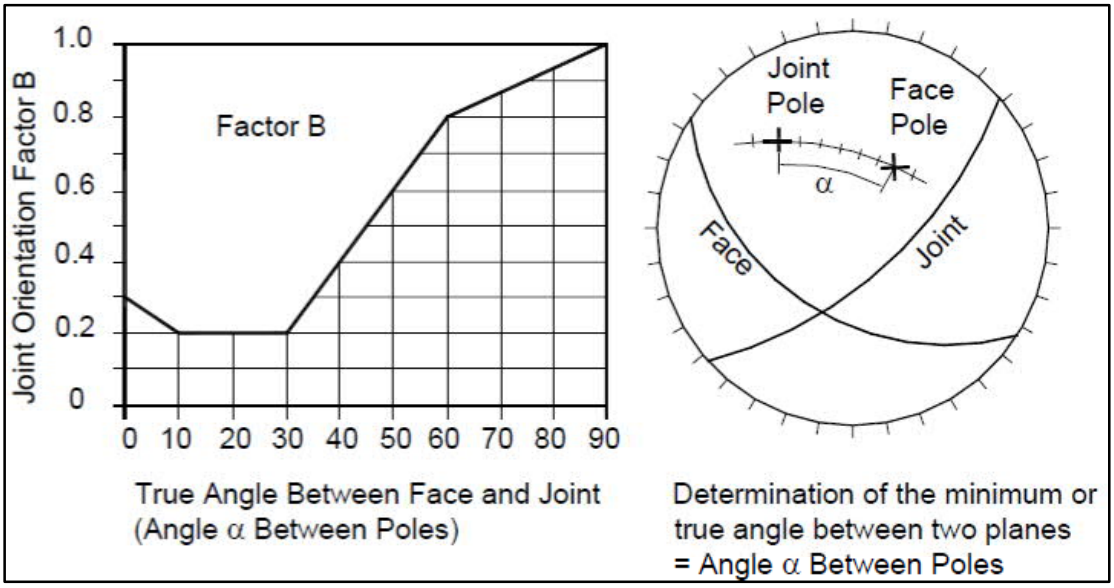

Figure A1.2: Determination of joint orientation factor B (after Potvin (1988), from Hutchinson and Diederichs (1996))

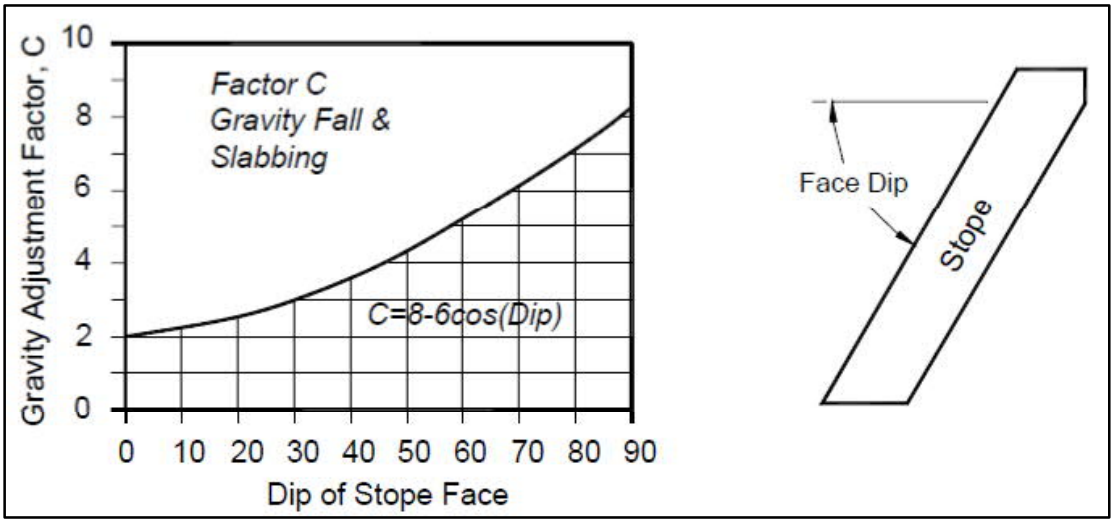

Figure A1.3: Gravity factor C for gravity fall and slabbing (after Potvin (1988), from Hutchinson and Diederichs (1996))

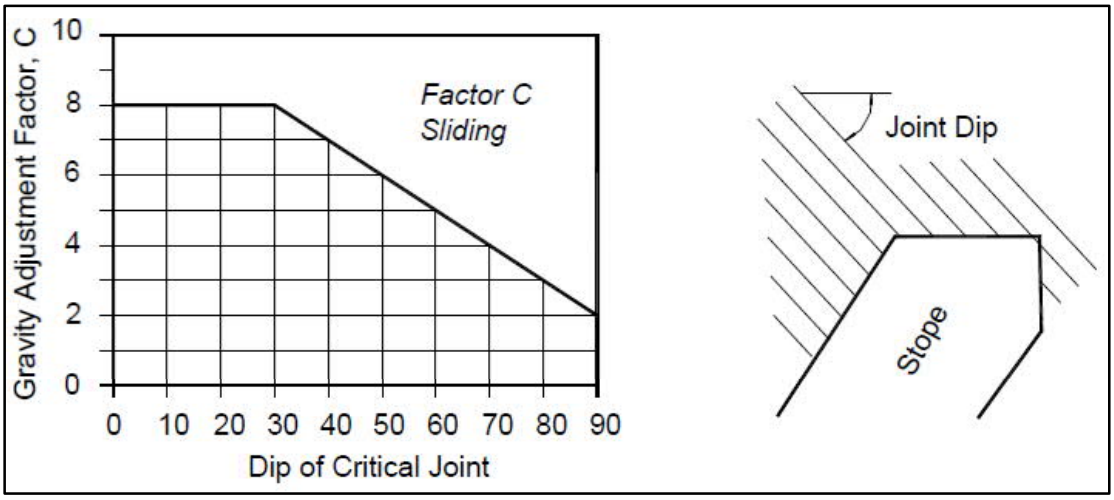

Figure A1.4: Gravity factor C for sliding (after Potvin (1988), from Hutchinson and Diederichs (1996))

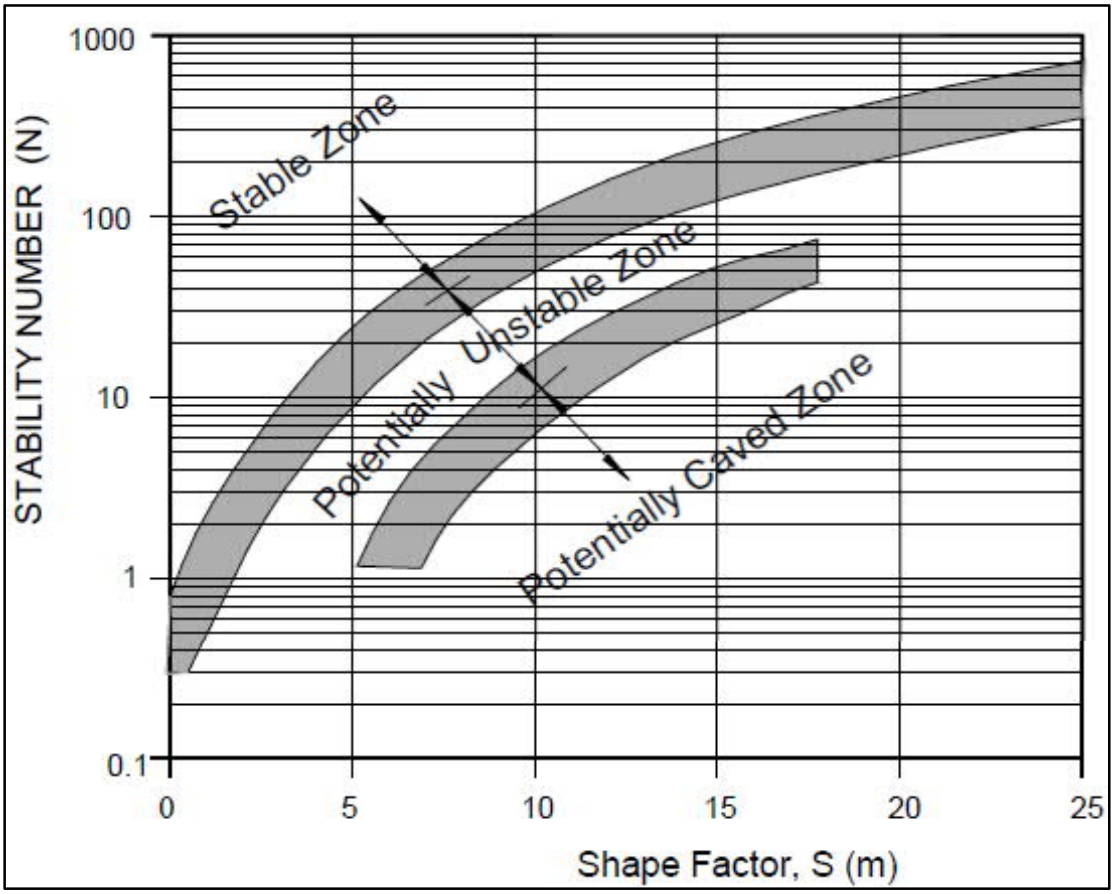

Figure A1.5: Stability graph (after Mathews et al. (1981), from Wang (2004))

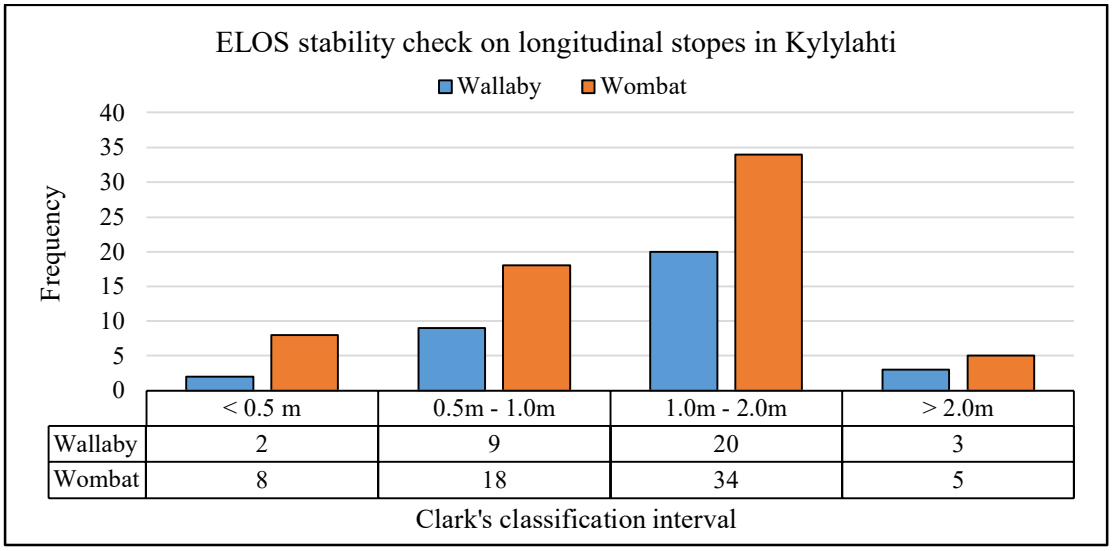

Figure A1.6: ELOS stability check on longitudinal stopes in Kylylahti

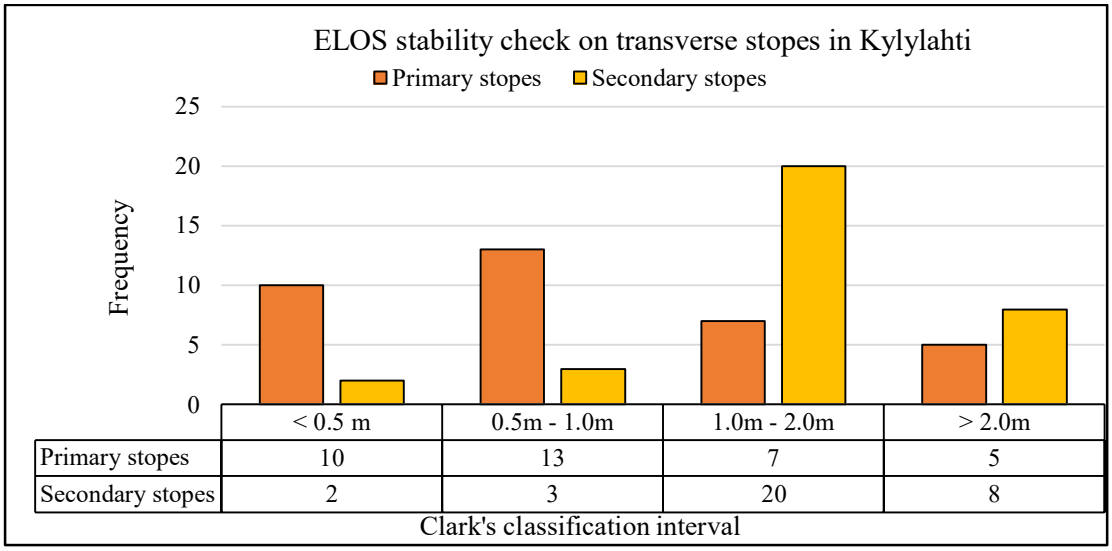

Figure A1.7: ELOS stability check on transverse stopes in Kylylahti

Appendix 2

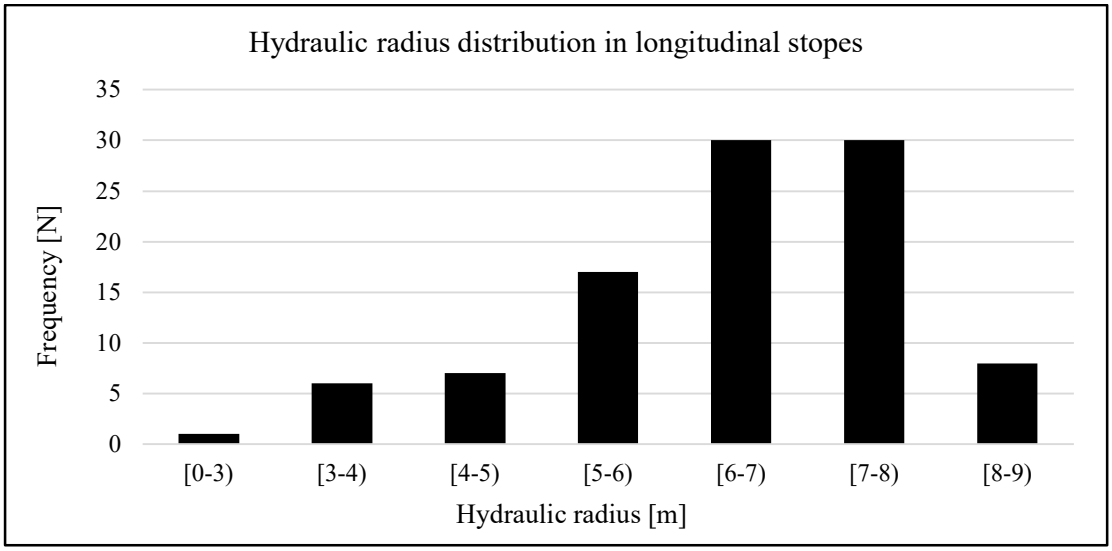

Figure A2.1: Hydraulic radius distribution in longitudinal stopes

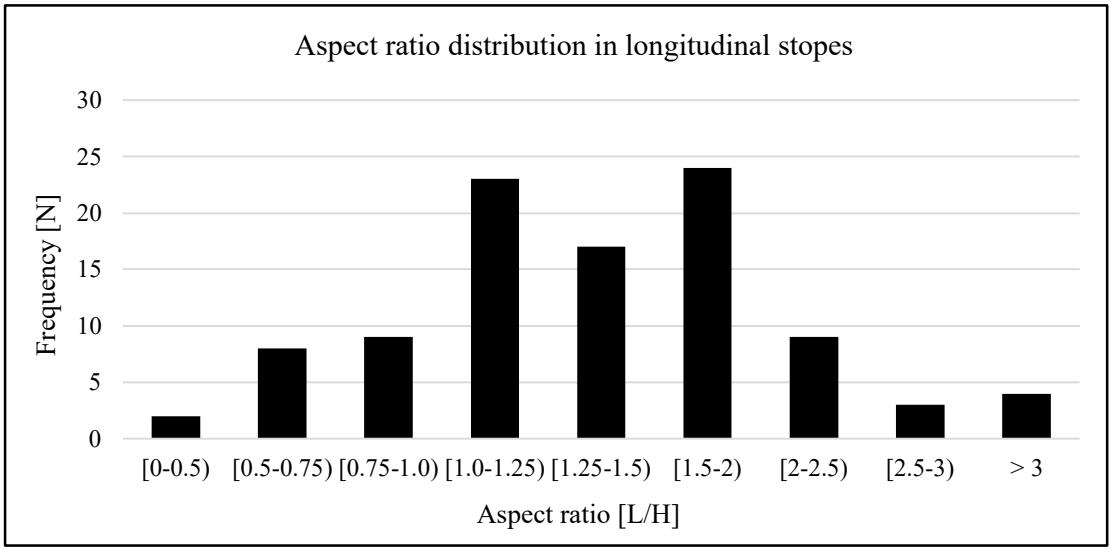

Figure A2.2: Aspect ratio distribution in longitudinal stopes

The accentuation in the plots is defined as the following:

- […) means the first shown number in the interval is mathematically included with second number being excluded

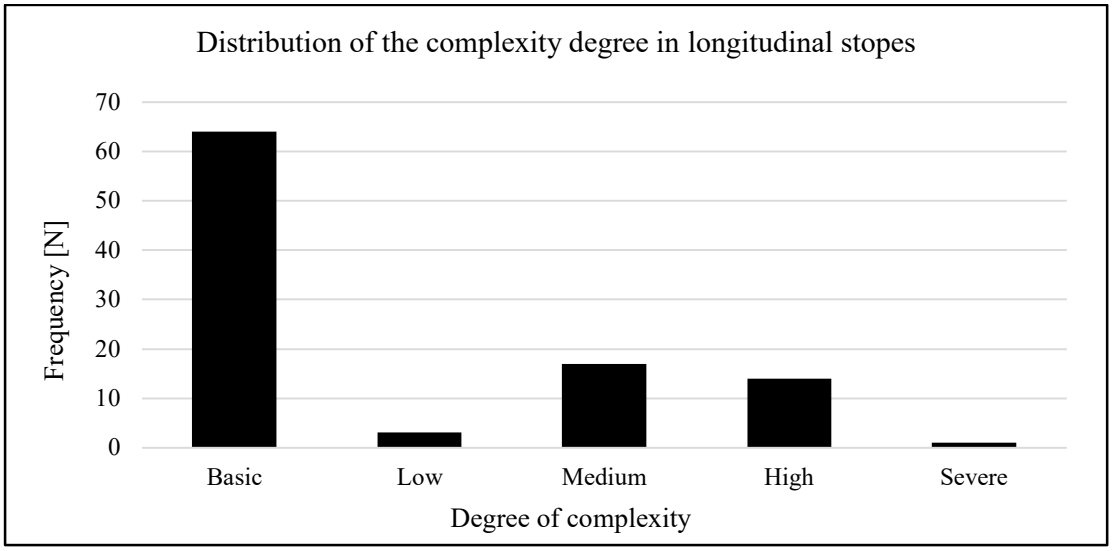

Figure A2.3: Distribution of the complexity degree in longitudinal stopes

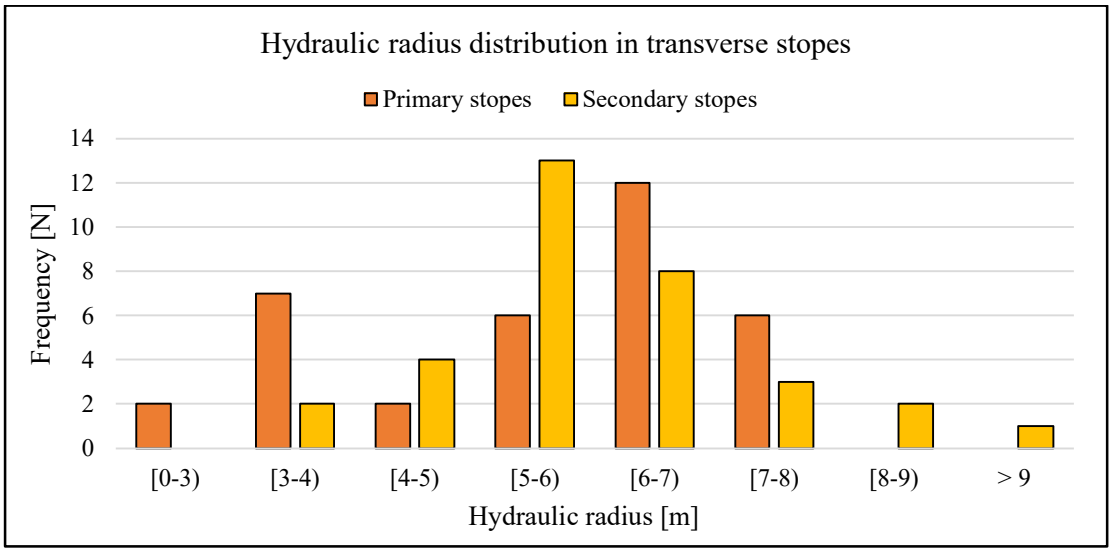

Figure A2.4: Hydraulic radius distribution in transverse stopes

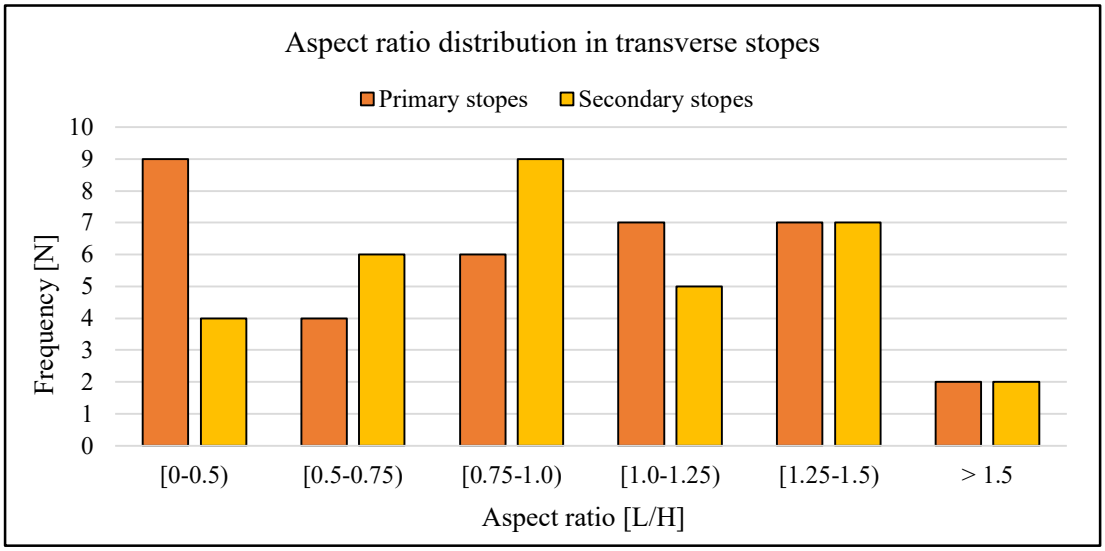

Figure A2.5: Aspect ratio distribution in transverse stopes

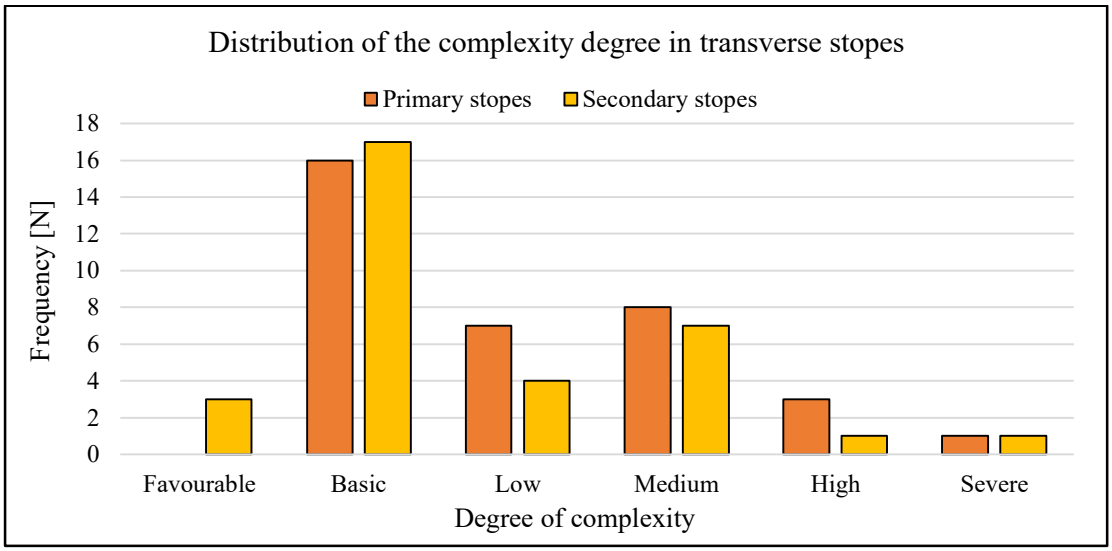

Figure A2.6: Distribution of the complexity degree in transverse stopes

Appendix 3

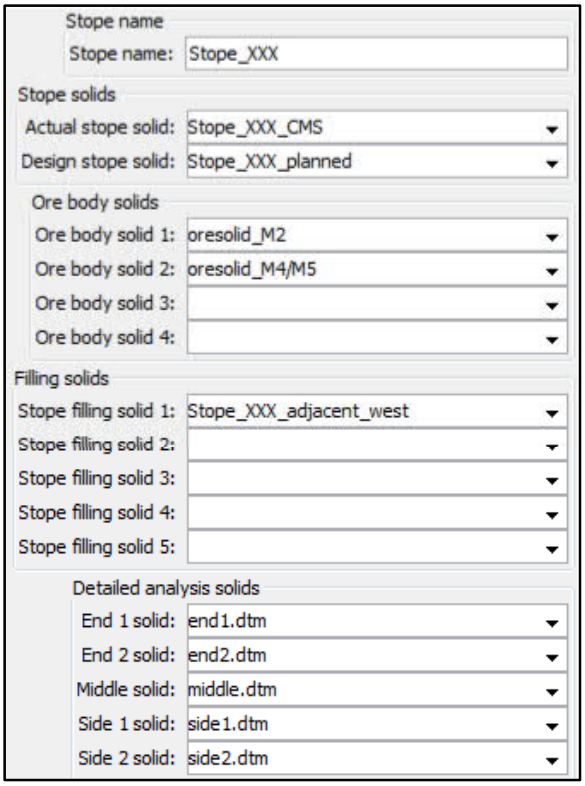

Figure A3.1: Macro interface illustration

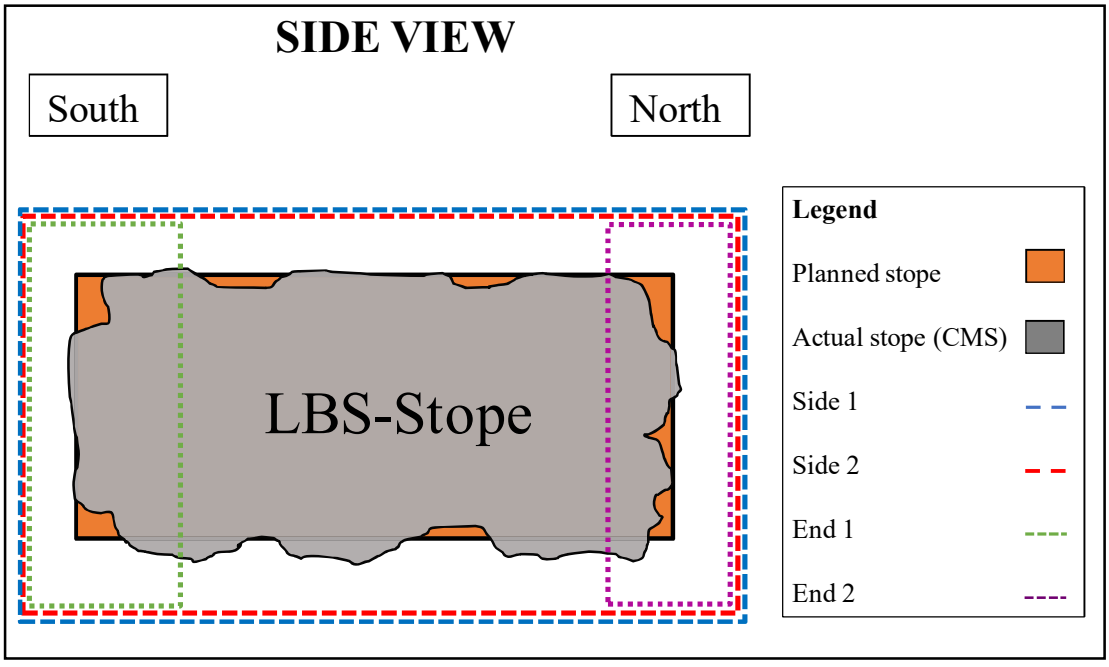

Figure A3.2: Box development on longitudinal stope looking west

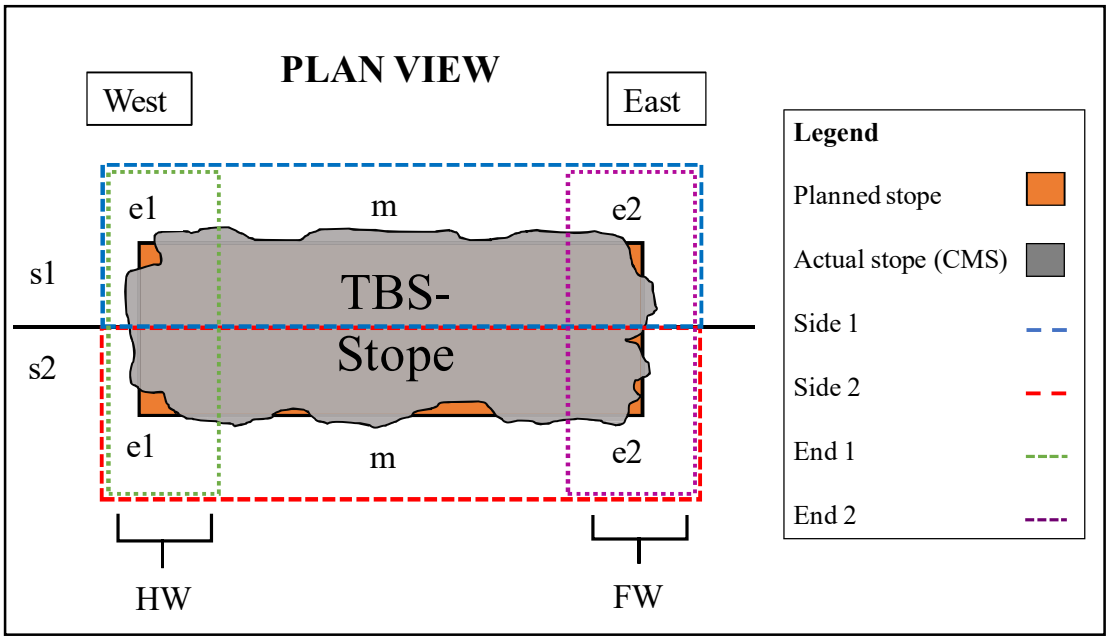

Figure A.3.3: Section development in transverse stopes in plan-view

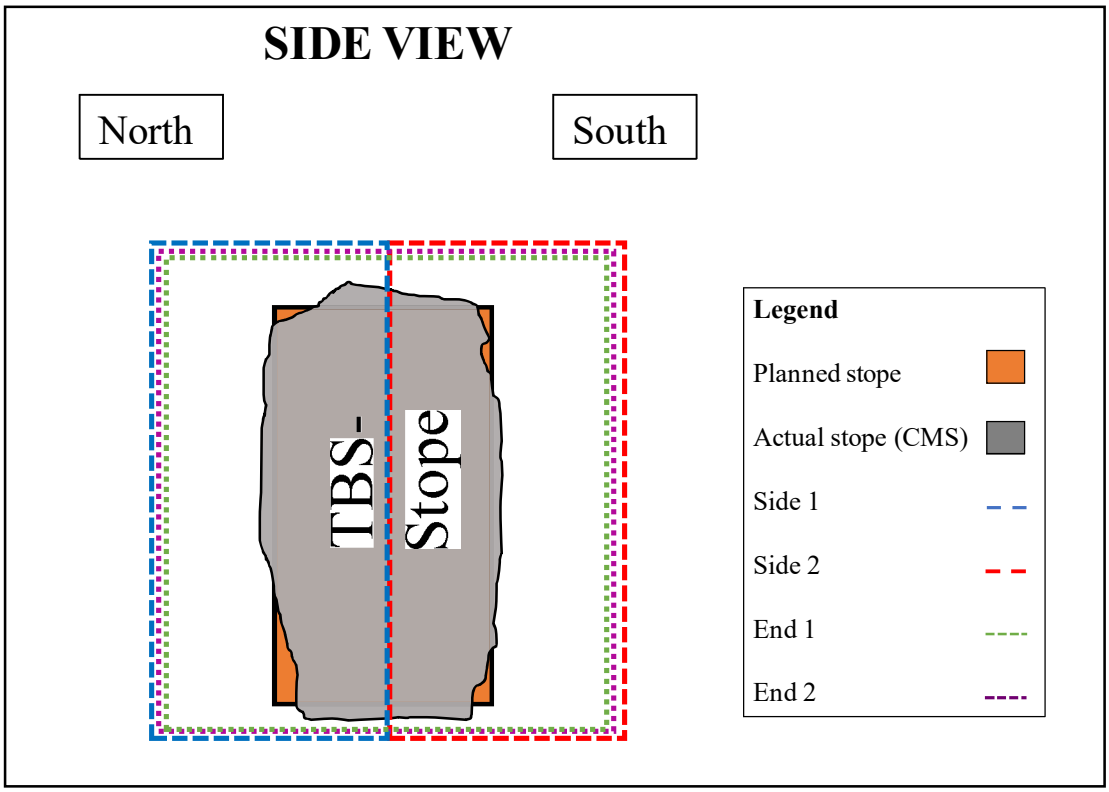

Figure A3.4: Box development in transverse stopes looking east

Table A3.1: Comprehensive macro output scheme

Stope XXX	Total	side1 end1	side1 end2	side1 middle	side2 end1	side2 end2	side2 middle
Units	[m³]	[m³]	[m³]	[m³]	[m³]	[m³]	[m³]
planned	6305	0	0	0	0	0	0
actual	6838	0	0	0	0	0	0
ore loss	404	19	81	41	25	101	134
total overbreak	937	75	24	669	3	17	134
overbreak ore1	445	24	13	344	3	11	37
overbreak ore2	0	0	0	0	0	0	0
overbreak ore3	0	0	0	0	0	0	0
overbreak ore4	0	0	0	0	0	0	0
crf1	0	0	0	0	0	0	0
crf2	0	0	0	0	0	0	0
crf3	0	0	0	0	0	0	0
crf4	0	0	0	0	0	0	0
crf5	0	0	0	0	0	0	0

Appendix 4

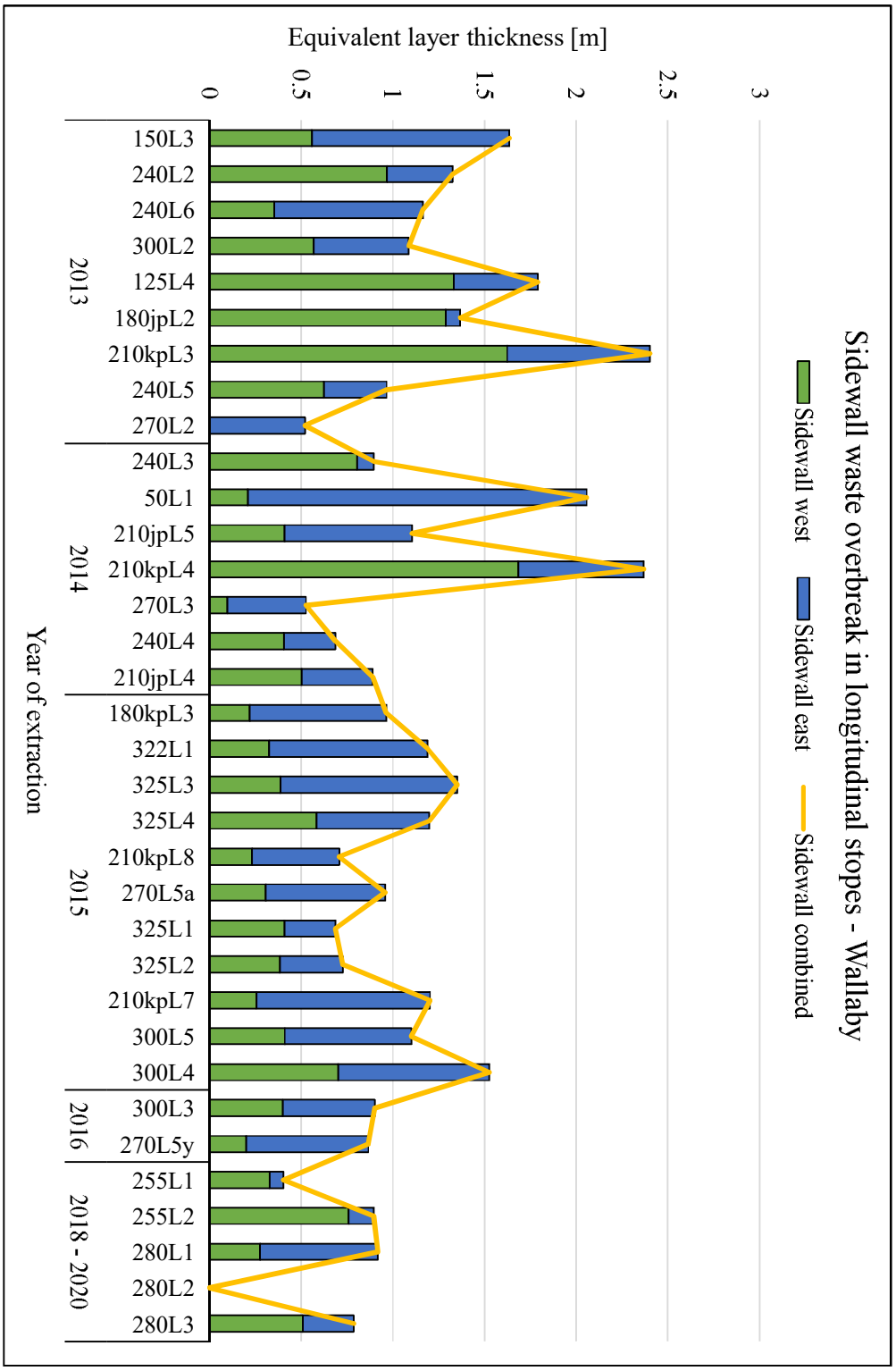

Figure A4.1: Sidewall waste overbreak in longitudinal stopes in Wallaby

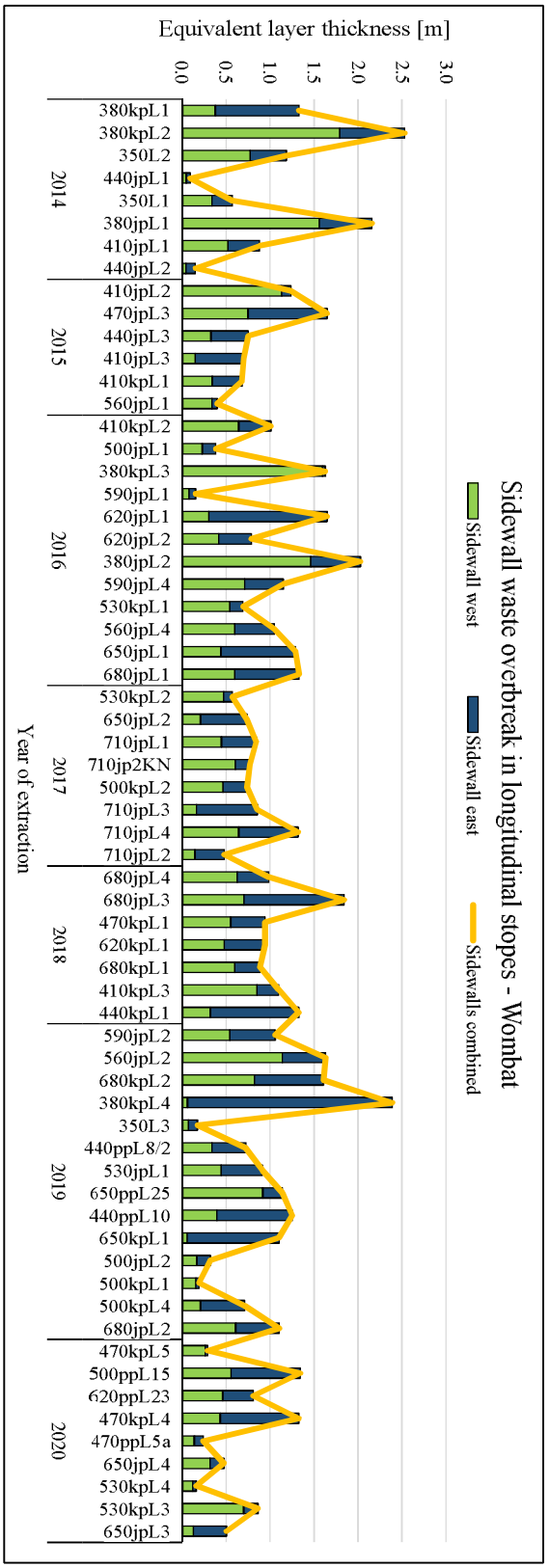

Figure A4.2: Sidewall waste overbreak in longitudinal stopes in Wombat

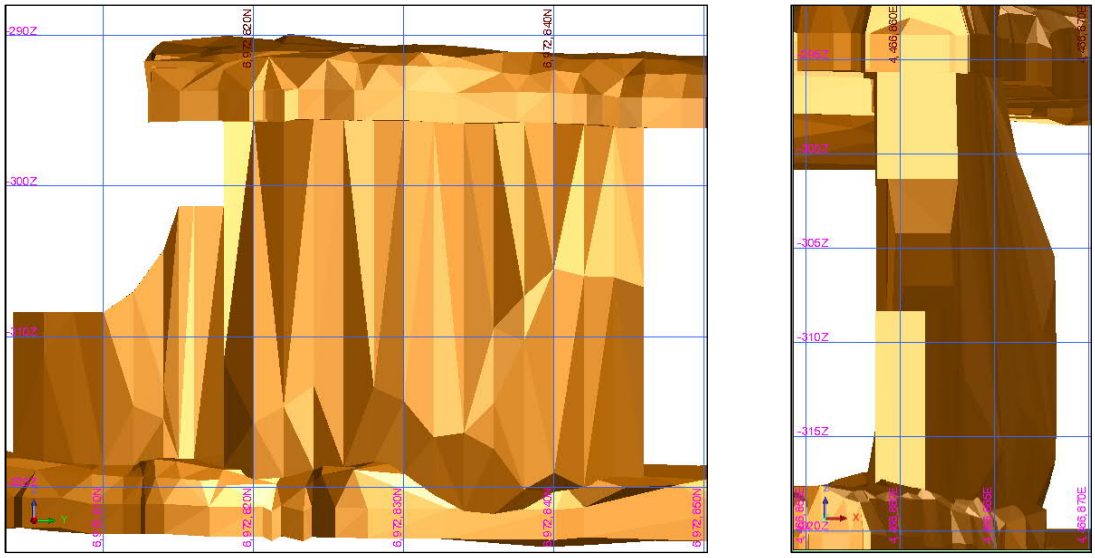

Figure A4.3: Stope example of basic geometric complexity, Stope 325L4

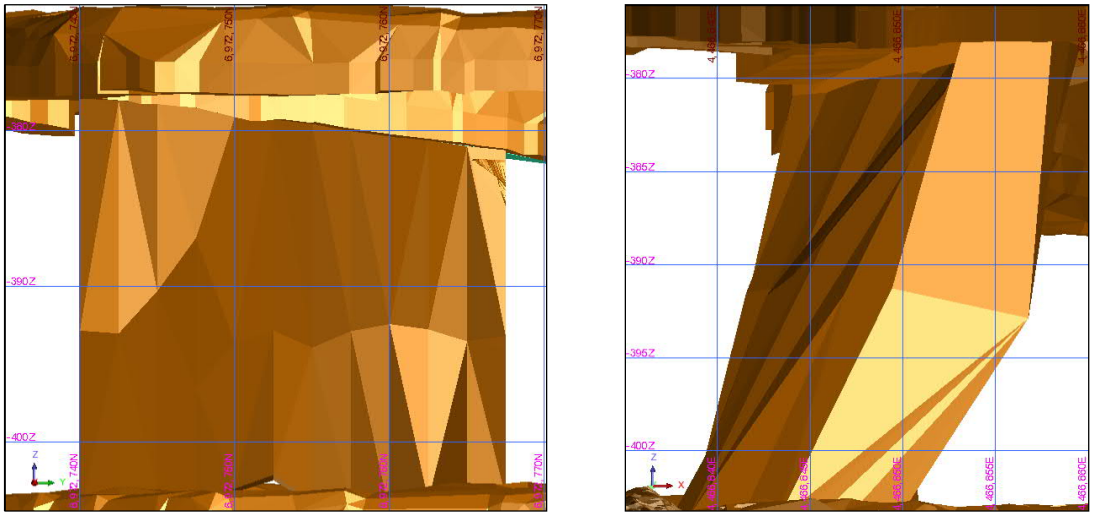

Figure A4.4: Stope example of high geometric complexity, stope 410kpL2

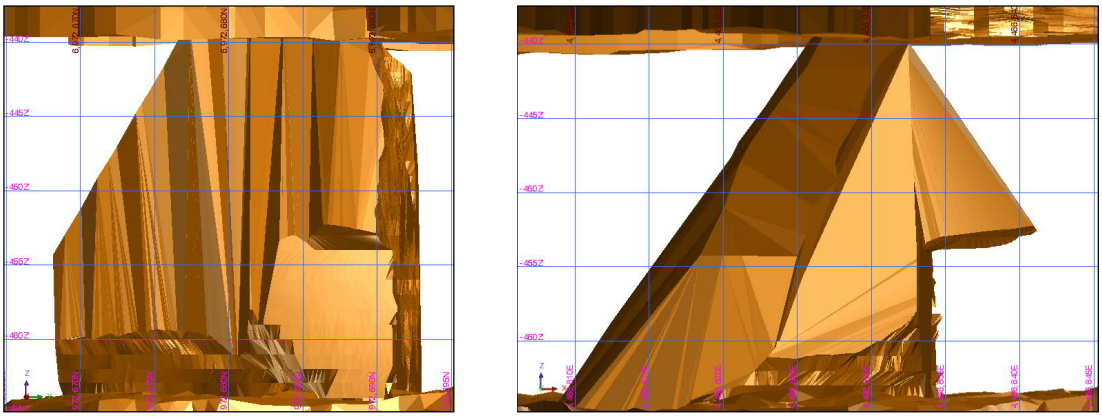

Figure A4.5: Stope example of severe geometric complexity (stope 470ppL11)

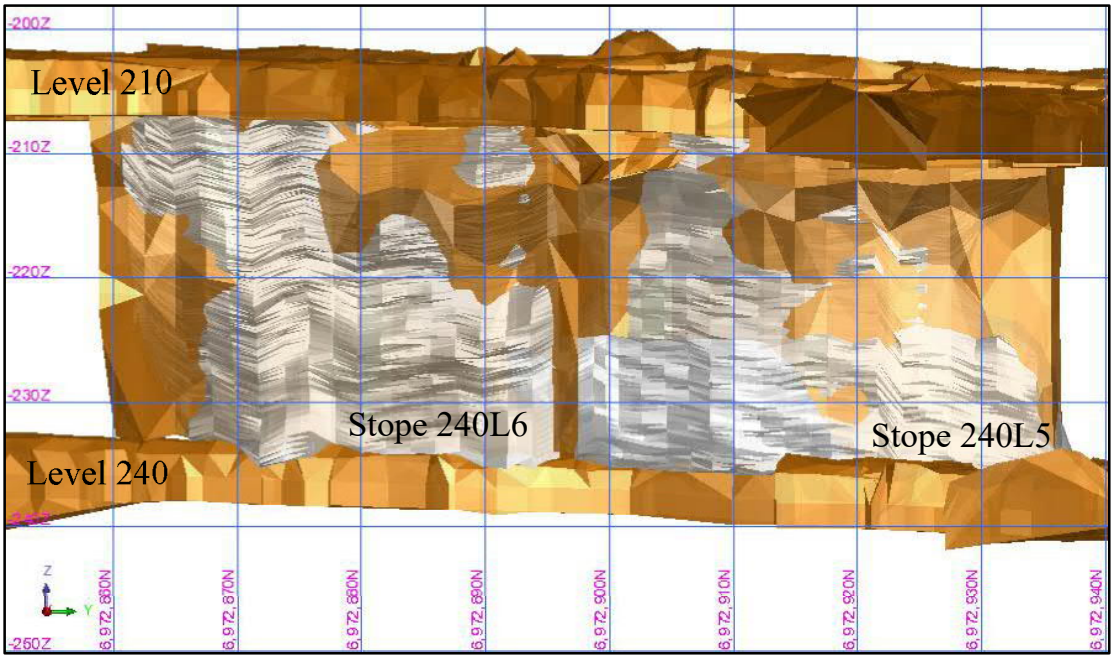

Figure A4.6: Vertical layers of black schist overbreak (grey) in stope 240L6 and 240L5

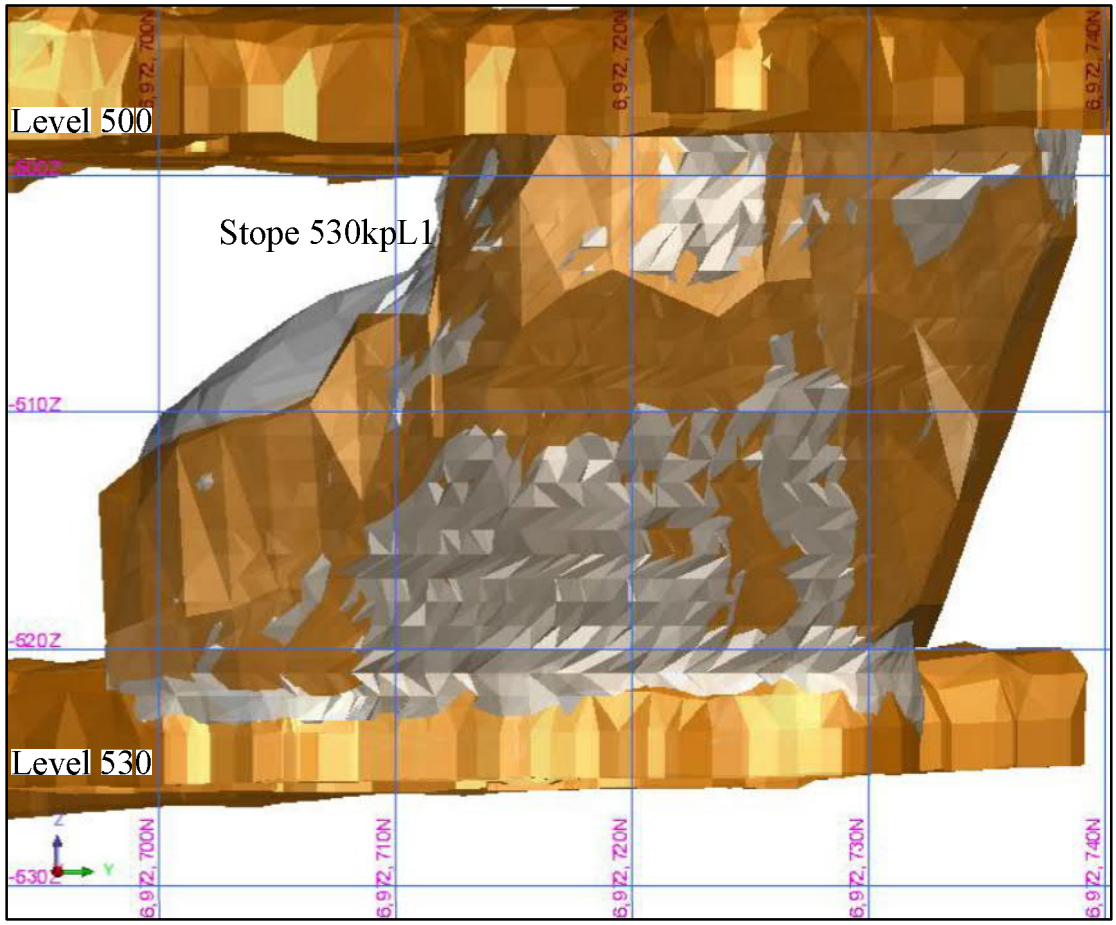

Figure A4.7: CMS scan of overbreak without black schist presence in stope 530kpL1

Appendix 5

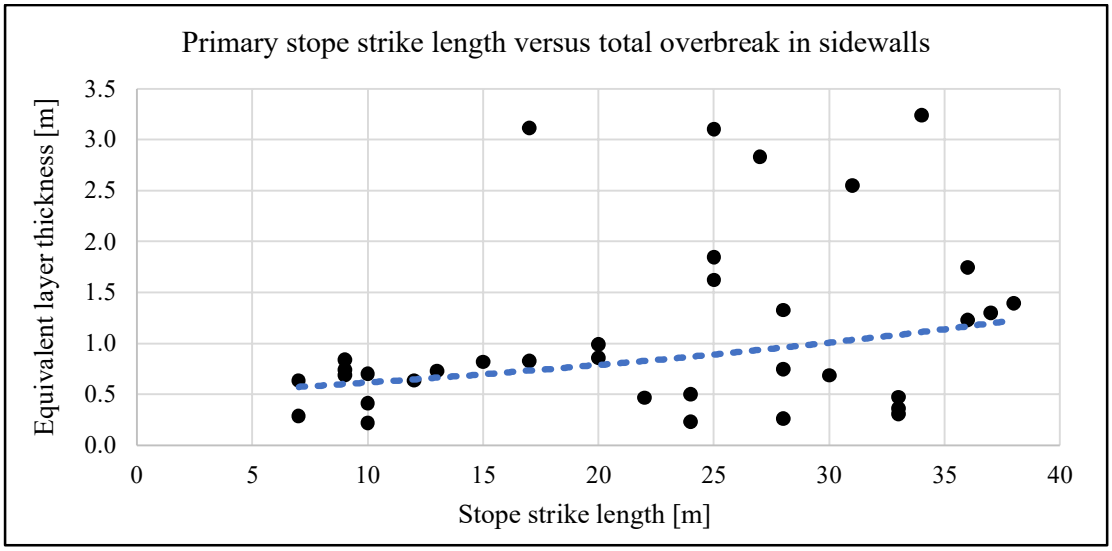

Figure A5.1: Primary stope strike length versus total overbreak in sidewalls, r = 0.33

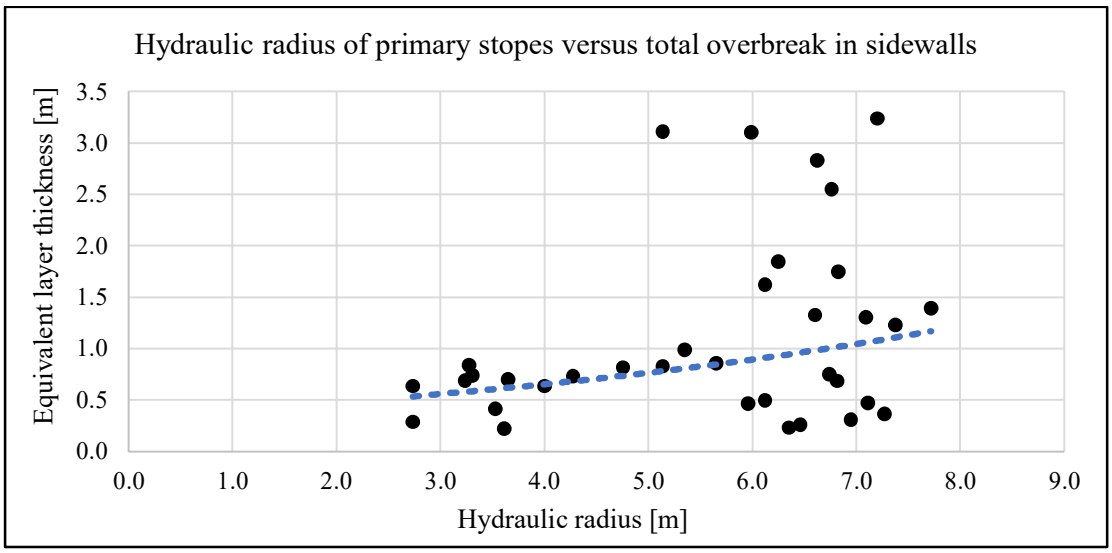

Figure A5.2: Hydraulic radius of primary stopes versus total overbreak in sidewalls, r = 0.33

Appendix 6

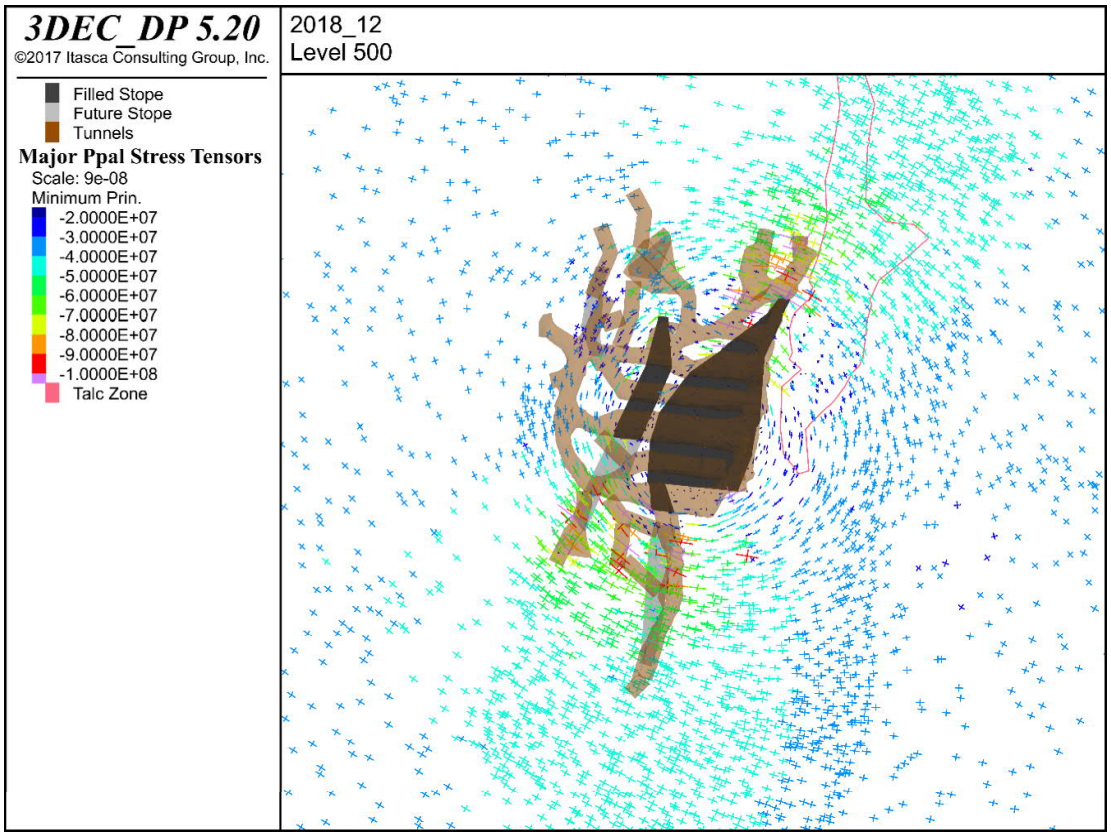

Figure A6.1: Large accumulation of high major principal stress values in the northern and southern ends of the level 500 by means of numerical modelling (Pöyry Finland Oy, 2017)

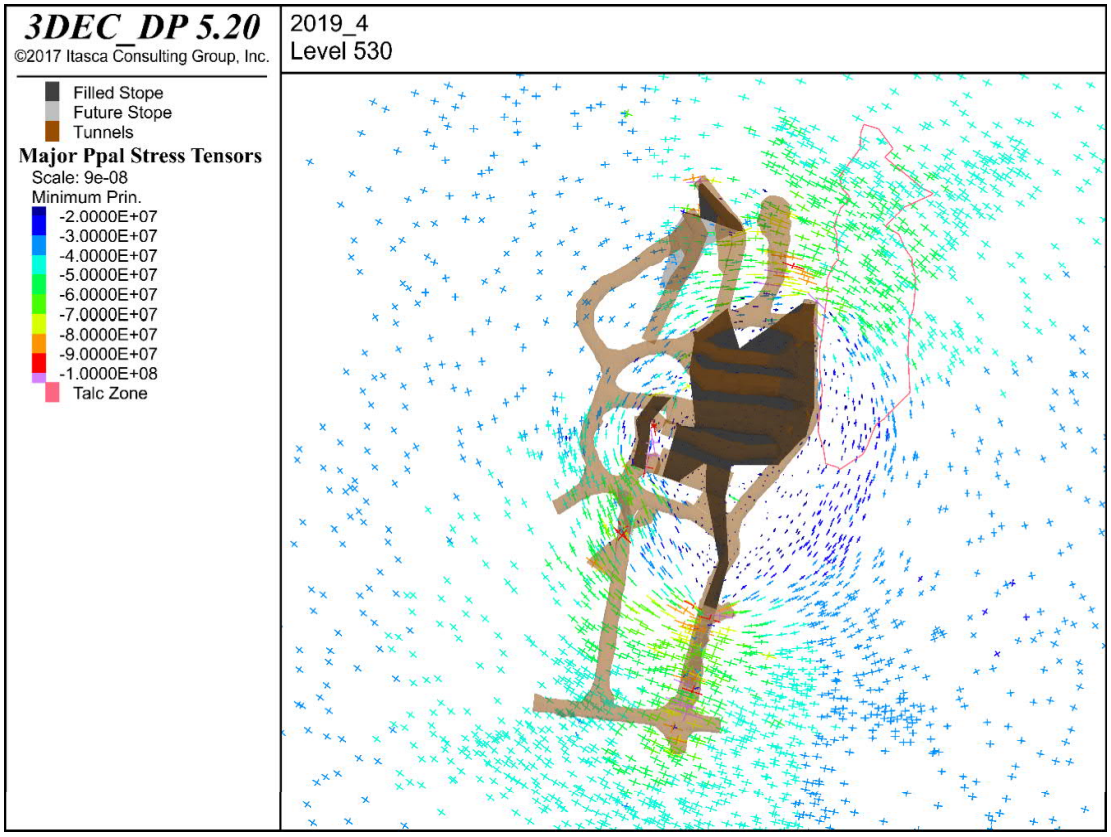

Figure A6.2: Large accumulation of high major principal stress values in the northern and southern ends of level 530 by means of numerical modelling (Pöyry Finland Oy, 2017)

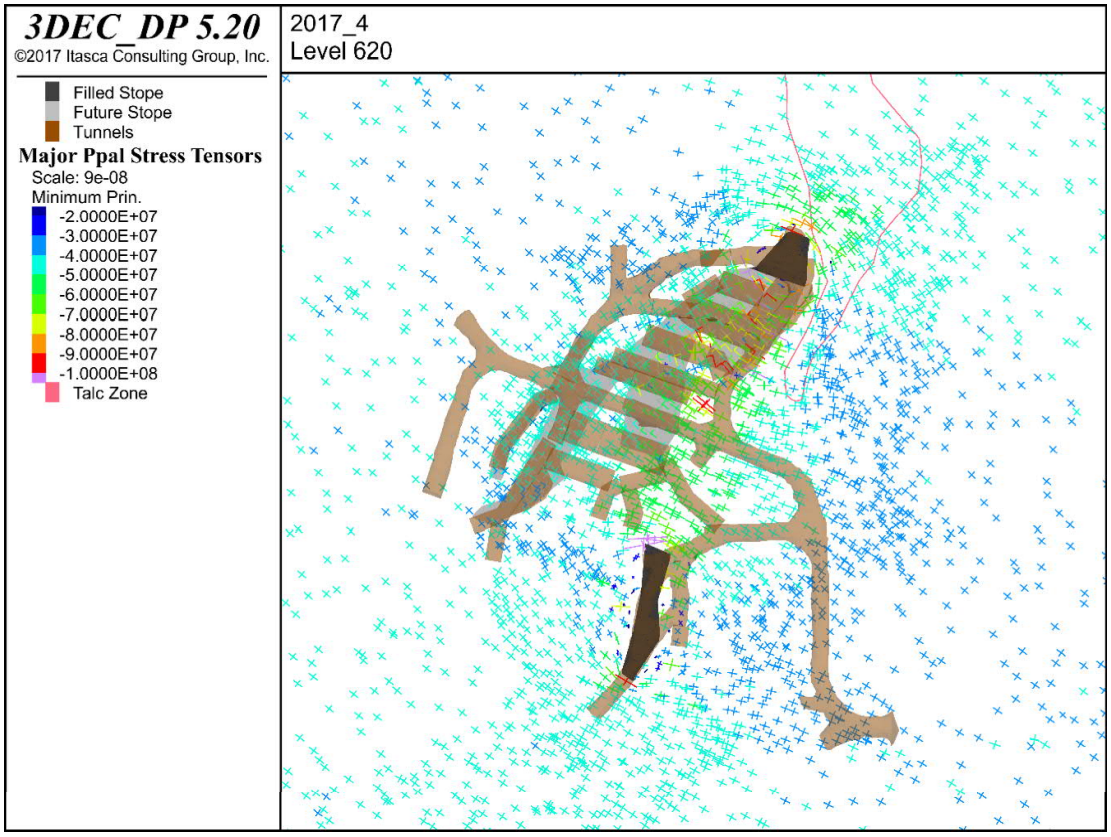

Figure A6.3: Large accumulation of high major principal stress values prior to mining in the level 620 by means of numerical modelling (Pöyry Finland Oy, 2017)

Appendix 7

Table A7.1: Comprehensive longitudinal dataset with required parameters

Comprehensive longitudinal dataset		
Sections	**Required parameters**	**Detailed selection**
General	Stope name	
	Orebody	
	Ore type	
	Mining sequence	
	Year	
	Production level	
Stope location	Regional HW/FW	
	North/South	
Black Schist	Presence	[yes/no]
	Located east	
	Located west	
Stope geometry	Undercutting	
	Overcutting	
	Geometric complexity	
	Stope length	
	Stope height	
	Stope width	
	Hydraulic radius	
	Aspect ratio (L/H)	
	Stope hanging wall	[west/east]
	Stope footwall	[west/east]
	Avg. HW dip	
	HW dip class	
	Avg. FW dip	
	FW dip class	
Stope production planning	Estimated dilution	
	Actual dilution	
	Estimated recovery	
	Actual recovery	
ELLO	Ore loss	
ELOS	Ore overbreak	
	Waste overbreak	
	CRF overbreak	

Table A7.2: Comprehensive transverse dataset with required parameters

Comprehensive transverse dataset		
Sections	**Required parameters**	**Detailed selection**
General	Stope name	
	Orebody	
	Ore type	
	Mining sequence	
	Year	
	Production level	
	Stope type	[Primary/Secondary]
	Vertical sequence	[Bottom/Middle/Top stope]
	Stope sub-type	[1.1/1.2] or [2.1/2.2]
Stope location	Orebody location	[Inside/Edge of orebody]
	North/South	
Stope geometry	Undercutting	
	Overcutting	
	Geometric complexity	
	Stope length	
	Stope height	
	Stope width	
	Hydraulic radius	
	Aspect ratio	
	Stope hanging wall	[west/east]
	Stope footwall	[west/east]
	Avg. HW dip	
	HW dip class	
	Avg. FW dip	
	FW dip class	
Stope production planning	Estimated dilution	
	Actual dilution	
	Estimated recovery	
	Actual recovery	
ELLO	Ore loss	
ELOS	Ore overbreak	
	Waste overbreak	
	CRF overbreak	